Durham E-Theses

Solitons in low-dimensional sigma models

Jens Gladikowski

How to cite:

Use policy

Solitons in Low-Dimensional Sigma Models
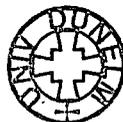
by

Jens Gladikowski

Thesis presented for the Degree of Doctor of Philosophy

at the University of Durham

Department of Mathematical Sciences

University of Durham

England

August 1997

1 6 DEC 1997

TO MY PARENTS

Preface

This thesis summarizes work done by the author between October 1994 and July 1997 in the Department of Mathematical Sciences at the University of Durham. No part of it has been previously submitted for any degree at this or any other University.

With the exceptions of chapter 1 and the introductions to each chapter, this material is believed to be original work, unless otherwise stated. The contents of chapter 2 derives from a paper that has been published in *Zeitschrift für Physik* [1]. The material of chapter 4 is the result of a collaboration with Meik Hellmund and is to appear in *Physical Review* D [2]. Parts of chapter 5 were also done in collaboration with Meik Hellmund.

There are a number of people who I wish to thank for making my stay in Durham enjoyable and productive. First and foremost I am deeply grateful to my supervisor Wojtek Zakrzewski for his constant encouragement, careful guidance and frankness. I am also very much indebted to Meik Hellmund for his genuine friendship and many valuable conversations. It is a pleasure to acknowledge various members of the Department of Mathematical Sciences for their interest in my work and their constructive criticism, especially I wish to thank Jacek Dziarmaga, Bernard Piette and Richard Ward. Also many thanks to Uli Harder for his irresistable outspokenness.

I thank the Department of Mathematical Sciences and the Engineering and Physical Sciences Research Council for Research Studentships.

Abstract

Solitons in Low-Dimensional Sigma Models

Jens Gladikowski

The aim of this thesis is to study topological soliton solutions in classical field theories, called sigma models, on a three-dimensional space.

In chapter 1 we review the general field-theoretical framework of classical soliton solutions and exemplify it on the main features of the $O(3)\,\sigma$-model and the Abelian Higgs model in (2+1) dimensions.

In chapter 2 a $U(1)$-gauged $O(3)\,\sigma$-model is discussed, where the behaviour of the gauge field is determined by a Chern-Simons term in the action. We find numerical solutions for radially symmetric fields and discuss those of degree one and two. They carry a non-vanishing angular momentum and can be interpreted as classical anyons.

A similar model is studied in chapter 3. Here the potential is of Higgs-type and chosen to produce a Bogomol'nyi model where the energy is bounded from below by a linear combination of the topological degree of the matter fields and the local $U(1)$-charge. Depending on internal parameters, the solutions are solitons or vortices. We study them numerically and prove for a certain range of the matter field's vacuum value that there cannot be a 1-soliton.

In chapter 4 we discuss a modified $O(3)\,\sigma$-model in (3+0) dimensions. The topological stability of the solitons is here implied by the degree of the map $S^3 \mapsto S^2$, which provides a lower bound on the potential energy of the configuration. Numerical solutions are obtained for configurations of azimuthal symmetry and the spectrum of slowly rotating solitons is approximated.

Chapter 5 deals with a theory where the fields are maps $\mathbb{R}^{2+1} \mapsto \mathbb{CP}^2$. The Lagrangian includes a potential and a fourth-order term in the field-gradient. We find a family of static analytic solutions of degree one and study the 2-soliton configuration numerically by using a gradient-flow equation on the moduli space of solutions.

We conclude this thesis with a brief summary and give an outlook to open questions.

Contents

Chapter 1

A Review of Topological Solitons

1.1 Solitons in Classical Field Theories

The general aim of this thesis is to explore classical solutions to certain non-linear field theories, called sigma models. If these solutions are non-singular, of finite energy and localised in space they will be called solitons. Solitons as such are abstractions of inherently non-linear wave phenomena whose description is related to several branches of pure mathematics and connects them to both physical theories and observations, the latter being exemplified by non-linear water waves, shock waves in a plasma medium, ATP-transport in muscles and non-linear electric pulses.

The theory of solitons is thus a prime example of a general tendency in contemporary theoretical physics, namely the increasing interchange of ideas and concepts between pure mathematics and physics. The work on the border between these two areas has been proven fruitful and inspiring for both sides. To mention just two relevant examples, many notions of Algebraic Topology and Differential Geometry, such as homotopy and (co-) homology groups or index theorems, are crucial for the physicists' understanding of soliton theory, while on the mathematics side the discovery of the inverse scattering transform — one of the main analytic tools in soliton theory — was inspired by a physical question that resulted in the initial value problem for the KdV equation [3]. It is in this spirit that the work presented in this thesis is motivated partly by the pure mathematical interest of finding solutions to a well-defined analytical problem irrespective of its physical applications and partly by the experimental evidence of non-linear waves in the broadest sense.

With the definition given above, solitons characteristically possess particle-like features and quite naturally physicists became intrigued by solitons in field theories and their applications to

particle physics. A prominent example of this is the Skyrme model. Being somewhat inspired by Kelvin's idea of a classical continuum theory of matter, Skyrme constructed, beginning in 1961, the first non-linear field theory for the description of baryonic matter, or more precisely, for fermions as solitons in a mesonic background field [4, 5]. Although being somehow overshadowed by the dramatic success of Quantum Chromodynamics (QCD) in the 1970's, Skyrme's model was revived in the early 1980's by Witten, who proposed it to be a good candidate for an effective theory in the low-energy range of QCD, which is beyond perturbation theory [6]. Witten's seminal proposal has inspired many subsequent investigations of the Skyrme and related models at both the classical and quantum mechanical level (see [7] for a comprehensive review). In a sense, some of the work presented in this thesis can be seen as spin-off of research performed on the Skyrme-model, although we are not directly interested in applications to nuclear physics. The Skyrme model is an example of a (modified) non-linear sigma model, the main objects of study of this thesis and its investigation has revealed many connections to other fundamental theories such as Yang-Mills and Yang-Mills-Higgs theory in (4+0) and (3+1) dimensions respectively. Below we will introduce two lower-dimensional relatives of these theories, the $O(3)$ σ-model and the Abelian Higgs model, but first we lay out the general field-theoretical framework for their description.

Solitons can be divided into two, almost disjoint, classes, corresponding to the origin of their stability. In one class, which is historically older, the solutions are called integrable and the governing equation(s) have an infinite number of quantities that are dynamically conserved. By definition, for the model to be integrable, these conserved quantities have to be in involution. Examples of integrable theories are the KdV-equation and the non-linear Schrödinger equation. Solitons in an integrable model cannot be rich in their dynamics: for two colliding solitons anything more than a shift of their phase is prohibited by the conservation laws. This makes solitons in integrable models less interesting from the particle physics point of view, where one is interested in non-trivial scattering, vibrations, radiation and the like, but there are many other areas in science where these solitons provide a fertile ground for various applications: hydrodynamics, plasma-physics and mathematical biology are just some of them. Generally speaking, integrable models are rare, especially if additional conditions (such as Lorentz-invariance) are imposed and most of them are confined to (1+1) dimensions. Integrability usually implies certain restrictions on the parameters of the model and one can say that the set of integrable models is of "measure zero" in the space of theories. Nevertheless these models carry important conceptual weight: the soliton solutions (if they can be found) can often be studied in analytical depth, and in a quantum theory — which, however, has to be defined for solitons — they offer, at least in principle, a

non-perturbative description which contrasts the perturbative approaches that are common in Quantum Field Theories.

For the other class of solitons, it is the topology of the theories' configuration space that can guarantee the solitons' stability. To be more precise, consider a classical field ϕ, which is defined as a smooth map from the physical space-time $X = \{\mathbf{x}, t\}$ into the field-manifold Φ, where $\mathbf{x}$ and t denote the space- and time-coordinates respectively; $\phi : X \mapsto \Phi$. The (classical) configuration space $\mathcal{C}$ is the infinite-dimensional space of all fields ϕ at a fixed time t. Consistently, we will frequently call a time-independent map a configuration. One defines a functional $V[\phi]$ on the configuration space, which is called the potential energy and maps $\mathcal{C} \mapsto \mathbb{R}$. Its finiteness is essential to allow for a meaningful physical interpretation of a field theory and we will henceforth impose this condition. For the theories considered in this thesis, an important consequence of $V[\phi] < \infty$ is that $\mathcal{C}$ decomposes into disjoint subsets $\mathcal{C}_N$, with integer N, which are separated by an infinite potential barrier:

$$\mathcal{C} = \bigcup_{N=-\infty}^{\infty} \mathcal{C}_N . \tag{1.1}$$

Elements of $\mathcal{C}_1$ are usually called 1-solitons, or simply solitons, and fields in the sector $\mathcal{C}_0$ are by definition topologically equivalent to the vacuum. The index N occurs under various names in the literature, such as degree of the map or topological charge. For the theories studied here it provides a lower bound on the potential energy $V[\phi]$.

The topology of the configuration space is canonically described in terms of homotopy groups [8]. Consider two maps $\phi_1(\mathbf{x})$ and $\phi_2(\mathbf{x})$ between two manifolds $\mathcal{M}$ and $\mathcal{N}$, $\phi_{1,2} : \mathcal{M} \mapsto \mathcal{N}$. They are called homotopic if there exists a continuous map $\phi : \mathcal{M} \times I \mapsto \mathcal{N}$, $I = [0, 1]$, such that $\phi_1(\mathbf{x}) = \phi(\mathbf{x}, 0)$ and $\phi_2(\mathbf{x}) = \phi(\mathbf{x}, 1)$. The map $\phi(\mathbf{x}, \xi), \xi \in [0, 1]$ is called the homotopy. A set of homotopic maps forms an equivalence class which is an element of the corresponding homotopy group. These are usually denoted $\pi_n(\mathcal{N})$ and they are composed of equivalence classes of maps $S^n \mapsto \mathcal{N}$. For $n = 0, 1$ there is a simple geometrical interpretation of the homotopy group. The relation $\pi_0(\mathcal{N}) = 0$ implies the arcwise connectedness of $\mathcal{N}$, while $\pi_1(\mathcal{N}) = 0$ means, that loops on $\mathcal{N}$ can be contracted to a point (trivialised), in this case $\mathcal{N}$ is called simply connected.

Homotopy is also the concept by which a time-evolution of the fields is incorporated. Let $\phi_1, \phi_2 \in \mathcal{C}_N$, then a continuous change of ξ from 0 to 1 defines a trajectory in $\mathcal{C}_N$, described by the homotopy $\phi(\mathbf{x}, \xi)$, which leads from ϕ_1 to ϕ_2. The parameter ξ can be interpreted as physical time so that the homotopy is a "time-dependent" field.

Finiteness of $V[\phi]$ makes it necessary to impose certain boundary conditions on the fields, such that $\phi(\mathbf{x}) \to \phi_\infty$ as $|\mathbf{x}| \to \infty$. Here ϕ_∞ lies in the vacuum manifold defined as $\Phi_{\text{vac}} \equiv \{\phi : |\mathbf{x}| \to \infty, V[\phi] < \infty\}$. Any smooth change into another topological sector of the configuration space would have to change the field at the boundary smoothly from one vacuum sector into a different one and by doing so the configuration would have to overcome an infinite potential barrier, which is prohibited by assumption. Therefore fields that belong to a certain $\mathcal{C}_N$ cannot be deformed smoothly into a different $\mathcal{C}_{\bar{N}}$, which in particular implies their stability against deformation into a configuration of arbitrary low energy, because of the above mentioned bound. This is the field-theoretical analogue to particle conservation in classical mechanics.

Topological solitons can be divided further into two different species, according to their topological classification. In the first category, the finiteness of the potential energy implies that the field at the *boundary* of the physical space (at a fixed time) is in an equivalence class which is a non-trivial element of the homotopy group that describes the map into Φ_{vac}. Denote the boundary of X at an arbitrary but fixed time t as ∂X_t, then the field at infinity $\phi_\infty : \partial X_t \mapsto \Phi_{\text{vac}}$ where for the theories of interest to us $X_t = \mathbb{R}^d$ and hence $\partial X_t = S^{d-1}$, the sphere at infinity, while Φ_{vac} is homeomorphic to S^m. Then the topology of the configuration is described by $\pi_{d-1}(\Phi_{\text{vac}}) = \pi_{d-1}(S^m)$, which equals zero for $d-1 < m$ and $\mathbb{Z}$ for $d-1 = m$. Examples for latter theories are Yang-Mills theory for $d = 4$ (which has instantons as solutions), Yang-Mills-Higgs theory for $d = 3$ (monopoles) and the Abelian Higgs model for $d = 2$ (vortices). These theories can have solutions, for a specific choice of their parameters, where the potential energy is proportional to the magnitude of the corresponding homotopy index N.

Alternatively, Φ_{vac} might consist just of a single point ϕ_∞. This means, all of ∂X_t gets mapped to ϕ_∞ and X_t can be one-point compactified to S^d. The fields fall into equivalence classes which are elements of $\pi_d(\Phi)$ and the topology is due to the *interior* of X_t. Such configurations are generally referred to as "textures", a name that stems from extended solitonic structures in solid state physics.

To describe textures topologically and can employ a useful theorem which relates the homotopy group of the configuration space $\mathcal{C}$ to the homotopy group of the field space Φ. In d space-dimensions [1] :

$$\pi_k(\mathcal{C}) = \pi_{k+d}(\Phi) \,. \tag{1.2}$$

---

[1] Strictly, this formula is true only for base-point preserving maps ϕ. All of the fields that are of interest to us are of this type.

Thus, if $k = 0$, the topology of the texture is related to the disconnectedness of the configuration space. Examples are the Skyrme model for $d = 3$ and the $O(3)\,\sigma$-model for $d = 2$. The homotopy index again provides a bound on the energy, which is, however, not saturated in the case of the Skyrme model.

Because of their conceptual relevance for the theories discussed in this thesis we will introduce below one model from each of the two classes for $d = 2$, namely the $O(3)\,\sigma$-model and the Abelian Higgs model.

1.2 The $O(3)\,\sigma$-model and its Relatives

Much of the work presented in this thesis is based on the non-linear $O(3)\,\sigma$-model and its modifications. Therefore we introduce it here in greater detail, but it also provides an excellent pedagogical example of a field theory which supports topological soliton solutions. The concepts discussed here are of relevance in various other theories, however, the $O(3)\,\sigma$-model in $(2+0)$ dimensions is special in the sense that it belongs to the few theories with topological solitons where the solutions to the Euler-Lagrange equations are analytically known. For the purpose of a well-composed introduction we first give some general background on σ-models before we proceed to the $O(3)\,\sigma$-model.

The original work on σ-models goes back to Gell-Mann and Lèvy, who introduced them in nuclear physics to describe the decay of the pion [9]. However, the soliton solutions which the model yields did not play a role in these theories, where interactions are described in terms of current algebras. Only later the soliton contents was discovered to be of great interest, partly as toy-models for higher-dimensional theories which seemed hard to tackle directly and partly in their own right as models in condensed matter physics and string theory, see the reviews in [10, 11].

The non-linear σ-models are real, scalar, non-linear field theories where the fields are maps

$$\phi \;:\; X \mapsto \Phi. \tag{1.3}$$

Here X is the $(d + 1)$-dimensional space-time with metric η and Φ the field-space which is a Riemannian manifold with metric g. The following action defines the non-linear σ-model:

$$S = \frac{1}{2} \int d^d x \, dt \; g_{ab} \partial_\alpha \phi^a \partial_\beta \phi^b \eta^{\alpha\beta} \,, \tag{1.4}$$

where we denote $\partial_\alpha \equiv \partial/\partial x^\alpha$. Here and throughout this thesis we assume the usual summation convention for repeated indices. We are interested in theories where X is a three-dimensional real

manifold, which has either a Euclidean or Minkowskian metric. Therefore η is flat and its signature is implied by the choice of space-time indices. We denote space indices in Euclidean space by latin characters $i, j, k...$ (running from 1 to d) and those in Minkowski space by greek indices $\alpha, \beta, \gamma...$ (from 0 to d). Indices in target space are $a, b, c....$ The equations of motion derived from the variation of (1.4) are

$$\partial_\alpha \partial^\alpha \phi^a + \Gamma^a_{bc} \partial_\alpha \phi^b \partial^\alpha \phi^c = 0 \,, \tag{1.5}$$

where Γ^a_{bc} is the Christoffel symbol, defined in the usual way [12]. For a flat target manifold $\Gamma^a_{bc} = 0$ and the equations of motion are the wave-equation for every component ϕ_a. Solutions to (1.5) are known in the mathematical literature as harmonic maps.

An alternative way to describe the curvature of the target space is by imposing a constraint to the fields ϕ and thinking of the target space as being embedded in Euclidean space. This leads to non-linear equations of motion despite g being flat. We discuss this procedure on the $O(3)\,\sigma$-model in (2+1) dimensions, where $X = \mathbb{R}^{2+1}$ and $\Phi = S^2$. Thus, the physical space is of signature $(+, -, -)$ such that the Lagrangian $L = T - V$, where T is the kinetic energy functional, defined on the tangent bundle of C and V is the potential energy functional as above. The field $\phi \,:\, \mathbb{R}^{2+1} \mapsto S^2$ is a three-component vector constrained to unit-length, $\phi_a \phi^a = 1$, $(a = 1, 2, 3)$. To shorten the notation, we use $\phi \equiv (\phi_1, \phi_2, \phi_3)$. Then the Lagrange-function L becomes

$$L = T - V = \frac{1}{2} \int d^2x\, \partial_t \phi \cdot \partial^t \phi - \frac{1}{2} \int d^2x\, \partial_i \phi \cdot \partial^i \phi \,, \tag{1.6}$$

where the dot-product is taken in field-space. This model is the relativistic extension of the continuum version of the Heisenberg ferromagnet. It is called the $O(3)\,\sigma$-model because the Lagrangian (1.6) and the constraint are invariant under global $O(3)$-rotations of the fields. From the symmetries point of view, the field-manifold is described by the action of a space-dependent matrix $R \in SO(3)$ on a constant unit vector, say $\mathbf{n}$, where all the fields obtained by those $SO(2)$-rotations which are orthogonal to $\mathbf{n}$ are identified. Thus the field-manifold Φ is described by the coset space $SO(3)/SO(2)$. To describe the topology of this coset space one can employ a useful formula from homotopy theory, namely

$$\pi_2 \left(\frac{G}{H} \right) = \pi_1 \left(H \right) \,, \qquad \text{if} \qquad \pi_1 \left(G \right) = 0 \,, \tag{1.7}$$

where G is a Lie-group and H is a closed subgroup. For the $O(3)\,\sigma$-model one can use the universal covering group of $SO(3)$ which is $SU(2)$, and deduce $\pi_2(SU(2)/U(1)) = \pi_1(U(1)) = \mathbb{Z}$.

This discussion might seem a bit artificial — after all $\pi_2(S^2) = \mathbb{Z}$ — but it serves nicely to illustrate (1.7), which is why we give it here.

In the Lagrangian formulation of the theory one must take care of the constraint by including a term $\sim \lambda(\phi \cdot \phi - 1)$, where λ is the Lagrange multiplier. This leads to the following equations of motion

$$\partial_\alpha \left(\partial^\alpha \phi \times \phi \right) = 0 \,, \tag{1.8}$$

where the cross-product is taken in field-space. Note that (1.8) is a conservation law for the current $\partial^\alpha \phi \times \phi$.

Topological Degree

As mentioned earlier, finiteness of the action induces the model's topology which is for the $O(3)\,\sigma$-model characterized by $\pi_2(S^2) = \mathbb{Z}$. For a given class of homotopically equivalent maps $\phi : S_x^2 \mapsto S_\phi^2$, the homotopy index can be computed using a simple formula from Differential Geometry [13]. This formula is valid for any maps $f : S^n \mapsto S^n$, $n > 0$ and we give therefore in generality. Let ω be the invariant volume form on target S^n, then the degree $N = \deg[f]$ equals the normalized integral of the pullback of ω by f^*, integrated over base S^n, the compactified physical space:

$$N = \int f^* \omega \bigg/ \int \omega \,. \tag{1.9}$$

This formula nicely illustrates the interpretation of N as the multiplicity of coverings of the target S^n. In this thesis we mostly work in the coordinate representation of all quantities and give the abstract versions for completeness only.

Therefore, in coordinates, the topological charge-density of the $O(3)\,\sigma$-model is given by $f^* \omega = \phi^* \omega = \varepsilon_{ij} \phi \cdot \partial_i \phi \times \partial_j \phi$ and

$$N = \frac{1}{4\pi} \int d^2 x \; \phi \cdot \partial_1 \phi \times \partial_2 \phi \,, \tag{1.10}$$

where 1,2 indicate cartesian coordinates x_1, x_2 on $\mathbb{R}^2$. Solutions with $N = 1$ are called solitons, those with $N = -1$ anti-solitons.

Bogomol'nyi Trick and Soliton Solutions

The equations of motion (1.8) are second-order partial differential equations. However, there is a procedure to find fields that describe absolute minima of $V[\phi]$ within a certain $\mathcal{C}_N$ — and therefore

solutions to the variational equations — by solving *first*-order differential equations. The argument goes back to Bogomol'nyi [14] and uses $(\partial_1\phi \pm \phi \times \partial_2\phi)^2 \geq 0$. If this inequality is expanded and integrated over $\mathbb{R}^2$, one obtains:

$$\frac{1}{2}\int d^2x\;(\partial_1\phi)^2 + (\partial_2\phi)^2 \;\geq \mp \int d^2x\,\phi\cdot\partial_1\phi\times\partial_2\phi \quad\Rightarrow$$
$$V[\phi] \;\geq 4\pi|N|\,. \tag{1.11}$$

where the sign ambiguity has been absorbed into the magnitude of N. The equality is clearly satisfied if and only if

$$\partial_1\phi = \mp\phi \times \partial_2\phi\,, \tag{1.12}$$

which defines the points of (anti-) self-duality. Self-duality is an important concept in many theories and we shall come back to it and explain it further in chapter 3. The solutions of (1.12) have a potential energy-density which equals the topological charge-density. To find these solutions, it is convenient to introduce a complex valued field, W, which is obtained by stereographic projection of S^2_ϕ from (for definiteness) the north pole:

$$W = \frac{\phi_1 + i\phi_2}{1 - \phi_3}\,. \tag{1.13}$$

The W's are called inhomogeneous coordinates on $\mathbb{CP}^1$, the one-dimensional complex projective space. This space consists of equivalence classes of points $z \in \mathbb{C}^2$, with the equivalence relation $z \sim \lambda z$, λ being complex. The W's have two real degrees of freedom, therefore they are not subject to any constraint. This alternative description of the $O(3)\,\sigma$-model is possible because of the exceptional property of $S^2 = \mathbb{CP}^1$, which implies that S^2 admits a complex structure. The self-dual equations (1.12) for W take a remarkably simple form if written in terms of a complex coordinate $x_\pm = x_1 \pm ix_2$ on the physical space. Let $\partial_{x_+}, \partial_{x_-}$ denote the derivatives with respect to x_+, x_-; it then holds from (1.12):

$$\partial_{x_\pm}W = 0\,. \tag{1.14}$$

From this it is clear that W is an (anti-) holomorphic function [15]. Thus W can be expressed as a rational function of degree, say, n and formula (1.10), in terms of W, yields a topological degree of $N = n$. A rational function of degree n has in general $(4n + 2)$ real parameters which determine the soliton's size, shape, position, orientation and various internal degrees of freedom. However, not all of those parameters lead to physically distinct solutions in the sense that they describe

configurations which differ only by certain (global) symmetries. To identify these symmetries is an important problem which is well-known from gauge theories such as Yang-Mills theory in (4+0) dimensions and Yang-Mills-Higgs theory in (3+1) dimensions. Here the Lagrange function (1.6) is invariant under global $O(3)$-rotations which removes three real parameters. Thus the "true" parameter space for minimum energy solitons is $4n - 1$-dimensional. Hence the holomorphic one-soliton solution has three real parameters and can be written as

$$W(x_+) = \frac{\mu}{x_+ - x_0}, \qquad (1.15)$$

where x_0 is complex and defines a pole of W, such that it can be identified with the soliton's position in the particle physics sense; μ is real and a measure for the decay of the energy density around x_0, hence it is a criterion the size of the soliton.

The $4n - 1$ parameter family of solutions spans a submanifold within the corresponding $\mathcal{C}_n$, namely the surface where the potential energy is minimal. Following an idea by Manton [16], this surface, called moduli-space, is used to describe the low-energy dynamics of solitons, where their time-evolution is approximated by a geodesic motion on the moduli space. The corresponding metric is induced by the kinetic energy functional. We will introduce this method more detailed in chapter 5 in the context of $\mathbb{CP}^2$-models.

The $O(3)\,\sigma$-model is relativistically invariant and thus moving solutions can be obtained from static ones by Lorentz-boosting them into a moving frame. Again, the topology remains untouched by this procedure and provides a conserved quantity, the degree.

The Hobart-Derrick Theorem

The Hobart-Derrick theorem is a very useful general argument which rules out that static solutions in certain theories are non-singular and non-trivial configurations [17, 18]. The input of the theorem is simply the Lagrangian that defines the theory and the argument itself is fairly straightforward, based on behaviour of the potential energy under scaling of the space coordinate. Its proof is rather short but also very instructive. We demonstrate it on the example of a theory whose fields are real vectors ϕ_a, $(a = 1 \ldots N)$. The $O(3)\,\sigma$-model is a special case for $N = 3$, $|\phi| = 1$. Consider the following potential energy functional $V[\phi]$ in d space-dimensions:

$$V[\phi] = \int d^d x \; \left[\partial_i \phi_a \partial^i \phi^a + \mathcal{U}(\phi) \right] \equiv V_2[\phi] + U[\phi], \qquad (1.16)$$

$(i = 1 \ldots d)$, where $U[\phi]$ is an arbitrary potential (a positive definite functional which does not include derivatives of ϕ). $V[\phi]$ can be thought of defining a surface in the theory's configuration

space where extrema of this surface are solutions to the Euler-Lagrange equations derived from (1.16):

$$\partial_i \partial^i \phi_a = \frac{\partial \mathcal{U}}{\partial \phi^a}\,. \tag{1.17}$$

Let $\hat{\phi}$ be such a solution. For those theories whose configuration space $\mathcal{C}$ decomposes into disjoint subspaces $\mathcal{C}_N$ in the way described above, one has to think of $\hat{\phi}$ as being an extrema of $V[\phi]$ within a certain $\mathcal{C}_N$. In other words, $\hat{\phi}$ carries an index N. Now consider a generalization of $\hat{\phi}$ to a one-parameter family of fields with parameter λ, such that $\hat{\phi}_\lambda(\mathbf{x}) \equiv \hat{\phi}(\lambda \mathbf{x})$. Under this transformation one finds

$$V[\hat{\phi}_\lambda] = \lambda^{2-d} V_2[\hat{\phi}] + \lambda^{-d} U[\hat{\phi}]\,. \tag{1.18}$$

$V[\hat{\phi}]$ is now a function of λ and for solutions to (1.17) it takes an extremum with respect to λ, which is by assumption realised for $\lambda = 1$. This implies:

$$\left. \frac{\partial V[\phi]}{\partial \lambda} \right|_{\lambda=1} = 0$$
$$= (2-d) V_2[\hat{\phi}] - d U[\hat{\phi}]\,. \tag{1.19}$$

Because $V_2[\phi]$ and $U[\phi]$ are both positive definite functionals, it depends on the space-dimension d whether the equation above can be satisfied. This leads to the following cases:

1. $d = 1$. One obtains immediately

$$V_2[\hat{\phi}] = U[\hat{\phi}]\,, \tag{1.20}$$

   which means that in one space-dimension the potential $U[\phi]$ is necessary for non-trivial solutions, because without its presence the field $\hat{\phi}$ had to be constant everywhere to yield $V_2[\hat{\phi}] = 0$.

2. $d = 2$. This case is particularly interesting form our viewpoint, because it includes the $O(3)\,\sigma$-model in (2+1) dimensions. Equation (1.19) gives

$$U[\hat{\phi}] = 0\,. \tag{1.21}$$

   In two dimensions $V_2[\phi]$ is conformally invariant which in particular implies that it is invariant under a scaling transformation $\mathbf{x} \to \lambda \mathbf{x}$. Therefore a change of λ is a zero-mode of the energy and the solution $\hat{\phi}$ does not correspond to a configuration of a definite size: the soliton is in

a neutrally stable state. If a potential U is added, the fields which are in one of the minima of U are energetically favoured (we call them ϕ_{vac}) and the minimum of the potential energy is where $\hat{\phi} = \phi_{\text{vac}}$ everywhere, unless some other conserved quantity like a topological charge prevents this. In this case, the configuration becomes singular. It is interesting to study the dynamical behaviour of solutions to $V_2[\phi]$. For the $O(3)\,\sigma$-model the evolution of its solutions have been studied numerically and analytically with the result that under perturbations the solitons shrink at a rate $\sim 1/t^2$ to a singular configuration [2] [19]. In order to allow stable, finite-sized solutions to the $O(3)\,\sigma$-model and various other theories, several modifications are possible; they will be mentioned below.

3. $d \geq 3$. Because $V_2[\phi]$ and $U[\phi]$ are positive definite, one reads off (1.19):

$$V_2[\hat{\phi}] = U[\hat{\phi}] = 0.$$ (1.22)

Therefore in $d \geq 3$ dimensions, the only solutions are the vacuum fields. This can be redeemed by the inclusion of higher derivative terms into $V[\phi]$, which scale as $(d-n)$, where n is the number of the derivatives. Especially interesting is the case $d = 3, n = 4$, because this is the modification of the σ-models that corresponds to the Skyrme-model. We will come back to this in chapter 4.

Modified $O(3)\,\sigma$-models

In this subsection we present some proposals to overcome the dilemma of unstable solutions by modifying sigma models. For definiteness we again refer to the $O(3)\,\sigma$-model, but the concepts laid out here are applicable to most $O(N)\,\sigma$- or $\mathbb{CP}^{N-1}$ models.

From the Hobart-Derrick theorem above it follows, that in $d = 2$ space-dimensions there are no stable static, non-singular solutions to the pure $O(3)\,\sigma$-model. The questions therefore is, whether there are modifications to this model which preserve Lorentz-invariance, but break the scale invariance of the Lagrangian (1.6), so that the configuration can be stable and lead to interesting dynamics. It seems, that there are at least three different ways of resolving the problem, each of which is worth studying in its own right.

- One can adapt the idea of Skyrme, who used that in $d = 3$ a quadratic and a quartic term in the field-gradient have opposite scaling behaviour, see point 3) above. In $d = 2$ dimensions, a

---

[2] By this we mean that the peak of the energy density $\sim 1/(t - t_c)^2$, where t_c is some critical blow-up time.

higher-order term in the field-gradient breaks the conformal invariance of the $O(3)\,\sigma$-model, but energetically favours small scales ($\lambda \to 0$ in the notation above), in other words the solution will spread out in space. To counter-balance this effect, a potential $U[\phi]$ can be added to the Lagrange function. Because one usually is interested in low-energy dynamics where the field-gradients are small on a relativistic scale, the next to leading order, which is positive definite, is a term $V_4[\phi] \sim (\partial_i \phi)^4$, by which we mean any combinations of four derivatives. The same energy considerations as above then result in a definite scale for the solution $\hat{\phi}$ and for minimal energy solutions one obtains the Virial-theorem:

$$V_4[\hat{\phi}] = U[\hat{\phi}]. \tag{1.23}$$

The choices for $V_4[\phi]$ and $U[\phi]$ are not unique *a priori*. With respect to $V_4[\phi]$, however, one usually wants to preserve the model's global $O(3)$-invariance. Also, in a relativistic extension of the theory, the kinetic energy T should not include terms higher than quadratic in its time-derivatives, in order to allow for a Hamiltonian interpretation of the equations of motion.

This excludes all fourth-order terms except $F_{\alpha\beta}F^{\alpha\beta} \equiv \sum_{\alpha\beta}(\partial_\alpha \phi \times \partial_\beta \phi \cdot \phi)^2$, which we will call Skyrme-term, in analogy to its (3+1)-dimensional counterpart. It is composed of a tensor $F_{\alpha\beta}$, the dual of which $B_\alpha = \varepsilon_{\alpha\beta\gamma}F_{\beta\gamma}/2$ is trivially conserved ($\partial_\alpha B^\alpha = 0$), due to the antisymmetry of F. The zero-component of B is the topological charge density $\mathcal{N}$, integrand of (1.10), with the geometrical interpretation given above. There is an interesting geometrical interpretation of the Skyrme energy functional due to Manton [16], which one can adapt to two dimensions and which we will give in chapter 5. In chapters 4 and 5 we investigate models in (3+0) and (2+1) dimensions respectively, which are modified by additional fourth-order terms. It is obvious that the addition of any positive definite term such as a potential or the Skyrme term will increase the potential energy and the Bogomol'nyi bound will not be saturated any longer.

- Unstable static solutions can possibly be stable dynamically. This would imply a fine balance between the forces that act on the soliton and favour its shrinkage and the forces of inertia such as a centrifugal force, that try to deform the solution in the opposite way. One can achieve this by including a potential term in the action (which favours a shrinking), and a time-dependent phase to the fields, which, however, leaves the energy density time-independent. This is very much in the spirit of Coleman's Q-balls in (3+1) dimensions, where

the stability of the solution is guaranteed by a global conserved charge and the rotation of the fields takes place in the corresponding symmetry direction.

- The model's scale invariance can in principle be broken by the introduction of a new field that is coupled to the $O(3)$-field. This can be a gauge field with the obvious physical motivation of coupling electrodynamics or non-Abelian gauge-dynamics to the model. Of course, the fact that the scale invariance is broken does not automatically imply the stability of the solution. However, usually the gauge field's dynamics is subject to some constraint such as Gauss' law which might imply stability. Alternatively, global quantities like the electric charge or flux can form a bound on the energy, thus also indicating stability. This is what we investigate in chapters 2 and 3. The Abelian Higgs model, to be described below, is an example of such a theory, although its solutions are not "textures".

Unfortunately, all these modifications suffer from an essential setback, namely that they usually destroy the integrability of the $O(3)\,\sigma$-model, although in some cases analytic static solutions to modified models are known. For almost none of the models discussed in this thesis even static solutions are analytically known. It is therefore necessary to approximate the solutions, especially if one is interested in time-dependent solutions. This can be done by an exclusively numerical procedure to solve the variational equations, which are given by a set of coupled PDE's. For radially or otherwise symmetrical solutions, the static system can often effectively be reduced to a lower-dimensional problem and sometimes to solving an ODE. For general time-dependent solutions, where no such reduction is possible, a popular method is to discretize the equations of motions on a spatial grid while the time-evolution is described by an ordinary differential equation for each gridpoint. It is interesting to ask, how the topological features of the model behave under this discretization. *A priori* there is no topology on a grid, by definition. Also, the choice of a lattice theory whose continuum limit is known, is not unique. However, it has been possible to construct theories on a grid which preserve the topological features of the $O(3)\,\sigma$-model and the $O(3)$ baby-Skyrme model, in particular the topological bound on the energy [20, 21].

As mentioned above, another method to approximate time-dependence is by employing a moduli space approximation for those models whose analytic solutions can be found. The time-evolution is then described by an initial value problem for ordinary differential equations in terms of the solutions parameter. This corresponds to a geodesic motion along a trajectory in the space of solutions with minimal potential energy.

1.3 The Abelian Higgs model

The Abelian Higgs model in (2+1) dimensions is a field theory which involves a complex scalar field and a $U(1)$-valued gauge field. It has soliton solutions called vortices which find an application in the theory of superconductors. These solutions can also be seen as orthogonal projections of their three-dimensional counterparts, the static solutions to the (3+1)-dimensional Abelian Higgs model, which are a simple model for a cosmic string. Although we are not presenting any research on the Abelian Higgs model in this thesis, it is a useful theory to introduce some fundamental concepts of which we will make much use in later chapters. These concepts are:

- The gauge principle. The theory is invariant under local $U(1)$-transformations of the fields. Due to Noether's theorem this implies a conserved (electric) charge.

- The spontaneous breakdown of a local symmetry and the Higgs mechanism. It is employed to generate massive gauge fields without destroying the model's gauge invariance.

- The Bogomol'nyi limit which yields self-dual equations, the solutions of which minimize the potential energy.

- The stability of configurations due to a topologically conserved quantity (the flux).

- The existence of multi-soliton solutions.

- A phase transition in the theory's parameter space, i.e. a transition between qualitatively different behaviour of the soliton solutions.

The purpose of this section is thus to set out these notions in more detail on a concrete example. The physical space $X = \mathbb{R}^{2+1}$, the Higgs field ϕ is a map $\phi : X \mapsto \mathbb{C}$ and the gauge field $A_\alpha \in U(1)$. As before, the space-time metric is of signature $(+, -, -)$. The relativistic version of the Abelian Higgs model is defined by the action:

$$S = T - V = \int d^2x\, dt\, \frac{1}{2}\overline{(D_\alpha \phi)}\, (D^\alpha \phi) - \frac{1}{4}F_{\alpha\beta}F^{\alpha\beta} - \frac{\lambda^2}{8}\left(|\phi|^2 - a^2\right)^2 , \qquad (1.24)$$

where the covariant derivative $D_\alpha \equiv \partial_\alpha + iA_\alpha$. The bar denotes complex conjugation. The electromagnetic coupling has been put to unity and the parameters a and λ are real. The field-strength $F_{\alpha\beta}$ is given by

$$F_{\alpha\beta} = -i\,[D_\alpha, D_\beta] = \partial_\alpha A_\beta - \partial_\beta A_\alpha . \qquad (1.25)$$

The magnetic field B corresponds to the only spatial component F_{12}. If the plane of motion is embedded into $\mathbb{R}^3$, B it can be thought of pointing perpendicular out of it. The Lagrangian $\mathcal{L}$, the integrand of (1.24), is invariant under

$$\begin{aligned}
\phi &\rightarrow e^{i\chi(\mathbf{x},t)}\phi, \\
A_\alpha &\rightarrow A_\alpha - \partial_\alpha\chi(\mathbf{x},t),
\end{aligned}$$

(1.26)

where $\chi(\mathbf{x},t)$ is a smooth, differentiable function, mapping $\mathbb{R}^{2+1} \mapsto \mathbb{R}$. Under these gauge transformations, the field-strength $F_{\alpha\beta}$ is unchanged and the covariant derivative

$$D_\alpha\left(e^{i\chi}\phi\right) = e^{i\chi}D_\alpha\left(\phi\right),$$

(1.27)

such that the $\mathcal{L}$ remains invariant. The gauge degree of freedom can be removed by fixing the gauge. A popular choice is the temporal gauge $A_0 = 0$, which does not, however, imply that the Euler-Lagrange equation for A_0 vanishes. This equation, called Gauss' law, has to be imposed as a constraint on the solutions:

$$\partial_i\partial_t A_i + \frac{1}{2}(\partial_t\phi\bar{\phi} - \partial_t\bar{\phi}\phi) = 0.$$

(1.28)

Note that Gauss' law is automatically satisfied for static fields $\partial_t A_i = \partial_t\phi = 0$.

For finite energy solutions the Higgs potential $\mathcal{U} \sim \left(|\phi|^2 - a^2\right)^2$ has to vanish at spatial infinity. Hence the Higgs field at infinity $\phi_\infty = ag$, where g is a pure phase, i.e. $g \in U(1)$. In the same limit, the covariant derivative $D_i\phi$ must approach zero. This implies for the gauge field A_i:

$$A_i(\mathbf{x}) \rightarrow ig^{-1}\partial_i g + \mathcal{O}\left(\frac{1}{r^2}\right), \quad \text{as} \quad |\mathbf{x}| \rightarrow \infty.$$

(1.29)

g maps $S^1_\theta \rightarrow S^1_g$ and can be represented as $\exp(i2\pi h(\theta))$, where θ is the angular coordinate on $\mathbb{R}^2$. Single valuedness of g requires $h(0) = h(2\pi) + n$, where $n \in \mathbb{Z}$. In other words, Φ_{vac}, the vacuum manifold of the theory is a circle of radius $|a|$ so that the Higgs field at infinity is homotopic to

$$\lim_{|\mathbf{x}|\rightarrow\infty} \phi \quad : \quad S^1_\theta \rightarrow S^1_g.$$

(1.30)

Such maps can be classified by the homotopy group $\pi_1(S^1) = \mathbb{Z}$. Thus the configuration space consists of disjoint sectors which are labeled by the winding number of the Higgs field at infinity.

Elements of the sector with winding number $n = 1$ are called vortices, those with $n = -1$ anti-vortices. The model is relativistic, hence vortices and anti-vortices are expected to show the same physical characteristics. More concretely, there is a (discrete) symmetry of $\mathcal{L}$, namely a reflection of the space-vector $\mathbf{x}$ on, say, the x_1-axis, which transforms vortices into anti-vortices and vice versa.

As mentioned earlier in this introduction, the vortices of the Abelian Higgs model are topologically of the same type as instantons ($d = 4$) or monopoles ($d = 3$). By this we mean that the topology of the theory is determined by fields which are maps from the boundary ∂X_t of the physical space X_t into the field-vacuum. For $SU(2)$ monopoles in $\mathbb{R}^{3+1}$ the boundary is a two-sphere S^2 which is mapped into the vacuum manifold of the Higgs-triplet. The Higgs vector lies on a two-sphere of radius v, where v is the equivalent of a above. Hence monopoles are classified by $\pi_2(S^2) = \mathbb{Z}$ where the integer is the monopole number. This is to be contrasted to the $O(N)$ σ-model, where the topology arises from the interior of the physical space.

Higgs mechanism

The Higgs mechanism is applied in gauge theories where the Lagrangian shows a symmetry which is broken in the ground state of the theory. The aim is to create massive gauge bosons without destroying the model's gauge symmetry. This interpretation in terms of particle physics is quantum mechanical in the sense that one talks about fluctuations around the classical ground state, but spontaneous symmetry breakdowns occur in many classical systems as well. In the model defined above, the Higgs field at infinity $\phi_\infty = ag$, such that there is a circle of energetically degenerate ground states. The explicit choice of the vacuum field breaks this symmetry spontaneously. This gives a mass to the Higgs field which is due to fluctuations orthogonal to the symmetry direction. Near the vacuum one approximates $\phi = a + \chi + i\xi$ which leads in the notation above to a mass $m_\chi = |\lambda||a|$. According to the Goldstone theorem, the spontaneous breakdown of a continuous symmetry also leads to a massless (zero-energy) mode, corresponding to fluctuations in the symmetry direction (described by ξ). However, this degree of freedom can be re-interpreted by performing a local gauge transformation. Such a transformation removes the massless mode from the particle spectrum and replaces it with what corresponds to the longitudinal direction of polarisation of the gauge field, thus giving the gauge field the correct (three) degrees of freedom. This procedure is called the Higgs mechanism.

Another implication, due to the broken gauge symmetry is that the magnetic flux Φ is quantized

and the winding number obtains a direct physical interpretation, namely the number of flux-quanta the solution carries. The only non-zero component of A_i at infinity is $A_\theta = dh/rd\theta$, which leads to:

$$\Phi_n = \int d^2x\, B = \oint_{S^1} d\mathbf{l} \cdot A = 2\pi \oint_0^{2\pi} d\theta\, h'(\theta) = 2\pi n \quad \Rightarrow \quad n = \frac{\Phi_n}{2\pi}, \qquad (1.31)$$

where we used (1.29). Note that the flux-quantisation here is a purely classical process. Also note that by continuity the Higgs field must vanish somewhere on the plane of motion.

Bogomol'ny bound

Similar to the $O(3)\,\sigma$-model, it is possible to establish an algebraic relation between the static energy of the fields and the topological degree. The self-dual limit is $\lambda = 1$, such that

$$V[\phi, A_i] = \frac{1}{2} \int d^2x \left[\overline{(D_1\phi \pm iD_2\phi)}\,(D_1\phi \pm iD_2\phi) + \left(B \pm \frac{1}{2}\left(|\phi|^2 - a^2\right) \right)^2 \right] + \frac{a^2}{2}\Phi_n + \text{bound. terms}.$$
$$(1.32)$$

The boundary terms vanish for the boundary conditions which were imposed above on ϕ and A_i. Since the integrand is clearly positive definite and the magnetic flux Φ_n is fixed by (1.31) for a given topological sector of the configuration space, it follows that V is minimized if the square brackets vanish. This is the case if and only if

$$D_1\phi = \mp iD_2\phi, \qquad B = \mp\frac{1}{2}\left(|\phi|^2 - a^2\right)^2. \qquad (1.33)$$

The solutions to these equations, being minima of $V[\phi, A_i]$, also satisfy the second-order Euler-Lagrange equations derived from (1.24). Moreover, it has been shown by Taubes [22] that *all* solutions of the static Euler-Lagrange equations are also solutions of (1.33).

From (1.32) we immediately read off a lower bound on the potential energy

$$V_n \geq \frac{a^2}{2}|\Phi_n|. \qquad (1.34)$$

with the equality holding only for solutions of the Bogomol'nyi equations. Note that the Bogomol'nyi equations correspond to the point $\lambda = 1$ in parameter space. It has been shown numerically that vortices repel each other for $\lambda > 1$ while they mutually attract for $\lambda < 1$. At the point of self-duality $\lambda = 1$ the vortices are free. In terms of the potential energy V it can be shown, that $V_n(\lambda) > nV_1(1)$ for $\lambda > 1$ and $V_n(\lambda) > \lambda^2 V_n(1)$ for $\lambda < 1$ [23]. Both these inequalities are strict [24].

The absence of any potential between static solutions is a typical feature of self-dual solutions which is also present for $SU(2)$-monopoles in the BPS-limit and can be understood quantum mechanically [25]. Due to the Higgs mechanism, both the gauge field A_α and the scalar ϕ are massive fields. At the self-dual point $\lambda = 1$, the attractive forces of the scalar field balance the repulsive force of the gauge field. Therefore the vortices are force-free, the space of minimal energy solutions, the moduli space, has no potential. In other words, for $\lambda = 1$ the energy has zero-modes which stem from the translational degrees of freedom, because energetically it is irrelevant where the vortices are positioned relative to each other.

It has been established, that the zeros of the Higgs field are the only zero-modes of the solution and thus they are natural coordinates on the moduli space. The potential energy of a vortex peakes around these zeros which makes them an obvious choice to describe the vortex' position. Taubes proved that for every n-tuple of positions $\{x_1, x_2, \ldots, x_n\}$, $x_i \in \mathbb{R}^2$, $i = 1, \ldots, n$ there is a solution to (1.33) where $\phi(x_i)$ are the zeros of ϕ on the plane [3]. The moduli space is thus $2n$-dimensional. In the case where two or more of the x_i coincide, the zeros of the Higgs have to be counted with multiplicity, the physical picture being that the vortices sit on top of each other. Let m be the multiplicity of a zero at x_j, then by encircling the point x_j on an arbitrarily small circle, the Higgs field will acquire a phase of $2\pi m$. Strictly speaking, the notion of a "position" of a vortex is only well-defined for sufficiently separated vortices which do not overlap. However, the Higgs field is massive and therefore falls off exponentially from the zero of the Higgs, such that the interpretation of separated vortices as independent "particles" is incorrect only by an exponential factor. Note that the exponential decay also implies a size for the vortex, which is a measure for the rapidity of the fall-off. This is to be contrasted to the $O(3)$ σ-model, the underlying difference being that (1.32) is not scale invariant.

It has not been possible to find analytic solutions to the Bogomol'nyi equations (1.33), in contrast to its (3+1)-dimensional counterpart, Yang-Mills-Higgs theory, where monopole solutions can be constructed. Therefore the actual vortex solutions have to be obtained numerically. For radially symmetric solutions, the following ansatz in polar coordinates (r, θ) is used

$$\phi = g f(r), \quad A_\theta = n b(r), \qquad A_r = 0. \qquad (1.35)$$

This leads to the boundary conditions $b(0) = f(0) = 0$ and $b(\infty) = 1, f(\infty) = a$.

---

[3]This choice of coordinates leads to conical singularities in the moduli space. See [26] how this problem can be resolved.

Interestingly, if the model is put on a hyperbolic space, the equations of motion are equivalent to the Liouville equation whose solutions are well known [27].

As indicated earlier, the applications of planar vortices are mainly due to non-relativistic theories in condensed matter physics, more precisely superconductivity. The potential energy V (1.32) is formally equivalent to the free energy of a Ginzburg-Landau theory. The Higgs field is there interpreted as a microscopic order-parameter and the two phases $\lambda < 1$ and $\lambda > 1$ correspond to type-I and type-II superconductivity respectively. This shows why the dynamics of vortices is important in their applications. In the self-dual limit numerical results have been obtained in a geodesic approximation by Samols [28], who found an approximation for the metric on the moduli space, and by Speight [23]. The scattering of vortices in a perturbation theory near the self-dual limit was studied by Shah [29]. There the moduli space has a potential and the true ground state of the energy is given by configurations that coalesce or, on a compact space, form a lattice, depending on the phase their are in. Another interesting results that has been obtained is that no mixed vortex-antivortex solutions exist. Dynamically, a vortex-antivortex pair annihilates, unless they have a non-zero relative angular momentum, in which case they can form a bound state by rotating around each other.

The rest of this thesis is laid out as follows. In chapter 2 we investigate a gauged $O(3)$ σ-model where the behaviour of the gauge field is determined by a Chern-Simons term. We find the static solutions to the model which carry a non-vanishing angular momentum. The potential in this model is chosen such that the solitons can be thought of being coupled to a constant external magnetic field. In chapter 3 we investigate a similar model which has self-dual solutions. In this case, the Bogomol'nyi bound is given by a linear combination of the topological $O(3)$ σ-bound and the local $U(1)$-charge. We discuss radially symmetric solutions which we computed numerically. Chapter 4 is concerned with an $O(3)$ σ-model in three space-dimensions. Such a model can have topological stable solitons because the third homotopy group of S^2 is isomorphic to the group of integers and this integer provides a lower bound on the static energy. We find minimal energy solutions numerically for topological charge one and two and discuss their shapes and energies. We also approximate the angular momentum of a slowly rotating soliton. In chapter 5 we study a generalisation of the $\mathbb{CP}^1$ model, the $\mathbb{CP}^2$ baby Skyrme-model. We find a family of analytic solutions for the one-soliton and study the two-soliton configuration using a gradient flow equation on the moduli space. The thesis ends with a short chapter presenting further conclusions and outlining some open questions.

Chapter 2

Topological Chern-Simons Solitons in the $O(3)\,\sigma$-model

2.1 Introduction

In (2+1)-dimensional space-time there is an alternative way to the Maxwell term of introducing dynamics to a gauge theory. This alternative expression is the Chern-Simons (CS-) term, which is a topological term that is not invariant under under discrete symmetry operations like parity and time reflection. For an Abelian gauge field $A_\alpha \in U(1)$, the CS-Lagrangian is given by

$$\mathcal{L}_{\text{CS}}^{\text{A}} = \frac{\kappa}{2}\varepsilon^{\alpha\beta\gamma}A_\alpha\partial_\beta A_\gamma\,, \tag{2.1}$$

while for a non-Abelian A_α^a which takes values in the algebra of a Lie-group G

$$\mathcal{L}_{\text{CS}}^{\text{NA}} = \frac{\kappa}{2}\varepsilon^{\alpha\beta\gamma}A^a{}_\alpha\partial_\beta A_\gamma^a + \frac{\kappa}{3}f_{abc}\varepsilon^{\alpha\beta\gamma}A_\alpha^a A_\beta^b A_\gamma^c\,, \tag{2.2}$$

(a is the group index), where f_{abc} are the structure constants of G and summation over repeated indices is assumed, as usual. Pure CS-theories are examples of topological field theories which means that they do not depend on the local properties of the underlying space-time metric. Let this metric be $g_{\alpha\beta}$, then the invariant volume element carries a factor $\sim \sqrt{|\det g|}$ while the antisymmetric tensor $\varepsilon_{\alpha\beta\gamma}$ transforms as $\sqrt{|\det g|}^{-1}$, hence both factors cancel in the action and consequently CS-actions depend only on global properties.

Chern-Simons terms were originally introduced in Differential Geometry to describe the topology of vector-bundles. A well-known example relevant to physics is the instanton number of four-

dimensional Yang-Mills theory, which is given by the second Chern-number [12]. The connection to the three-dimensional CS-term is made by writing the topological charge-density of the instanton number as a total divergence of a Euclidean four-current. The zero-component (or rather, fourth component) of this current is equivalent to the CS-term.

As an aside we remark that non-Abelian CS-theories are used to describe invariants of knots [30], (2+1)-dimensional gravity [31] and integrable models [32].

We will concentrate on the Abelian version and henceforth drop the indices (NA/A) that distinguish it from the non-Abelian theory. The Abelian CS-*action* is invariant under small gauge transformations while the Lagrange density is not. Under $A_\alpha \to A_\alpha + \partial_\alpha \chi$, $\chi = \chi(\mathbf{x}, t)$ being a real, non-singular, differentiable function on $\mathbb{R}^{2+1}$, $\mathcal{L}_{\text{cs}}$ transforms as

$$\mathcal{L}_{\text{cs}} \to \mathcal{L}_{\text{cs}} + \varepsilon^{\alpha\beta\gamma} \partial_\alpha (\chi \partial_\beta A_\gamma). \tag{2.3}$$

The term created by the gauge transformation is a surface term and vanishes for a small gauge transformation, i.e. if the function χ goes smoothly to a constant at infinity.

From the general field-theoretical point of view it is interesting to observe, that a CS-term in combination with a Maxwell term gives rise to a massive gauge theory [33]. In detail, consider the Lagrangian

$$\mathcal{L} = -\frac{1}{4e^2} F_{\alpha\beta}^2 + \frac{\kappa}{4} \varepsilon^{\alpha\beta\gamma} A_\alpha \partial_\beta A_\gamma. \tag{2.4}$$

Its Euler-Lagrange equations are given by

$$-\frac{1}{e^2} \partial_\alpha F^{\alpha\beta} + \kappa \varepsilon^{\alpha\beta\gamma} F_{\alpha\gamma} = 0. \tag{2.5}$$

where the field-strength is defined in the usual way $F_{\alpha\beta} = \partial_\alpha A_\beta - \partial_\beta A_\alpha$. Using this and defining the dual field-strength $F^\alpha = \varepsilon^{\alpha\beta\gamma} F_{\beta\gamma}/2$, one can easily see that $\partial_\alpha F^\alpha = 0$, which is the Bianchi-identity. If one inserts the dual field-strength into (2.5) and employs $\partial_\alpha F^\alpha = 0$, after taking a derivative ∂_α,

$$-\frac{1}{e^2} \partial_\alpha \partial^\alpha F^\gamma + \kappa \partial_\alpha F^{\alpha\gamma} = 0 \tag{2.6}$$

is obtained. If the equation of motion (2.5) is substituted for the second term and the definition of the dual field-strength is inserted, one finds

$$\left(\partial_\alpha \partial^\alpha + e^4 \kappa^2 \right) F^\gamma = 0. \tag{2.7}$$

This is the massive Klein-Gordon equation for the dual field F^γ, describing a boson of rest-mass $e^2\kappa$. In the limit of $\kappa \to 0$ (vanishing CS-term) one is, of course, left with the usual wave equation of electrodynamics.

However, most of the recent interest in theories which include CS-terms originates in their ability to create fractional statistics (that is quantum statistics that is neither fermi nor bose). To explain this in more detail, consider a theory with a conserved current j_α (that can be Noether or topological), coupled to a CS-gauge field A_α,

$$\mathcal{L} = -A_\alpha j^\alpha + \frac{\kappa}{2} \varepsilon^{\alpha\beta\gamma} A_\alpha \partial_\beta A_\gamma , \tag{2.8}$$

from which the following equations of motion are derived

$$-j^\alpha = \kappa \varepsilon^{\alpha\beta\gamma} \partial_\beta A_\gamma . \tag{2.9}$$

After fixing the gauge one can solve this relation for A_γ in terms of j^α. This shows that A_γ is just a convenient abbreviation to describe a self-interaction of the current j^α. In other words, the CS-term does not introduce independent dynamics for the gauge field A^γ, it really defines a constraint. If in (2.9) the $\alpha = 0$ component of j^α is integrated over d^2x, one obtains an important relation between the conserved charge associated with j_0, denoted Q_j and the flux Φ_{cs} that stems from the CS-gauge field:

$$Q_j = -\kappa \Phi_{\text{cs}} . \tag{2.10}$$

This is the CS-version of Gauss' law. Because of this relation particles in a theory (2.8) are sometimes called charge-flux composites. In a quantum mechanical description, the term $A_\alpha j^\alpha$ generates an Aharonov-Bohm phase on the wave function of a particle which winds around a flux-tube of strength Φ_{cs}. This phase is proportional to the CS-coupling which is not quantized or otherwise restricted [1] and therefore can generate an arbitrary phase, labeled by the flux which is encircled. The particles which are subject to such a non-standard phase are called anyons (see [34] for a review of fractional statistics and its physical implications).

To introduce the notion of fractional statistics from a geometrical point of view, consider the trajectory of two identical particles winding around each other. In space-dimensions $d \geq 3$ the winding angle (by which we mean the number of interchanges counted in multiples of π) is defined

---

[1]This is true only for Abelian CS-theories. In the non-Abelian (quantum mechanical) version κ has to be quantized to make $\exp(iS_{\text{cs}})$ gauge invariant.

mod 2π and thus allowing only for fermi or bose statistics. In two dimensions, however, this angle can be summed up as the particles continue to move around each other. By defining a map of this angle to the interval $[0, 2\pi]$ one obtains wave-functions with *any* phase, hence the term anyons.

Now consider a set of two identical, point-like particles on $\mathbb{R}^{2+1}$, described by the centre of mass vector $\mathbf{R}$ with respect to the origin and their relative position $\mathbf{r}$. The statistics of the two particles is entirely described by the time evolution of $\mathbf{r}$, which can take values on all of $\mathbb{R}^2$ except $\mathbf{r} = \mathbf{0}$, to consistently allow for phases other than zero. The two identical particles cannot be distinguished and therefore one also has to identify their permutation, $\mathbb{Z}_2$. Hence the two-particle configuration space $\mathcal{C}_2$ is

$$\mathcal{C}_2 = \frac{\mathbb{R}^2 - \{\mathbf{0}\}}{\mathbb{Z}_2} \,. \tag{2.11}$$

This space is multiple-connected, since

$$\pi_1(\mathcal{C}_2) = \mathbb{Z} \,, \tag{2.12}$$

which means that there are sets of trajectories (consisting of two particle trajectories), which have the same initial and final positions in space-time but are not homotopic to each other and thus they cannot be smoothly transformed into one another, see Fig. 2.1. One can think of these trajectories as being knots embedded in a three-dimensional space-time. In the path-integral formulation a different weight is given to every homotopically different path in the configuration space and this weight is the anyonic phase.
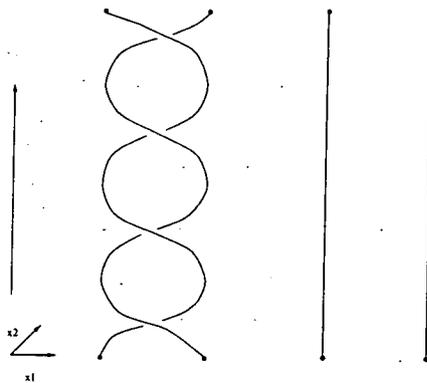

fig. 2.1: Two topologically distinct trajectories in $\mathbb{R}^{2+1}$. In $\mathbb{R}^{3+1}$, similar paths could be deformed into each other.

For an n-particle configuration, it is straightforward to generalize (2.11). Let $\{0_i\}$ denote the set of positions where any i particles coincide (and thus their relative vectors are identically zero)

and P_n is the group of all permutations of the n-particle set. Then $C_n = (\mathbb{R}^{2n} - \sum_i \{0_i\})/P_n$ and $\pi_1(C_n)$ is given by the braid group B_n. Consequently, the statistics of the configuration is in the n-particle case described by the (one-dimensional) representations of B_n, which is a generalization of the permutation group P_n whose representations describe fermi/bose statistics in $d \geq 3$.

One of the most important physical applications of particles with fractional statistics is the Fractional Quantum Hall Effect (FQHE). It occurs in special semiconducting devices which are exposed to high magnetic fields and low temperatures. At a heterojunction between two layers the sample is effectively reduced to a two-dimensional system of electrons. Theoretically, the FQHE can be described as a hierarchy of quasiparticles, where the quasiparticles are local density fluctuations in an otherwise homogeneous band-structure of electrons. A universal parameter to label the FQHE is the filling fraction and the quasiparticles carry charges proportional to it. By describing an adiabatical motion in a closed loop the quasiparticle obtain a Berry-phase on their wave-function. This phase is proportional to the quasiparticles' charge or, due to (2.10), to its flux and thus fractional.

Here we investigate a CS-theory which is based on the gauged non-linear $O(3)$ σ-model. The interest in gauged sigma models goes back to early work by Faddeev [35]. His idea was revived later for the description of charged baryons in the Skyrme model [36]. It was first proposed by Dzyaloshinskii et.al. to use a CS-action in order to stabilise solitons in a Heisenberg antiferromagnet [37]. The greater computational power that became available during recent years lead to a reexamination of gauged sigma models and their soliton solutions. Much work has been done on this since the original proposals, especially on the $O(3)\sigma/\mathbb{C}P^1$-model, starting with the work by Nardelli and later Aitchinson et. al. [38, 39]. This lead to a stream of papers, many of which are concerned with self-dual models in (2+0) and (1+1) dimensions. These self-dual models play a very important role on general physical grounds and will be discussed in the next chapter.

In this chapter we consider a static classical CS-model, whose potential term preserves the gauge symmetry and is chosen to produce exponentially localized configurations. They carry fractional angular momentum and have a lower topological bound on the energy which is, however, not saturated. We solve the equations of motion numerically for radially symmetric fields and study the dependence of the solutions on the coupling strength to the gauge field. We also look at two solitons on top of each other and on their mutual attraction dependent on their coupling. The asymptotic behaviour of the fields is studied analytically and conclusions about intersoliton forces are drawn.

Recently, static solitons were found in a gauged $\mathbb{CP}^1$-model which includes a CS-term and a potential term equivalent to the one considered here [40]. In its ungauged version the $\mathbb{CP}^1$-model represents merely a different choice of fields to the $O(3)$ σ-model. In [40], however, the gauged symmetry is the internal $U(1)$ symmetry of the two-component complex $\mathbb{CP}^1$ vector which lies on S^3. Therefore we expect our solutions to be different to the ones presented in [40], but it is nevertheless instructive to compare them.

2.2 The Chern-Simons $O(3)$ σ-model

We consider the following Lagrangian of a gauged $O(3)$ σ-model, defined on $X = \mathbb{R}^{2+1}$. It contains a potential term and the behaviour of the Abelian gauge field A_α is governed by a CS-term

$$\mathcal{L} = \frac{1}{2}\left(D_\alpha\phi\right)^2 - \frac{\kappa}{2}\varepsilon^{\alpha\beta\gamma}\partial_\alpha A_\beta A_\gamma - \mu^2(1 - \mathbf{n}\cdot\phi)\,. \tag{2.13}$$

The fields ϕ are three-component real vectors and subject to the constraint $\phi\cdot\phi = 1$, hence they take values on the two-sphere S^2_ϕ. We have suppressed the Lagrangian multiplier in (2.13) and the metric is flat, as before, and of signature $\mathrm{diag}(+,-,-)$. We chose units in which the velocity of light $c = 1$. κ and μ are real coefficients of dimension length and 1/length respectively and for dimensional reasons the Lagrange density should be thought of as being multiplied by an overall factor of dimension energy. We fix our mass scale by putting this factor to one. We borrow from the notation of nuclear physics and refer frequently to S^2_ϕ as iso-space and to ϕ as matter fields (in distinction to the gauge fields). The potential term in (2.13) reduces the symmetry of the model to $O(2)_{\mathrm{iso}}$, i.e. to rotations and reflections perpendicular to the vector $\mathbf{n}$. It is this symmetry that is to be gauged and by choosing $\mathbf{n} = (0,0,1)$ we select the $SO(2)_{\mathrm{iso}}$ subgroup which consists of unimodular rotations about the z-axis. Its generator Λ can be written as

$$\Lambda = \begin{pmatrix} 0 & -1 & 0 \\ 1 & 0 & 0 \\ 0 & 0 & 0 \end{pmatrix}\,. \tag{2.14}$$

Note that $\Lambda\phi = \mathbf{n}\times\phi$. Consider a real, non-singular, differentiable function $\chi(\mathbf{x},t)$ on $\mathbb{R}^{2+1}$. The gauge transformation under which the quadratic and the potential term are invariant, are

$$\phi \rightarrow e^{-\chi\Lambda}\phi\,,$$

$$A_\alpha \rightarrow A_\alpha + \partial_\alpha\chi\,. \tag{2.15}$$

$D_\alpha\phi$ is the covariant derivative and given by:

$$D_\alpha\phi = \partial_\alpha\phi + A_\alpha(\mathbf{n}\times\phi)\,, \qquad (2.16)$$

such that $D_\alpha\left(e^{-\chi\Lambda}\phi\right) = e^{-\chi\Lambda}D_\alpha\phi$, as required. The ungauged Lagrangian shows symmetry under combined reflections in space and iso-space:

$$P: \quad (x_1, x_2) \to (-x_1, x_2) \qquad \text{and} \qquad C: \quad (\phi_1, \phi_2) \to (-\phi_1, \phi_2)\,, \qquad (2.17)$$

which can be thought of as a parity operation and charge conjugation. The CS-term breaks the parity symmetry explicitly by changing its sign under P. It also breaks the time-reflection symmetry which corresponds to $A_0(t) \to A_0(-t)$ and $\mathbf{A}(t) \to -\mathbf{A}(-t)$. However, the Lagrangian is still symmetric under CPT.

The potential term can be thought of physically as an analogue to a Zeeman term which couples the spin fields ϕ to an external, constant magnetic field of strength μ^2 in $\mathbf{n}$-direction. Such terms can occur in the description of the Quantum Hall Effect.

Finite energy requires that the potential term and the covariant derivative vanish at spatial infinity. Hence we impose:

$$\lim_{|\mathbf{x}|\to\infty} \phi(\mathbf{x}) = \mathbf{n}\,. \qquad (2.18)$$

This boundary condition allows to one-point compactify $\mathbb{R}^2$ such that fields ϕ are effectively maps:

$$\phi \quad : \quad S_x^2 \to S_\phi^2\,. \qquad (2.19)$$

As mentioned above, these maps are elements of homotopy classes which form a group isomorphic to the group of integers. This integer can be written as the integral over the zero-component of a topologically conserved current

$$l_\alpha = \frac{1}{8\pi}\varepsilon_{\alpha\beta\gamma}\phi\cdot(\partial^\beta\phi\times\partial^\gamma\phi)\,, \qquad (2.20)$$

such that the degree N is obtained from

$$N = \int d^2x\, l_0\,, \qquad (2.21)$$

where the range of integration is $\mathbb{R}^2$, see formula (1.10). The current (2.20) is the topological current of the fields in the ungauged $O(3)\,\sigma$-model and obviously not gauge invariant. We will therefore address this question in detail below.

The equations of motion derived from (2.13) can be written in terms of the matter current J_α and the electromagnetic current j_α

$$\mathbf{J}_\alpha = D_\alpha \phi \times \phi, \qquad j_\alpha = \mathbf{n} \cdot \mathbf{J}_\alpha. \tag{2.22}$$

The Euler-Lagrange equations are

$$D_\alpha \mathbf{J}^\alpha = \mu^2 (\mathbf{n} \times \phi), \tag{2.23}$$

$$j_\alpha = -\kappa \varepsilon_{\alpha\beta\gamma} \partial^\beta A^\gamma. \tag{2.24}$$

Note that by equation (2.24) the gauge fields are completely determined by first-order equations which illustrates our earlier remark that they do not have own dynamics in the strict sense. Equation (2.24) for $\alpha = 0$ is Gauss' law

$$D_0 \phi \cdot (\mathbf{n} \times \phi) = \kappa B, \tag{2.25}$$

where we have used $B = \varepsilon_{0ij}\partial^i A^j$, taking $\varepsilon_{012} = 1$. Note that, since $-1 \leq \mathbf{n} \cdot \phi \leq 1$ it follows that $|A_0| \geq |\kappa B|$ for static fields. The equation of motion (2.24) implies for non-singular A_α that the electromagnetic current j_α is conserved ($\partial_\alpha j^\alpha = 0$). It can be written conveniently as $j_\alpha = (\rho, \mathbf{j})$, where ρ is the charge density of the soliton while $\mathbf{j}$ denotes its electric current. By inserting (2.22), the Lagrangian (2.13) can be expressed in terms of j_α:

$$\mathcal{L} = \frac{1}{2}(\partial_\alpha \phi \cdot \partial^\alpha \phi) - \frac{1}{2}A_\alpha j^\alpha - \frac{1}{2}A_\alpha A^\alpha (1 - (\mathbf{n} \cdot \phi)^2) - \mu^2 (1 - \mathbf{n} \cdot \phi). \tag{2.26}$$

This shows explicitly that the gauge fields A_α are coupled to the electromagnetic current j^α which is to be contrasted to the gauged Chern-Simons system considered by Wilczek and Zee [41], where an $U(1)$ gauge field was coupled to the topological current.

The electric field $\mathbf{E}$ and the magnetic field B are related to j_α as follows:

$$B = -\frac{\rho}{\kappa} \quad , \quad E_i = \varepsilon_{ij} \frac{j^j}{\kappa}. \tag{2.27}$$

The first equation leads to the relation (2.10) between the magnetic flux Φ and the electric charge Q of the configuration

$$\Phi = \int d^2x\, B = -\frac{1}{\kappa} \int d^2x\, \rho = -\frac{Q}{\kappa}. \tag{2.28}$$

The theory's energy-momentum tensor is obtained by the variation of the Lagrangian with respect to the space-time metric $\eta_{\alpha\beta}$

$$T_{\alpha\beta} = (D_\alpha\phi)\cdot(D_\beta\phi) - \eta_{\alpha\beta}\left(\frac{1}{2}(D_\gamma\phi)\cdot(D^\gamma\phi) - \mu^2(1 - \mathbf{n}\cdot\phi)\right). \tag{2.29}$$

The integral over the component T_{00} is the sum of kinetic and potential energy of the soliton:

$$E_{\text{cs}}[\phi, A] = \int d^2x\, \frac{1}{2}(D_0\phi)^2 + \frac{1}{2}(D_i\phi)^2 + \mu^2(1 - \mathbf{n}\cdot\phi). \tag{2.30}$$

Note that the Chern-Simons term does not contribute directly to the energy because of its metric independence. The rotational symmetry of the Lagrangian leads to a conserved angular momentum M of the soliton

$$\text{M} = \int d^2x\, (\mathbf{x} \wedge \mathbf{p}), \tag{2.31}$$

where the wedge-product stands for $x_1 p_2 - p_1 x_2$. If the plane of motion is embedded into $\mathbb{R}^3$ one can think of M as a vector pointing perpendicular out of it. The components of the momentum density $\mathbf{p}$ are given by

$$p_i = T_{0i} = D_0\phi \cdot D_i\phi. \tag{2.32}$$

Due to the gauge field the momentum is non-vanishing even for static fields and so is the angular momentum.

2.3 Bogomol'nyi Bound in the Gauged Model

Next we give a proof that E_{cs}, the energy of the configurations, is bounded from below by a topologically conserved quantity. This is not obvious, because the gauged pure $O(3)$ σ-model does not have a lower bound on the energy, unlike its ungauged counterpart where the solutions saturate the Bogomol'nyi limit. In our argument we adapt a proof by Schroers for the Maxwell-gauged self-dual $O(3)$ σ-model [42]. Because we wish this section to be self-contained, we repeat below parts of the analysis given in this reference. We employ an auxiliary energy functional $E_{\text{aux}}[\phi, A]$ which is of Bogomol'nyi type. First, we show that the energy gap between E_{cs} and E_{aux} is positive and then complete the argument by demonstrating that $E_{\text{aux}} \geq 4\pi|N|$.

E_{aux} reads as:

$$E_{\text{aux}}[\phi, A] = \frac{1}{2} \int d^2x \, B^2 + (D_i\phi)^2 + (1 - \mathbf{n} \cdot \phi)^2 \,. \tag{2.33}$$

In order to be consistent in the notation of dimensions, both the potential term and the magnetic field must be thought of as being multiplied by a parameter of dimension 1/length squared and length respectively. For the above model to be self-dual, these couplings are algebraically related and can consistently be put to one.

To relate E_{CS} to E_{aux}, one first observes that for E_{CS}, $A_0^2 \geq \kappa^2 B^2$, due to Gauss' law (2.25). Now we carry out a rescaling of $\mathbf{x}$ in E_{CS}, namely $\mathbf{x} \to \kappa\mathbf{x}$, which transforms $B \to B/\kappa^2$ and $\phi(\mathbf{x}) \to \phi(\kappa\mathbf{x})$. The potential term then transforms into $\kappa^2\mu^2(1 - \mathbf{n} \cdot \phi)$ and is greater than $(1 - \mathbf{n} \cdot \phi)$ if $\kappa \geq 1/\mu$. Let us consider this case first, while we deal with $\kappa < 1/\mu$ below. To verify that E_{aux} is smaller than E_{CS} we use that since $0 \leq (1 - \mathbf{n} \cdot \phi) \leq 2$, it follows that $(1 - \mathbf{n} \cdot \phi) \geq \frac{1}{2}(1 - \mathbf{n} \cdot \phi)^2$ and one sees that for E_{aux} holds

$$E_{\text{CS}} \geq E_{\text{aux}} \quad \text{if} \quad \kappa \geq 1/\mu \,. \tag{2.34}$$

In the case $\kappa < 1/\mu$ we assess an energy bound by multiplication of each individual term in the energy density with $\kappa^2\mu^2$. This gives

$$E_{\text{CS}} \geq \kappa^2\mu^2 E_{\text{aux}} \quad \text{if} \quad \kappa < 1/\mu \,. \tag{2.35}$$

This already proves the bound for E_{CS}, but it is instructive to see in detail that the functional E_{aux} defines a Bogomol'nyi model. To demonstrate this, we rewrite E_{aux} as

$$E_{\text{aux}}[B, \phi] = \frac{1}{2} \int d^2x \, (D_1\phi \pm \phi \times D_2\phi)^2 + (B \mp (1 - \mathbf{n} \cdot \phi))^2 \pm \int d^2x \, L_0 \,. \tag{2.36}$$

L_0 is composite of the cross-terms and can be interpreted as the zero-component of the solitons gauge invariant, conserved topological current:

$$L_\alpha = \frac{1}{2}\varepsilon_{\alpha\beta\gamma}\left(\phi \cdot (D^\beta\phi \times D^\gamma\phi) + \partial^\beta A^\gamma(1 - \mathbf{n} \cdot \phi)\right) \,. \tag{2.37}$$

Up to a surface term, this current is equivalent to l_α, the topological current of the ungauged $O(3)\,\sigma$-model (2.20). If the solutions are required to have finite energy, then ϕ must tend to zero faster than $1/r$ as r goes to infinity, hence it follows by Stokes' theorem that the corresponding

surface term integrates to zero. In order to saturate the Bogomol'nyi bound, both squares in (2.36) have to vanish, such that the following two (anti-) self-dual equations are read off

$$D_1 \phi = \mp \phi \times D_2 \phi \,, \qquad B = \pm(1 - \mathbf{n} \cdot \phi) \,. \tag{2.38}$$

These equations were discussed in [42] for a special choice of the fields in the context of a Maxwell-baby Skyrme model. There it was shown that they yield a one-parameter family of solutions which are degenerate in their energy but differ in their magnetic flux.

By using the sign ambiguity in front of the integral over L_0 in (2.36), we can restrict our discussion to the case $B > 0$ and the upper sign without a loss of generality. Equation (2.36) then implies

$$E_{\text{aux}} \geq \int d^2x \, L_0 = 4\pi |N| \,. \tag{2.39}$$

The equality holds for self-dual solutions.

2.4 Static Fields of Radial Symmetry

To find soliton solutions in our model we exploit the symmetries of (2.30) with the aim to reduce the two-dimensional static problem to a one-dimensional system, which is governed by ordinary differential equations.

According to the "principle of symmetric criticality", sometimes also called "Coleman-Palais" theorem, given a functional with a certain (global) symmetry, solutions of that symmetry can be found by variation of the functional of fields invariant under this symmetry. These solutions will also be stationary points of the energy functional of "non-restricted" (i.e. non-invariant) fields [43]. In abstract terms this corresponds to finding equivariant fields, that is maps which satisfy

$$\phi(\mathbf{x}) = R\phi(g^{-1}\mathbf{x}) \,, \tag{2.40}$$

where $g \in G$, the group under which the functional is invariant and R is an operator in a certain representation of G.

The energy functional (2.30) is symmetric under global $O(2)$-rotations in space and iso-space separately, however, fields of such a symmetry are necessarily of degree zero. The maximal compact symmetry group with non-vanishing degree for the fields ϕ is given by

$$G = \text{diag}\left[O(2)_x \otimes O(2)_\phi\right] \,. \tag{2.41}$$

Fields of that symmetry which are invariant under combined rotation in space and iso-space are called hedgehog fields, in analogy to the diag$[O(3) \otimes O(3)]$ invariant Polyakov-'t Hooft ansatz for $SU(2)$-monopoles. Hedgehog configurations are also used in the Skyrme-model in (3+1) dimensions [44, 45, 46], where they are the appropriate ansatz for the solution of topological charge one.

In (2+1) dimensions, symmetry under G implies that one of the two angles which parametrize the target S^2_ϕ is identified with θ, the polar angle on $\mathbb{R}^2$ (up to a multiplicative constant). Due to our choice of the gauged x_1/x_2-plane, we can write

$$\phi(r,\theta) = \begin{pmatrix} \sin f(r) \cos n\theta \\ \sin f(r) \sin n\theta \\ \cos f(r) \end{pmatrix}. \tag{2.42}$$

For this field, the topological charge density, the integrand of (2.21), equals

$$l_0 = \frac{n}{4\pi r} f' \sin f. \tag{2.43}$$

By integration one easily sees that $n = -N$. We will refer to finite energy solutions of degree one simply as CS-solitons. Note that the Lagrangian (2.13) is invariant under $n \to -n$ hence solitons and anti-solitons will exhibit the same physical features, as expected in a relativistic model. We therefore do not strictly distinguish between them and adopt a somewhat sloppy notation.

The next step is to find a suitable ansatz for the gauge field A_α. We use the most general ansatz which can lead to radially symmetric and static electromagnetic fields:

$$A_0 = nv(r), \quad A_\theta = na(r), \quad A_r = h(r)t, \tag{2.44}$$

where t denotes the time and the factor n is introduced for convenience. We fix our gauge by putting $A_r = 0$ and obtain the equations

$$f'' + \frac{f'}{r} = n^2 \left(\frac{(a+1)^2}{r^2} - v^2 \right) \sin f \cos f + \mu^2 \sin f, \tag{2.45}$$

$$v' = -\frac{1}{\kappa} \frac{(a+1)}{r} \sin^2 f. \tag{2.46}$$

Gauss' law (2.25) reads in terms of a and v:

$$a' = -\frac{1}{\kappa} r v \sin^2 f \,. \tag{2.47}$$

Finite energy requires that $D_\alpha(\phi) \to 0$ as $r \to \infty$. To guarantee this and the regularity of the fields at the origin, we impose the following boundary conditions

$$a(0) = 0 \,, \quad f(0) = \pi \,, \quad v(0) = v_0 \,,$$

$$\lim_{r \to \infty} f(r) = 0 \,, \quad \lim_{r \to \infty} a(r) = a_\infty \,, \quad \lim_{r \to \infty} v(r) = v_\infty \,, \tag{2.48}$$

where v_0, v_∞ and a_∞ are constants. With these boundary conditions it is clear that constant fields a and v are not a solution of (2.46) and (2.47), which can be shown by contradiction. If a were a constant it would have to be zero everywhere in which case (2.46) implies that v is not a constant which in turn, via (2.47) leads to a non–constant a. A similar argument applies for the case of v being constant. Hence the equations of motion will not lead to vanishing flux and charge.

The energy E_{cs} is given as the integral over the energy density e, which reads in terms of the fields f, a and v (2.30)

$$e = \frac{f'^2}{2} + \frac{n^2}{2} \left(\frac{(a+1)^2}{r^2} + v^2 \right) \sin^2 f + \mu^2 (1 - \cos f) \,. \tag{2.49}$$

For the angular momentum (2.31) we obtain

$$M = -\pi \kappa N a_\infty (a_\infty + 2N) \,. \tag{2.50}$$

Hence we see that the angular momentum of the soliton is fractional (because it depends on κ and a_∞) and in that sense the solitons are anyons. The electromagnetic fields (2.27) are radially symmetric by construction and in terms of the gauge field can be written as

$$B = N \frac{a'}{r} \,, \qquad E_r = N v' \,. \tag{2.51}$$

The electric charge and magnetic flux are not topologically quantized (unlike in the Abelian Higgs model, for instance) and depend on the model's parameters.

$$\Phi = N \int r dr d\theta \, \frac{a'}{r} = -2\pi N a_\infty = -\frac{Q}{\kappa} \,. \tag{2.52}$$

2.5   Asymptotic Behaviour of the Fields

The boundary conditions (2.48) allow to derive asymptotic solutions to the equations of motion
(2.45). By approximating $\sin f \approx f$ and $\cos f \approx 1$ for large r, the equation for $f(r)$ simplifies to

$$f'' + \frac{f'}{r} = n^2 \left(\frac{(a_\infty + 1)^2}{r^2} + k^2 \right) f \,, \tag{2.53}$$

where

$$k^2 = \mu^2 - n^2 v_\infty^2 \,. \tag{2.54}$$

The asymptotic values of f depend on the value k takes. There are three possible cases.

1.) $|\mu| > |n v_\infty|$, k real.

The solutions to (2.53) for real k are given by modified Bessel functions $f(r) \sim K_m(kr)$,
$m = n(a_\infty + 1)$, with the asymptotic behaviour

$$f \sim \frac{1}{\sqrt{r}} e^{-kr} \,. \tag{2.55}$$

This shows that k can be interpreted as the effective mass of the matter fields ϕ, being a measure
of the inverse decay-length of the profile function.

The asymptotics of the field are determined by the potential term which defines the theory's vacuum
structure. Therefore it is not a surprise that the soliton's matter field looks asymptotically like the
baby Skyrmion investigated in [47], where the same potential term was used.

2.) $\mu < |n v_\infty|$, k imaginary.

This case leads to oscillating fields with an amplitude that falls off proportional to $1/\sqrt{r}$ in leading
order. The substitution $\tilde{k} = ik$ in (2.55) verifies this instantly and shows that k is proportional to
the inverse wavelength of the oscillations. The energy density of these solutions is asymptotically
proportional to $1/r$ in leading order and hence the energy of these solitons is infinite. This, of
course, is not a physically relevant solution so that we impose the following constraint on the
solutions:

$$|\mu| > |n v_\infty| \,. \tag{2.56}$$

$$3.)\ \mu = |nv_\infty|,\ k = 0.$$

The critical case involves a vanishing exponential such that the profile function $f \sim 1/r$. The energy of these solutions is also infinite, because the leading term in the energy density is proportional to $v_\infty^2 f^2$. Numerically we find that all these solutions occur but restrict our discussion to the case 1.), which has solutions of finite energy.

For the electric and the magnetic field we find in the asymptotic limit of large r, using expression (2.55)

$$E_r \sim \frac{1}{r} e^{-2kr}, \quad B \sim \frac{1}{r} e^{-2kr}. \tag{2.57}$$

This shows that the electromagnetic fields fall off much faster than the matter field f. Therefore the electromagnetic interactions are expected to be negligible in the context of long-range forces between the solitons. The electric field is a vector lying in the plane of motion while the magnetic field B is a pseudoscalar and can be thought of as pointing perpendicular out of the plane of motion (again, if it is thought of embedded into $\mathbb{R}^3$). The asymptotic behaviour of B is similar to the magnetic field of Skyrme-Maxwell solitons as discussed in [48], where it was argued that such a magnetic field resembles a magnetic dipole in two-dimensional electrodynamics.

For small r, the fields can be approximated by power series

$$f \approx \pi + cr^{|n|}, \quad v \approx v_0 + dr^{2|n|}, \quad a \approx gr^{2|n|+2}, \tag{2.58}$$

where c and v_0 are free parameters while d and g are given as functions of n, κ, c and v_0. Note that for finite energy solutions c and v_0 are not completely independent on each other. Finite energy solutions define a subset of solutions which satisfy specific boundary conditions (2.48) on the fields. These boundary conditions limit the parameter range not only separately for each field but also — as a result of the coupled equations of motion — mutually.

For the Skyrme-Maxwell solitons [48] it was found that the electromagnetic short-range interaction decreases the energy per soliton and leads, in particular, to stronger bound 2-soliton states. Here, having a non-zero electrical charge distribution we expect this effect to be weakened by the inner repulsion of the soliton's electric field.

Interestingly, the asymptotic behaviour of the fields (2.58) implies that both the electric and the magnetic field vanish at the origin. For the energy density e not to be divergent at the origin, B and $\mathbf{E}$ have to approach zero faster than $r^{|n|}$ for small r.

2.6 Numerical Methods

We solved the set of equations (2.45) numerically by using a shooting method and a relaxation method.

The shooting method is a systematic trial-and-error method for the numerical integration of boundary-value problems, in which the free parameters of the integration are adjusted until the required boundary conditions are met. To illustrate this procedure, consider a family of functions $g(r, \xi)$ which is to be integrated within the closed interval $[r_1, r_2]$ and depends on a parameter ξ. If, say, the boundary condition at r_2 is $g(r_2, \xi) = h$ and is to be met by the variation of the function g at r_1, one can start with an initial guess for the parameter's range at r_1. Denote this range $\Xi = \{\xi : \xi_{\min} \leq \xi \leq \xi_{\max}\}$; then Ξ corresponds to a range of values $g_2(\xi) \equiv g(r_2, \xi)$, $\xi \in \Xi$. Given that h is within the interval $[g_2(\xi_{\min}), g_2(\xi_{\max})]$, one can find the value $\hat{\xi}$ that corresponds to $h = g_2(\hat{\xi})$ by bisecting Ξ or by Newton's method until the required accuracy is achieved.

Here, however, we have two parameters to vary (c and v_0 in (2.58)) which are indirectly dependent on each other and therefore it is not obvious which method should be used to determine both simultaneously and with efficiency. To find a systematic approach, we took two large ranges for both c and v_0 and put a grid on the range of v_0. This grid typically consists of 200 points and to find c for each point we applied the shooting method described above. The boundary conditions on the fields were always met by a subset of points on the grid v_0. For this subset we obtained the energy E_{cs} (2.30) as a function of v_0 and used this information to place a finer grid around the global minimum of $E[v_0]$. This process was continued iteratively until the difference of v_0 for subsequent iterations was within the limit of the imposed precision (which was of order 10^{-5}). We obtained a quasi-periodical structure for E_{cs} dependent on v_0, showing many local minima, however the global minimum $E_{\min} \equiv E(v_0^{\min})$ was in all cases given by the local minimum closest to $v_0 = 0$ with $v_0^{\min} > 0$.

The relaxation method, on the other hand, works on basis of the diffusion equation. Here the fields are initially "guessed" and then undergo a dissipative time-evolution, determined by a linear first-order time-derivative. This ensures that the energy is decreasing during time-evolution. If the Euler-Lagrange equation (2.45) is written as $F(f, a, v) = 0$, then the dissipative equation is given by

$$-D \frac{df}{dt} = F(f, a, v), \qquad (2.59)$$

where D is a positive real coefficient which determines the rapidity with which the energy decreases. Similar expressions are used in the equations for a and v. Although the relaxation method is strictly

defined only for elliptic differential equations, we could employ it successfully here. The initial fields are chosen in such a way that their boundary conditions are satisfied and the boundary remains fixed as the fields "relax". We used this method to solve the coupled set of equations (2.45)-(2.47) on several grids containing between 700 and 2000 points. For the range of integration $r \in [0, r_{\text{max}}]$ we took $r_{\text{max}} = 10$ or $r_{\text{max}} = 15$, dependent on the shape of the soliton. For both the shooting method and the time evolution in the relaxation method we used a fourth-order Runge-Kutta integration routine. While the stepwidth for the shooting method was typically $dx = 0.01$, the gridspacing dx in the relaxation method is related to the time-step dt by $dx = dt^2/2$. We used several values between $dt = 10^{-3}$ and $dt = 10^{-5}$.

2.7 Numerical Results

In order to perform the numerical integration we had to fix the parameters in our model. Using geometric units in which the energy and length are of unit one, we are left with μ and κ to be fixed. However, the parameter space is in fact one-dimensional which can be verified by carrying out a rescaling $x \to \kappa x$, $B \to B/\kappa^2$. This leads to a redefinition of the coupling to the potential which is the only remaining parameter. Thus we can fix μ for all our computations without loss of generality. We choose $\mu = \sqrt{0.1}$, a value which allows to compare our numerical values with the ones obtained in the Skyrme-Maxwell model [48] and in the gauged $\mathbb{CP}^1$ model [40], where the same value had been used.

We looked at the dependence on κ of solutions of degree $N = 1$ and $N = 2$. This parameter determines the strength of the CS-term and is proportional to the square root of the inverse coupling to the gauge field, $A_\alpha \to A_\alpha/\sqrt{\kappa}$.

Fig. 2.2 shows the dependence of the static energy or mass on κ. Small κ, which corresponds to strong coupling, leads to lighter solitons for both the one-soliton and the two-soliton. For large κ the energy E_{CS} tends to a constant but remains relatively close the the Bogomol'nyi bound, staying below 1.1 (in units of $4\pi|N|$) for the one-soliton and the two-soliton. Thus our solitons are significantly lighter than gauged baby Skyrmions, which for weak coupling tend to $E_{\text{SM}} = 1.546$. The energy gap arises partly due to the Skyrme term which is not present here.

It is particularly interesting to look at the relative energy per soliton. The energy difference $\Delta E = E^2 - 2E^1$ can be interpreted as binding and excess energy of the 2-soliton for $\Delta E < 0$ and $\Delta E > 0$ respectively. In case $\Delta E < 0$ the solitons form bound states while for $\Delta E > 0$ we expect that solitons on top of each other are unstable under perturbations and experience a

repulsive force. From Fig. 2.2 it is clear that in our model both cases occur. For small κ the two-soliton is in an attractive regime as it is for large κ, however there is an intermediate region $\kappa_{cr}^l < \kappa < \kappa_{cr}^h$ for which the 2-soliton configuration is unstable (in the sense that its decay is energetically favourable). Numerically we find that $\kappa_{cr}^l = 0.632$ and $\kappa_{cr}^h = 2.215$.
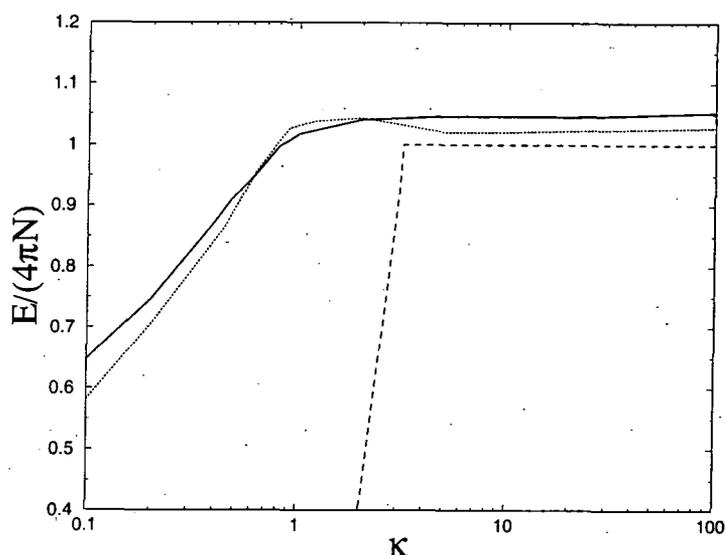

fig. 2.2: The energy E_{CS} (2.30) in units of $4\pi|N|$ as a function of the Chern-Simons coupling κ for $N = 1$ (solid line) and $N = 2$ (dotted line). The plot includes the Bogomol'nyi bound (dashed line).

In the limit of large κ the gauge fields decouple and become very small when compared with the matter fields. The study of ungauged solitons in a model which uses the same potential showed that pure matter forces are attractive for two solitons [47]. This is also the case here. For very small κ, however, the magnetic flux tends to a constant. Increased coupling (small κ) leads to a configuration which is stronger bound. The intermediate range is a regime in which a repulsion dominates the attractive forces of matter and magnetic field. It is within this range that the electric charge has its maximum value $Q_{max} = Q(\kappa_{max})$, where numerically $\kappa_{max} = 0.75$ (for $N = -1$) and $\kappa_{max} = 0.92$ ($N = -2$), see Fig. 2.3.
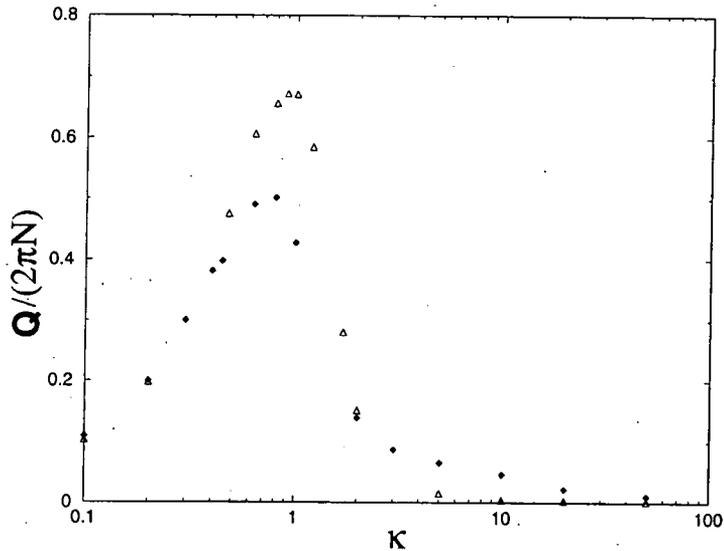
fig. 2.3: The electric charge Q (2.52) in units of $2\pi|N|$ as a function of the Chern-Simons coupling parameter κ for $N = 1$ (solid diamonds) and $N = 2$ (triangles up).

In showing such a behaviour, CS-solitons resemble the vortices of the Abelian Higgs model where a similar transition between repulsive and attractive regime occurs, depending on the strength of the potential term. The shape of our soliton solution shows a strong dependence on κ, which is foreseeable by the interpretation of κ as a coupling parameter to the gauge field. Increased magnetic flux, as it occurs for small κ, in the Skyrme-Maxwell model is known to cause more localized configurations [48]. On the other end of the scale, for large κ the electromagnetic interaction is only very weakly coupled. If the asymptotic value $\kappa = \infty$ is taken, the Lagrangian reduces to the $O(3)\sigma$-model term plus the potential term, such defining a configuration which is known to be unstable against shrinkage due to the Hobart-Derrick theorem [17, 18]. Actually taking the limit therefore leads to a different model.

Figs. 2.4-2.7 show the energy density, profile function and gauge field for several values of κ. In agreement with our expectations one sees that for large κ the soliton becomes more localized. This illustrates that the potential term in the Lagrangian favours a shrinkage of the soliton. For decreasing κ the soliton tends to spread out and reaches its maximum width at $\kappa \approx 1$. On the other hand, for smaller κ the soliton becomes more localized again. This can also be seen in Figs. 2.4-2.5.
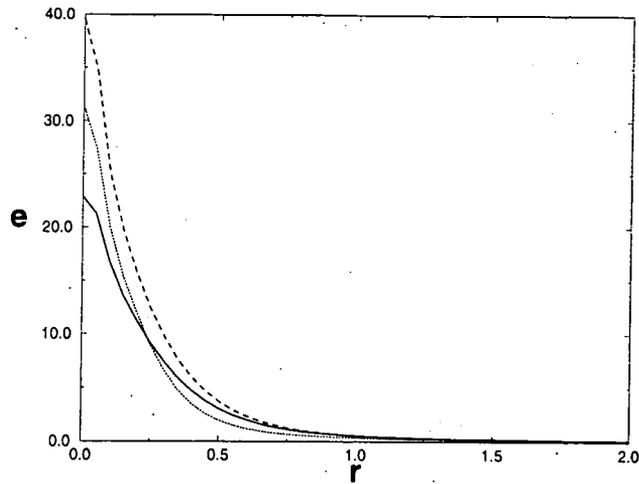
fig. 2.4: The energy density e (2.49) as a function of r for $N = -1$ and $\kappa = 0.3$ (long-dashed), $\kappa = 0.4$ (dotted) and $\kappa = \kappa_{\text{cr}}^{\text{l}} = 0.632$ (solid).

For very small κ, both the gauge fields a and v tend to functions that are singular at the origin, in particular, a tends to -1 everywhere except at $r = 0$, which is fixed by the boundary conditions. In that the behaviour of a is similar to the gauge field in the Skyrme-Maxwell model. We conjecture that the origin of this coincidence is the particular ansatz chosen for the gauge field, which leads to terms proportional to $(a + 1)^2$ in the energy density, thus making the value $a = -1$ exceptional. The limit of strong coupling therefore also leads to a dynamically quantised flux (2.52) and in addition implies via (2.52) that the electric charge vanishes for $\kappa \to 0$. From (2.58) it follows that the electric and the magnetic field form a ring, a feature usually seen for 2-solitons.
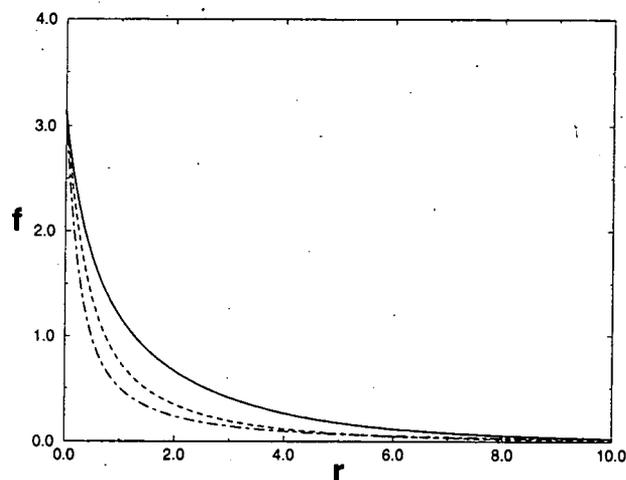

fig. 2.5: The profile function f as a function of r for $N = -1$ and $\kappa = \kappa_{\text{cr}}^{\text{l}} = 0.632$ (solid), $\kappa = 2$ (dashed), $\kappa = 0.4$ (dotted).

We also looked at the solitons for $N = -2$ and its dependence on κ. The 2-soliton has the shape of a ring, a familiar picture in many soliton theories in (2+1) and (3+1) dimensions. For the same given coupling, the fields of the 2-soliton decay slower than those of the 1-soliton, which can be understood from formula (2.54). Our numerical results show that v_∞ depends strongly on the coupling κ but weakly on the topological charge N so that the effective mass k is smaller for the 2-soliton and hence its exponential decay slower.

In Figs. 2.8-2.10 we show the energy density, profile function and electromagnetic fields of the one- and two-soliton. The coupling here is the lower critical coupling κ^l_{cr}.
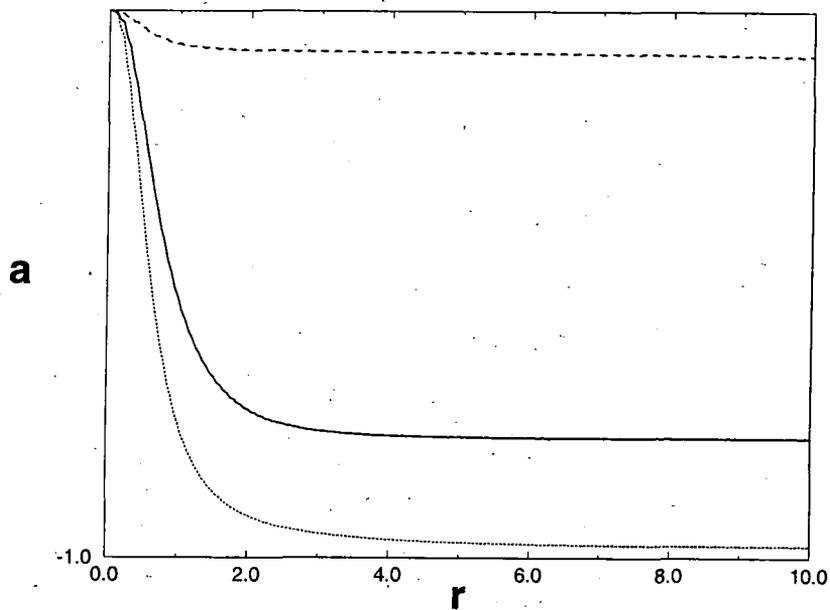

fig. 2.6: The gauge field a as a function of r for $N = -1$ and $\kappa = \kappa^l_{cr} = 0.632$ (solid),$\kappa = 2$ (dashed), $\kappa = 0.4$ (dotted).
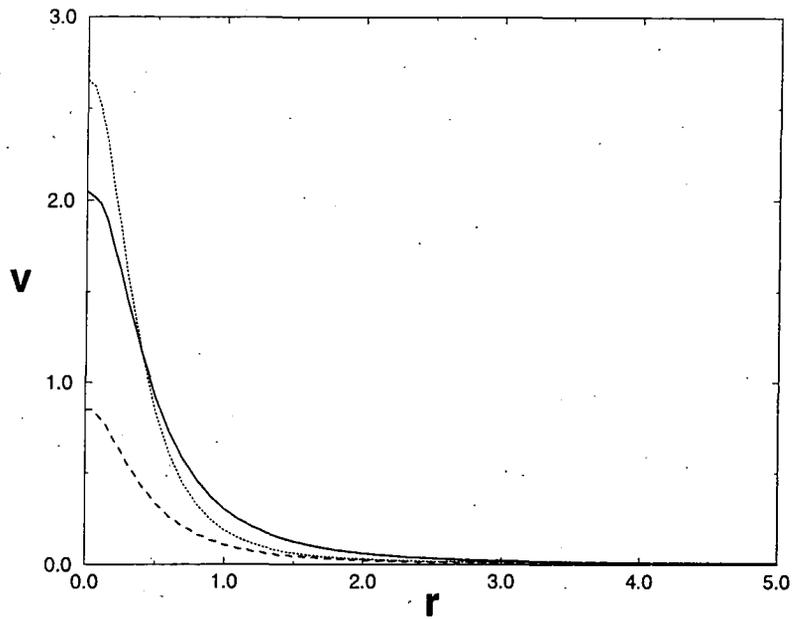
fig. 2.7: The gauge field v as a function of r for $N = -1$ and $\kappa = \kappa_{cr}^{1} = 0.632$ (solid), $\kappa = 2$ (dashed), $\kappa = 0.4$ (dotted).
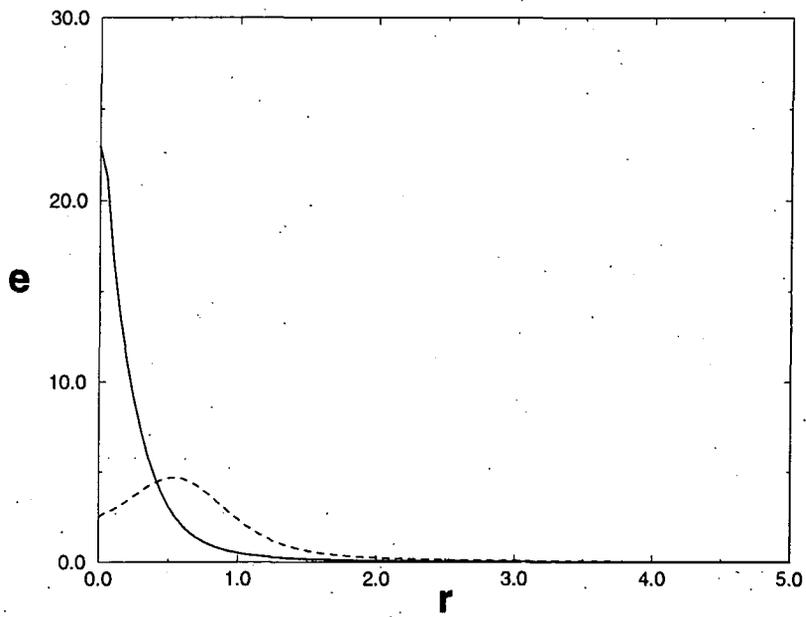

fig. 2.8: The energy density e (2.49) as a function of r for $\kappa = \kappa_{cr}^{1} = 0.632$, $N = -1$ (solid) and $N = -2$ (dashed).
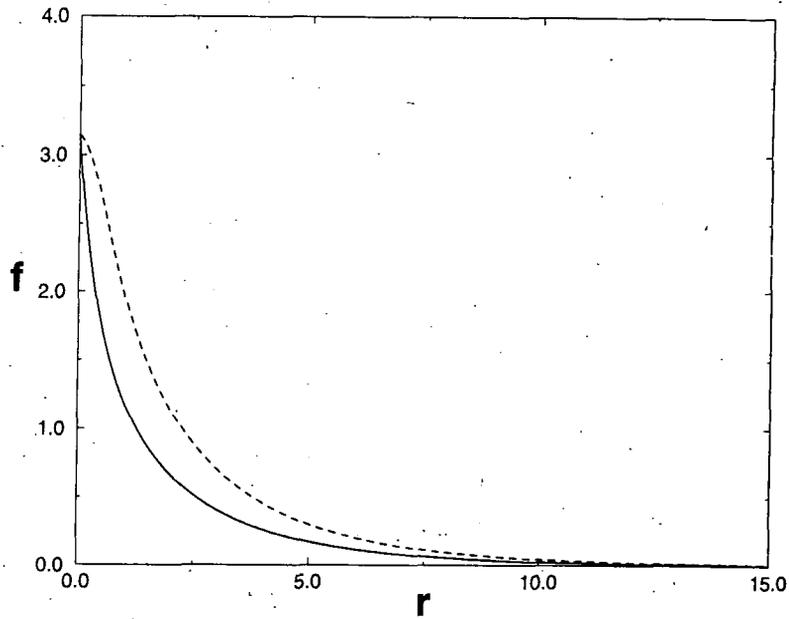
fig. 2.9: The profile function f as à function of r for $\kappa = \kappa_{\mathrm{cr}}^{\mathrm{l}} = 0.632$, $N = -1$ (solid) and $N = -2$ (dashed).
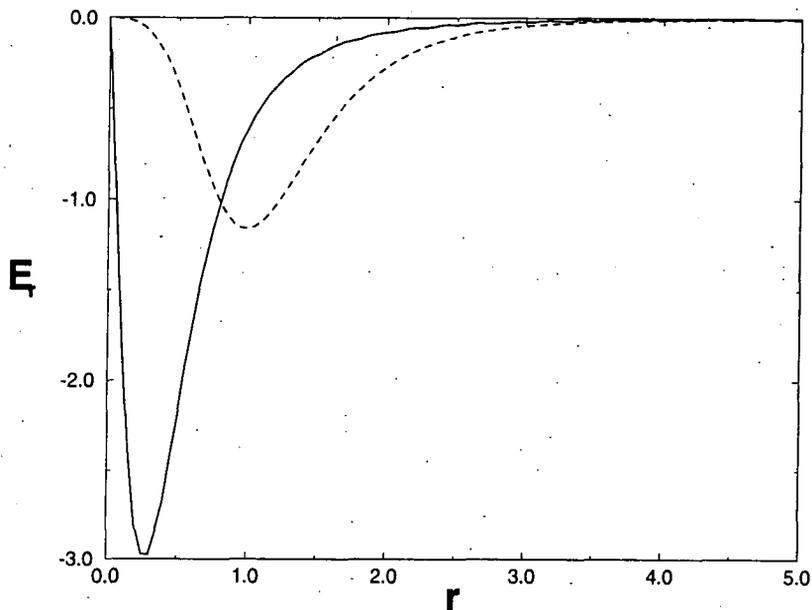
fig. 2.10: The radial component of the magnetic field $\mathbf{E_r}$ as a function of r for $\kappa = \kappa_{\mathrm{cr}}^{\mathrm{l}} = 0.632$, $N = -1$ (solid) and $N = -2$ (dashed).

2.8 Conclusions

We have studied classical static soliton solutions in an $O(3)\sigma$-Chern-Simons system with unbroken $U(1)$ gauge symmetry. The solitons have an electric charge which shows a unique maximum dependent on the coupling to the gauge field. The magnetic flux in the model is effectively quantised in the limit of strong coupling while the angular momentum of the solitons is fractional such that they can be seen as classical anyons.

In the case of two solitons sitting on top of each other, the model has a repulsive and two attractive phases, depending on the parameter which couples the gauge and matter fields. This has interesting consequences for interactions of multisolitons. In the repulsive regime they will presumably try to move away from each other and for a finite region this would lead to a configuration similar to an Abrikosov-lattice with solitons in equidistant and fixed positions. Such configurations occur in the description of type-II superconductors, although the theoretical description there is given in a non-relativistic model.

In the attractive regime, however, solitons which are not too widely separated from each other will be likely to coalesce. In this context it is worth investigating whether the solitons of higher winding number show a similar dependence on the coupling, in particular whether their critical couplings κ_{cr}^l and κ_{cr}^h are of the same value as they are here. The inter-soliton forces at large and medium distances will be dominated by the matter fields, because the electromagnetic fields decay faster by a factor of e^{-kr}. Thus, the interactions should be asymptotically well described by the dipole picture developed in [47]. A full numerical simulation of the time-dependent fields is not an easy task and one could therefore start with a study of truncated dynamics. As an example for such an investigation it would be interesting to look at rotating CS-solitons. Due to the hedgehog ansatz for the matter fields, a rotation in space is equivalent to a rotation in iso-space and thus it can be imposed by making θ a function of time. If one wants to take into account the back-reaction to the matter fields, $f(r)$ had to become time-dependent and would be deformed due to centrifugal forces. Such investigations would also be interesting in comparison to the ungauged spinning baby Skyrmions described in [49].

Chapter 3

Self-Dual Solitons in a Gauged $O(3)\,\sigma$-model

3.1 Introduction

The concept of self-duality is applied for the construction of a class of theories in which certain terms in the action and their couplings are not free but constrained by relations between each other. If these relations are satisfied — thus defining the self-dual fields — some positive valued functionals (usually the potential energy) take their minima. The equations of motion at the point of self-duality are reduced to first-order differential equations, which are more accessible to an analytic investigation and, in some cases, can be solved explicitly.

The notion of self-duality (sd) originates in Yang-Mills (YM-) field theory. Historically, Yang and Mills introduced the idea of making the global $SU(2)$ iso-spin symmetry of nuclear physics local. It has later turned out that in four-dimensional Euclidean space pure YM-theory possesses classical, finite-action solutions to the sd-equations. These solutions are called instantons. The YM-action, on its own, does not describe any known physical system, but apart from its conceptual value it is of course one of the fundamental building-blocks of the Standard Model. More interestingly, from our viewpoint, YM-theory shows various relations to other important models with topological soliton solutions. This is our main reason for describing it here in more detail (see also [50] for a review).

The model is defined on $X = \mathbb{R}^4$, the coordinates of which are (x_1, x_2, x_3, x_4). The $su(2)$ gauge field $A_i = \sum_a A_i^a \sigma_a/(2\mathrm{i}),\, (a = 1, 2, 3)$ is in its adjoint representation and the field-strength is given

by $F_{ij} = \partial_i A_j - \partial_j A_i + [A_i, A_j]$, (here $i, j = 1, 2, 3, 4$), while σ_a denotes the Pauli matrices. Taking the coupling-strength to unity, the YM-action can be written as

$$S_{\text{YM}} = -\int d^4x \ \text{Tr} \ \left(F_{ij} F^{ij}\right),$$

where the trace is taken over the group index. Now the Bogomol'nyi trick is applied and introducing the dual field-strength $\tilde{F}_{ij} = \varepsilon_{ijkl} F_{kl}/2$, the action is rewritten,

$$S_{\text{YM}} = -\frac{1}{2} \int d^4x \ \text{Tr} \ \left(F_{ij} \mp \tilde{F}_{ij}\right)^2 \mp \int d^4x \ \text{Tr} \ \left(F_{ij} \tilde{F}^{ij}\right). \tag{3.1}$$

To guarantee finite action, the gauge field A_i at the boundary of the physical space $\partial X = S^3_\infty$ has to be a pure gauge $A_i = U^{-1} \partial_i U$, where $U = U(\alpha) \in SU(2)$ depends on a set of coordinates $\alpha = (\alpha_1, \alpha_2, \alpha_3)$, which parametrise S^3_∞. Therefore $U : S^3_\infty \mapsto SU(2)$, which is topologically S^3 and hence U falls into a homotopy class that corresponds to $\pi_3(S^3) = \mathbb{Z}$. Consequently, the configuration space of the theory is composed of disjoint subsets labeled by their integer-valued index which counts the winding of the gauge field at infinity. This also illustrates our earlier claim that YM-instantons are topologically of the same type as vortices in the Abelian Higgs model.

We denote the degree, often called Pontrjagin index, by k. Its analytic expression is given by a multiple of the second integral in (3.1). Therefore (3.1) yields:

$$S_{\text{YM}} \geq c|k|,$$

where c is the normalization constant, $c = 8\pi^2$. Within each topological sector labelled by k, S_{YM} is absolutely minimized and the bound saturated at the points of self-duality

$$F_{ij} = \pm \tilde{F}_{ij}. \tag{3.2}$$

The solution to this equation of index $k = \pm 1$ is called the (anti-) instanton. Solutions to the sd-equation are known for all k and, being a minimum of the action, they also solve the Euler-Lagrange equations of motion $D_i F_{ij} = \partial_i F_{ij} + [A_i, F_{ij}] = 0$. The converse is in general not true, there can be saddle-point solutions to the equations of motion which are not self-dual.

As mentioned above, one reason for the interest in YM-theory stems from its manifold relations to various other theories, which are usually established by some form of dimensional reduction. Probably the most important of these is the connection to three-dimensional Yang-Mills-Higgs (YMH-) theory. In essence, if the four-dimensional YM-fields are made independent of, say, x_4 and A_4^a is identified with the Higgs field Φ^a in its adjoint representation, the theory is equivalent

to YMH-theory in three space-dimensions which has — in the limit of vanishing Higgs potential — self-dual soliton solutions known as BPS-monopoles.

The sdYM equations are also related to the notion of integrability in lower dimensions. In a space of signature $(+, +, -, -)$, the sdYM equations can be dimensionally reduced to $(1+1)$ or $(2+1)$ dimensions and reinterpreted as consistency conditions for systems of complex linear differential equations. These systems often resemble the Cauchy-Riemann equations and thus relate the problem to the theory of holomorphic functions. A prominent example where this method can be applied is the chiral model [51, 52].

Our third example relates the sdYM-theory to the model we discuss in this chapter, that is to self-dual Chern-Simons (sdCS-) theories. The $SU(2)$-sdYM equations, again reduced from $(2+2)$ dimensions, yield non-relativistic, non-Abelian sdCS equations in $(2+1)$ dimensions, see ref. [53]. The matter fields here are complex scalar fields ψ. Non-relativistic sdCS-theories are relevant in condensed matter physics, as indicated in chapter 2. Self-duality requires in this case a fourth-order Higgs potential $U(|\psi|)_{\text{NR}} \sim |\psi|^4$. The matter equation of motion is the non-linear Schrödinger equation and the sd-solutions are static solutions of the corresponding Euler-Lagrange equations. For an Abelian gauge field these solutions are of zero energy [54]. Interestingly, the sd-equations can be solved explicitly for an Abelian as well as for a non-Abelian gauge field [55]. In the Abelian case the equations can be combined to the Liouville equation, while in the more general non-Abelian case they become Toda field equations.

Relativistic sdCS-theories, on the other hand, do not have known analytic solutions. These theories include a sixth-order potential with degenerate symmetric/asymmetric vacua which allows for (non-) topological solitons as well as for (non-) topological vortices: $U(|\psi|)_{\text{R}} \sim |\psi|^2(|\nu|^2 - |\psi|^2)^2$ [56, 57, 58]. In the sd-limit the Higgs' mass equals the mass of the gauge field. Abelian and non-Abelian versions have been investigated and in both cases the Bogomol'nyi bound is given by a $U(1)$ charge. It would be interesting to know if non-Abelian models with more complicated bounds, like a linear combination of various charges or BPS-type bounds, can be constructed. To the best of our knowledge this has not been done yet. In the non-Abelian relativistic sdCS-model the Higgs- and gauge field spectra are rather rich and their masses can differ. However, for $su(N)$-valued gauge fields they are given as (integer or half-integer) multiples of the same fundamental mass scale $m = \nu^2/\kappa$, (κ being the CS-coupling). For completeness we also want to mention that these sd-models have been generalized to accommodate a Maxwell/Yang-Mills term, thus giving the gauge field some true dynamics. To make such a model self-dual, a

neutral scalar field has to be introduced [59].

It is an amusing observation that for all those models the self-dual bound, or a modification of it, provides a bound on the energy even if the couplings are perturbed. Take the energy functional $E[\phi, A_\alpha]_{\mathrm{SD}} = \sum_{i=1}^{n} \kappa_i^{\mathrm{SD}} E_i[\phi, A_\alpha]$ with positive definite $E_i[\phi, A_\alpha]$ and let the sd-couplings $\kappa_i^{\mathrm{SD}} > 0$ for all i. For solutions of the sd-equations, denoted $(\tilde{\phi}, \tilde{A}_\alpha)$, it holds in the N-soliton sector that $E_{\mathrm{SD}}[\tilde{\phi}, \tilde{A}_\alpha] = c_N > 0$, where c_N is a constant. Now use coupling constants which are different from the sd-limit: $\kappa_i^\pm = \kappa_i^{\mathrm{SD}}(1 \pm \mu_i/(1 + \mu_i))$, $\mu_i > 0$ for all i. Then one obtains for the energy $E_\kappa^\pm \equiv \sum_{i=1}^{n} \kappa_i^\pm E_i$:

$$
\begin{aligned}
E_\kappa^+ &= E_{\mathrm{SD}} + \sum_{i=1}^{n} \frac{\kappa_i^{\mathrm{SD}} \mu_i}{1 + \mu_i} E_i > c_N \,, \\
E_\kappa^- &= \sum_{i=1}^{n} \frac{\kappa_i^{\mathrm{SD}}}{1 + \mu_i} E_i \\
&= \left(\prod_{k=1}^{n} (1 + \mu_k) \right)^{-1} \sum_{i=1}^{n} \left\{ \kappa_i^{\mathrm{SD}} E_i \prod_{j \neq i} (1 + \mu_j) \right\} \\
&= E_{\mathrm{SD}} \left(\prod_{k=1}^{n} (1 + \mu_k) \right)^{-1} + \left(\prod_{k=1}^{n} (1 + \mu_k) \right)^{-1} \sum_{i=1}^{n} \left\{ \kappa_i^{\mathrm{SD}} E_i \left(\prod_{j \neq 1}^{n} (1 + \mu_j) - 1 \right) \right\} \\
&> c_N \left(\prod_{k=1}^{n} (1 + \mu_k) \right)^{-1} .
\end{aligned}
\tag{3.3}
$$

In both cases the bound is insaturable for non-trivial fields, because its saturation would imply that each E_i vanishes individually, which means that the fields are constant.

In this chapter we present a relativistic sdCS-theory which is based on the $O(3)$ σ-model [38]. It is similar to the relativistic scalar CS-Higgs- (CSH-) model discussed above in that it exhibits a symmetric and an asymmetric vacuum which are degenerate. The gauged $O(3)$ σ-model has a self-dual realization for Maxwell-dynamics, as shown by Schroers [42]. In this model the gauge symmetry remains unbroken, hence the flux is not quantized and the topological bound is entirely due to the topology of the matter fields. However, the gauged $O(3)$ σ-model exhibits two conserved charges: the topologically conserved degree of the matter field ϕ and the dynamically conserved Noether charge arising from local gauge symmetry. In this chapter we pursue the idea to find a self-dual model where the energy-bound is given by a linear combination of these two charges. For the construction of this theory we apply the Bogomol'nyi argument described above. In contrast to the Bogomol'nyi equations of the pure $O(3)$ σ-model, the self-dual equations in our model cannot be solved analytically. Nevertheless, because they are of first order, an analysis of them is more accessible than one of the second-order Euler-Lagrange equations.

The non-relativistic version of the theory discussed below is potentially interesting as a model for planar ferromagnets. In this context the field ϕ is interpreted as a spin vector and the Euler-Lagrange equations are the gauged Landau-Lifshitz equations. Such a model was investigated very recently in [60] where it was shown that it yields a variety of topological and non-topological soliton solutions. If a background charge is included, it turns out that for a specific value of this charge the soliton solutions are the same as those in the (non-relativistic) Abelian sdCS-theory, as discussed by Jackiw and Pi [61].

3.2 The Self-Dual Chern-Simons $O(3)\,\sigma$-model

Our model is defined by the following Lagrangian on (2+1)-dimensional Minkowski space of signature $(+,-,-)$:

$$\mathcal{L} = \frac{1}{2}\left(D_\alpha\phi\right)\left(D^\alpha\phi\right) \pm \frac{\kappa}{2}\epsilon^{\alpha\beta\gamma}A_\alpha\partial_\beta A_\gamma - \mathcal{U}(\mathbf{n}\cdot\phi)\,, \tag{3.4}$$

where we omit the Lagrangian multiplier. ϕ is the $O(3)\,\sigma$-model matter field introduced above and $A_\alpha \in U(1)$, $\mathbf{n} = (0,0,1)$. With respect to the covariant derivative and the indices, we use the same notation as in chapter 2. For the moment, we leave the sign of the Chern-Simons coupling κ arbitrary. Being interested in static sd-configurations, we consider the energy functional for time-independent fields, which can be written as

$$E_{\text{cs}}[A,\phi] = \int d^2x\,\frac{1}{2}\left(A_0^2(\mathbf{n}\times\phi)^2 + (D_1\phi)^2 + (D_2\phi)^2\right) + U[\phi]\,. \tag{3.5}$$

Gauss' law yields $A_0 \stackrel{\text{!}}{=} \mp\kappa B/(\mathbf{n}\times\phi)^2$, $B = \partial_1 A_2 - \partial_2 A_1$. Using this to to eliminate A_0 and chosing the potential $\mathcal{U}(\mathbf{n}\cdot\phi) = |\mathbf{n}\times\phi|^2(\nu - \mathbf{n}\cdot\phi)^2/(2\kappa^2)$, $\nu > 0$, we can rewrite the energy

$$E_{\text{cs}}[\phi,A] = \int d^2x\,\frac{1}{2}(D_1\phi \pm \phi\times D_2\phi)^2 + \frac{1}{2}\left(\frac{\kappa B}{|\mathbf{n}\times\phi|} \mp \frac{|\mathbf{n}\times\phi|(\nu - \mathbf{n}\cdot\phi)}{\kappa}\right)^2 \pm$$
$$\int d^2x\,(D_1\phi\cdot\phi\times D_2\phi + B(1 - \mathbf{n}\cdot\phi)) \pm (\nu - 1)\int d^2x\,B\,. \tag{3.6}$$

As shown in chapter 2, the second integral is proportional to deg$[\phi]$, the degree of the map $\phi: S^2 \mapsto S^2$. The third integral gives a multiple of the magnetic flux Φ, which is due to Gauss' law proportional to the electric charge and therefore conserved in time. The electric charge-density is here $\rho = A_0(\mathbf{n}\times\phi)^2$. The integrand of the first term in (3.6) clearly is positive definite, from which we derive the following bound on the energy:

$$E_{\text{cs}} \geq 4\pi|\deg[\phi]| + (\nu - 1)|\Phi|. \tag{3.7}$$

Here the sign ambiguities of κ and in the square brackets in (3.6) were removed by taking the magnitude of $\deg[\phi]$ and Φ. The energy bound (3.7) is a conserved quantity and therefore solutions which saturate it will have the same E_{cs} throughout their time-evolution [1].

Due to the choice of the potential $\mathcal{U}$, the model exhibits two or three degenerate vacua, depending on ν. In radial coordinates (r, θ):

$$
\begin{aligned}
&\text{a)} \quad \nu \geq 1, \quad \lim_{r \to \infty} \phi(r) = \pm\mathbf{n}, \\[2mm]
&\text{b)} \quad \nu < 1, \quad \lim_{r \to \infty} \phi(r) = \pm\mathbf{n} \quad \text{or} \quad \lim_{r \to \infty} \mathbf{n} \cdot \phi = \nu.
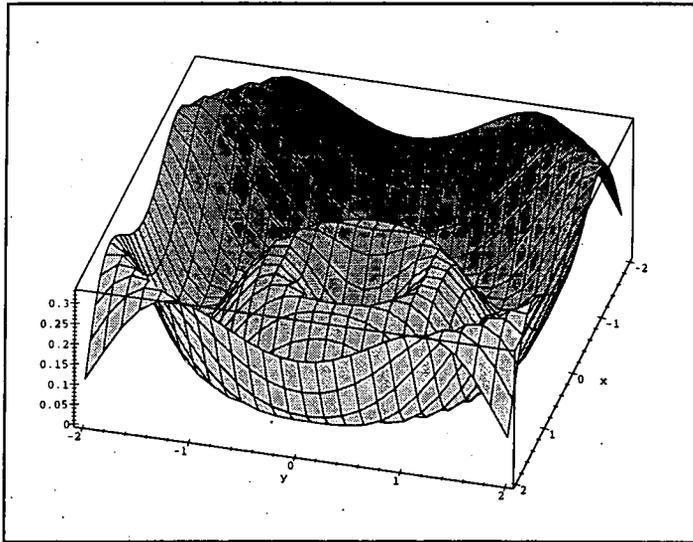\end{aligned}
\tag{3.8}
$$

fig. 3.1: Higgs potential $\mathcal{U} = \sin^2 r(\nu - \cos r)^2$, where $\phi_3 = \cos r$, $r = \sqrt{x^2 + y^2} \in [0, \pi]$. $\nu = 0.1$.

For $\nu = 1$ both cases coincide. We refer to the vacua $\phi = \pm\mathbf{n}$ as symmetric vacua and to $\mathbf{n} \cdot \phi = \nu$ as an asymmetric vacuum.

---

[1]Note that E_{cs} is not simply the potential energy because it includes contributions from the temporal part of the covariant derivative of ϕ.

a) Topology for $\nu \geq 1$

This case gives rise to soliton solutions with the degree of the map $N = \deg[\phi]$ being integer valued. The gauge symmetry remains unbroken and hence the flux is not quantized. If the degree $N \neq 0$, we speak of topological solitons. For $N = 0$ there is no topologically preserved quantity, the energy of the solutions is proportional to the flux which in turn is proportional to the θ-component of the gauge field at infinity. These are non-topological solitons.

b) Topology for $\nu < 1$

This case allows for any of the three vacua where the symmetric phase is analogue to case a). In the asymmetric phase the vacuum manifold of the field is a circle of radius $\sqrt{1 - \nu^2}$ in the plane $\phi_3 = \nu$, i.e. $\phi_\infty \equiv \lim_{r \to \infty} \phi = (\phi_\infty^1, \phi_\infty^2, \nu)$. The model's local $U(1)$-symmetry gets spontaneously broken by the choice of the vacuum $\phi_\infty^1, \phi_\infty^2$ and the magnetic flux is quantized. One can combine $\phi_\infty^1, \phi_\infty^2$ into a complex scalar field, $\varphi \equiv \phi_\infty^1 + i\phi_\infty^2$ and proceed in the discussion analogously to the Abelian Higgs model of section 1.3, such that $\varphi \to \nu \exp(iM\theta)$. The covariant derivative then becomes $D_i\varphi = \partial_i\varphi + iA_i\varphi$ and for it to vanish at infinity, the θ-component of the gauge field has to satisfy:

$$\lim_{r \to \infty} A_\theta(r, \theta) = i\frac{|\partial_\theta \varphi|}{|\varphi|} = -\frac{|\partial_\theta \phi|}{|\mathbf{n} \times \phi|} = -M \,. \tag{3.9}$$

Hence the boundary of the physical space (S_∞^1) gets mapped onto the circle $\phi_3 = \nu$ and such maps are classified by $\pi_1(S^1) = \mathbb{Z}$, giving them an integer degree M. We call solutions of degree $M > 0$ topological vortices. Note that the map ϕ is not surjective any longer and that one cannot one-point compactify $\mathbb{R}^2$ to S^2, because the fields at infinity are not constant. The notion of a degree $\pi_2(S^2)$ in the way we used it so far is therefore not applicable. However, formula (1.10) for N produces a value of $N < 1$ which can be visualised as the fraction of target S^2 that is covered by ϕ.

Hence there are two topological charges of relevance in our model: $\pi_2(S^2)$ for the symmetric vacuum and $\pi_1(S^1)$ for the asymmetric vacuum of case b). We will discuss solutions to cases a) and b) in detail below.

To find these solutions, we study the Bogomol'nyi equations of our model. The static energy functional (3.6) is minimized and the bound saturated if and only if the first integral vanishes. This leads to the following sd-equations:

$$D_1\phi = \mp\phi \times D_2\phi,$$

$$B = \pm\frac{|\mathbf{n} \times \phi|^2(\nu - \mathbf{n} \cdot \phi)}{\kappa^2}.$$

(3.10)

For further discussion it is helpful to rephrase these equations in terms of coordinates on the complex projective space $\mathbb{CP}^1$. The coordinates of $\mathbb{CP}^1$ are scalar fields depending on the coordinates of the plane of motion, for which the complex variables $x_+ = x_1 + ix_2$ and $x_- = x_1 - ix_2$ are introduced. Let W be such a complex field, related to ϕ through the stereographic projection from the south pole of S^2 onto the complex plane:

$$W = \frac{\phi_1 + i\phi_2}{1 + \phi_3}.$$

(3.11)

Then the Bogomol'nyi equations in terms of W are:

$$D_1 W = \mp i D_2 W, \qquad B = \frac{|W|(1 + 3|W|)}{(1 + |W|)^3},$$

(3.12)

where the covariant derivative is now $D_i W = \partial_i W + iA_i W$. After some algebraic manipulations these two equations can be rewritten as a second-order equation for W:

$$\partial_{x_+ x_-} W + \partial_{x_+} W \partial_{x_-} W = \frac{4|W|(1 + 3|W|)}{(1 + |W|)^3} W.$$

(3.13)

From this equation it is immediately clear that W cannot be a (anti-) holomorphic function. We did not succeed in solving this equation and to progress numerically we resort to an appropriate ansatz for the fields. The same symmetry considerations as discussed in the previous chapter apply for the matter fields and hence we make use of ansatz (2.42) again. We restrict ourselves further and use for the gauge field the rotationally symmetric ansatz $A_\theta = na(r)$. Then the sd-equations (3.10) become

$$f' = -n\frac{a+1}{r}\sin f,$$

$$a' = -\frac{r\sin^2 f}{n\kappa^2}(\nu - \cos f).$$

(3.14)

For the fields to be well-defined at the origin and for the energy to be finite, one has to impose the following boundary conditions, similar to (2.48):

$$a(0) = 0, \quad \lim_{r \to \infty} a(r) = a_\infty, \quad f(0) = m_1\pi, \quad \lim_{r \to \infty} f(r) = m_2\pi,$$

(3.15)

for the symmetric phase and

$$\lim_{r \to \infty} \cos f(r) = \nu \tag{3.16}$$

for the asymmetric phase. In the symmetric phase, fields ϕ which satisfy these boundary conditions are of degree $N = (\cos(m_1\pi) - \cos(m_2\pi))n/2$. For simplicity we restrict ourselves to $m_1 = 1, m_2 = 0$. In the asymmetric phase we find $\Phi = -2\pi M$ and $N = -(\nu + 1)n/2$.

The classical vacuum structure of the model is the starting point of any quantum mechanical approximation for the mass-spectra of the particles. We expand the potential for the fields close to the vacuum and obtain for the symmetric vacuum $\phi_\infty = \pm\mathbf{n}$ a mass of $m_\phi = |\nu - 1|/|\kappa|$ and a massless gauge boson. In the asymmetric phase the Higgs effect takes place. It gives a mass $(1 - \nu^2)/|\kappa|$ to the gauge field and to the Higgs particle (which corresponds to the ϕ_3-degree of freedom). The fact that the masses of the scalar and the vector particle are the same is not a coincidence. In the $M > 1$ sector of the configuration space the vortices do not exercise any mutual forces, because if they did, their static energy would not be constant (unless repulsive and attractive forces cancel each other in the potential energy, which is unlikely). However, having a magnetic field and non-linear matter fields, it is not obvious how this effect occurs. The standard interpretation for BPS-monopoles (where the Higgs and photon are massless in the sd-limit) is that in the Bogomol'nyi limit the attractive matter-forces are just compensated by the repulsive magnetic forces [25].

The solutions to our model also have a non-vanishing angular momentum. It is determined by the quadratic term in the action and the CS-term only and it does not depend on the potential. Therefore the angular momentum M in the sd-model is the same as in the non-sd-model of chapter 2, cf.(2.31) . In table 3.1 we summarize some of the features of the theory that were mentioned so far.

The energy-density (3.6) can be expressed in terms of our ansatz (3.14), which yields:

$$E[f, a] = \frac{1}{2} \int d^2x \left(f'^2 + \kappa^2 \frac{n^2 a'^2}{r^2 \sin^2 f} + \frac{n^2 (a + 1)^2 \sin^2 f}{r^2} + \frac{\sin^2 f(\nu - \cos f)^2}{\kappa^2} \right). \tag{3.17}$$

For the numerical treatment it is important to know the asymptotic behaviour of the fields for small r. We approximate the fields around the origin by a power series and obtain:

$$
\begin{aligned}
f &\approx \pi + \alpha r^{|n|}, \\
a &\approx \frac{(\nu + 1)\alpha^2}{2\kappa^2 |n|(|n| + 1)} r^{2(|n|+1)}.
\end{aligned}
\tag{3.18}
$$

From this expansion it is clear that the magnetic field $B = na'/r$ vanishes at the origin. Also note that the powers are the same as for the non-sd-model discussed in the previous chapter, eq.(2.58).

	$\nu \geq 1$	$\nu < 1$
ϕ_∞	$\pm\mathbf{n}$	$(\phi_\infty^1, \phi_\infty^2, \nu)$
Φ	$2\pi a_\infty n$	$-2\pi M$
M	$\pi\kappa n a_\infty(2n + a_\infty)$	$-\pi\kappa M(2M - 1)$
m_A	0	$(1 - \nu^2)/\kappa$
m_ϕ	$|\nu \pm 1|/\kappa$	$(1 - \nu^2)/\kappa$
N	$-n, 0$	$-(\nu + 1)n/2$

$$(3.19)$$

Tab. 3.1 Characteristics of solutions in the self-dual Chern-Simons $O(3)$ σ-model.

3.3 Topological Solitons in the Range $\nu > 1$

In the parameter range $\nu > 1$ there are two symmetric vacua, namely $\phi_\infty = \pm\mathbf{n}$. We concentrate on $\phi_\infty = \mathbf{n}$, which has for boundary condition (3.15) a non-vanishing topological charge $N = -n$. The self-dual equations (3.14) and the boundary conditions (3.15) constitute a well-defined problem, which can be discussed analytically. We prove, that there is a one-parameter family of solutions for all $\nu > 1, |N| > 1$ and $\nu = 1, |N| \geq 1$. The proof requires several steps, in some of which we follow Schroers [42].

a) limits on f

The profile function f is limited to the range $[\pi, 0)$. To prove this, we use in the vicinity of π: $\tilde{f} = f - \pi$. Then (3.14) can be simplified to

$$\frac{\tilde{f}'}{\tilde{f}} = \frac{|N|(a + 1)}{r}.$$

$$(3.20)$$

If integrated over dr this gives $\ln\tilde{f} = |N| \int dr\, (a + 1)/r$, the left hand side of which clearly diverges as $\tilde{f}$ approaches zero, while the right hand side remains finite (as long as the upper limit of

integration is finite). This means that if $f > \pi$ for any value of $r > 0$, then it will be larger than π for all r. But this excludes the possibility of meeting its boundary condition at infinity, hence $f \leq \pi$. If $\tilde{f}$ is replaced by f, the above argument also shows, that $f > 0$, for all r, hence

$$0 < f \leq \pi. \qquad (3.21)$$

b) limits on a

From (3.14) it follows, that $a' \leq 0$ for all r, hence a is a monotonically decreasing function. Moreover, using $0 \leq \sin^2 f(\nu - \cos f) \leq (\nu + 1)$ it follows that $a' \geq -(\nu + 1)r/(|N|\kappa^2)$. Hence, for a given $R \in [0, \infty)$, by using the mean value theorem and (3.15), we find

$$-\frac{(\nu + 1)}{|N|}R^2 \leq a(R) \leq 0. \qquad (3.22)$$

c) lower limit on a

If $\nu \geq 1$ it is easy to show that $a \geq -1$. For if it became smaller than -1 at a certain R then the derivative of f would change its sign so that f would increase. Since a is a decreasing function for all r, f would increase for all $r \geq R$ and could not meet its boundary value at infinity. Hence $a \geq -1$.

d) asymptotic behaviour

The first three steps of the proof tell us that the boundary value for a, $a_\infty \in (0, -1]$. By using that f becomes small for large r, we approximate the fields in eq. (3.14) by a power series in r. For f we find $f \sim f_1 r^{-|N|(a_\infty + 1)}$, f_1 being positive and constant. This inserted into the second sd-equation yields $a \sim |N|f_1^2(\nu - 1)r^{-2|N|(a_\infty + 1) + 2}$ and $a \sim |N|f_1^2(\nu - 1)r^{-4|N|(a_\infty + 1) + 2}$ for $\nu > 1$ and $\nu = 1$ respectively. Hence, for a to converge, we find two cases:

$$\nu > 1 : a_\infty > \frac{1}{|N|} - 1, \qquad \nu = 1 : a_\infty > \frac{1}{2|N|} - 1. \qquad (3.23)$$

While the first case rules out the possibility of a one-soliton solution due to the boundaries on a, there is no such restriction for $\nu = 1$. It is interesting to note, that the result for $\nu > 1$ coincides with the result for the sd-Skyrme-Maxwell system [42]. The case $\nu = 1$ was in fact discussed before in ref. [62] as the first sdCS-$O(3)$ σ-model. However, to the best of our knowledge, the announced numerical results of the model for $\nu = 1$ never appeared in print. We present our solutions in the next section.

We solved equations (3.14) numerically by using a shooting method and show here the plots of the energy density and the magnetic field for various values of ν. For each ν there may be (and probably are) other solutions which satisfy the boundary conditions (3.15). They are labelled by their flux.

It follows from (3.14) that the magnetic field has a minimum where

$$\cos f_{min} = \frac{1}{3}(\nu - \sqrt{\nu^2 + 3})$$ (3.24)

and a saddle point at $r = 0$. In the plot of the profile-function $f(r)$, Fig. 3.2 we indicate f_{min} by a vertical line.
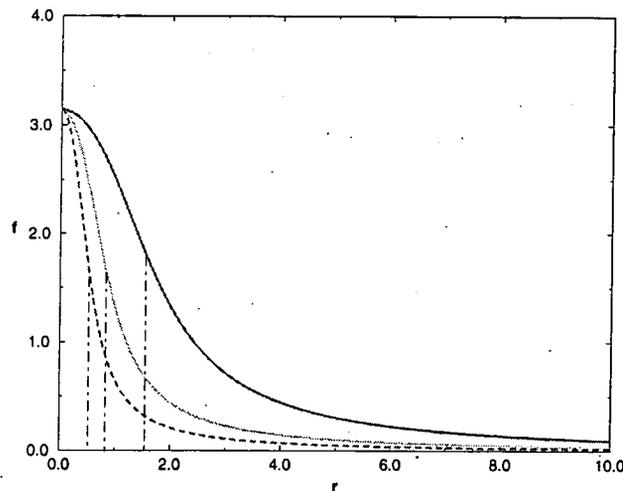

fig. 3.2: Profile function f of the 2-soliton $N = 2.$ as a function of the radius r for various $\nu \geq 1$. Solid line: $\nu = 2$, Dotted line: $\nu = 8$, Dashed line: $\nu = 20$. The vertical dot-dashed lines indicate the radii of maximal magnetic field according to (3.24), cf. Fig. (3.4).

Inserting (3.24) into the sd-equations gives:

$$B_{min} = B(f_{Bmin}) = \frac{4|N|}{9\kappa^2}\left(1 - \frac{\nu}{3}\left(\nu + \sqrt{\nu^2 + 3}\right)\right)\left(\nu + \frac{\sqrt{\nu^2 + 3}}{2}\right).$$ (3.25)

For comparison with Fig. 3.4, the three plotted values for ν give

ν	2	8	20
B_{min}	-0.0422	-0.1603	-0.4002

(3.26)

Tab. 3.2 Minima of the magnetic field for $\nu \geq 1$.

As mentioned above, the model also supports solutions whose vacuum is $\phi_\infty = -\mathbf{n}$. With boundary condition (3.15), the topological charge of such a configuration $N = 0$, but due to the non-vanishing magnetic flux there is a non-zero bound on the energy and hence the self-dual solutions cannot be deformed into the vacuum.
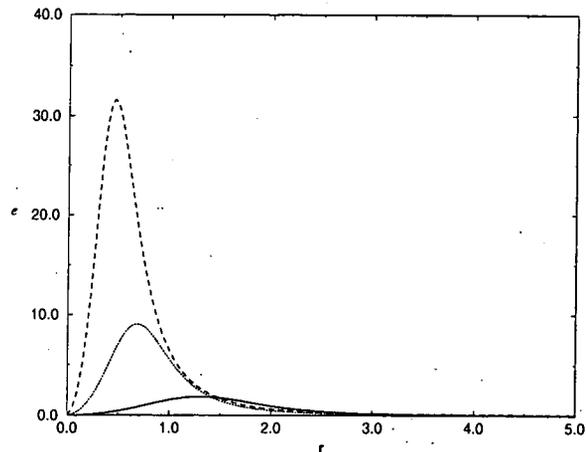

fig. 3.3: Local energy density e, integrand of (3.6) of the 2-soliton $N = -2$ as a function of the radius r for various $\nu \geq 1$.

Solid line: $\nu = 2$, for which the energy $E = 1.254e + 01$ and $a_\infty = -8.996e - 02$.

Dotted line: $\nu = 8$, $E = 4.602e + 01, a_\infty = -2.381e - 01$.

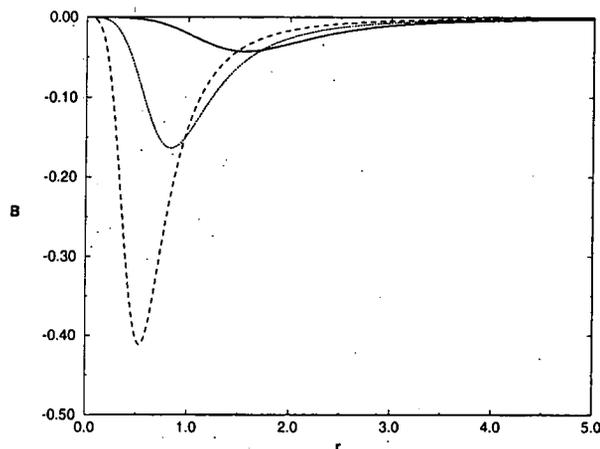Dashed line: $\nu = 20$, $E = 8.574e + 01, a_\infty = -2.541e - 01$.

fig. 3.4: Magnetic field B per soliton of the 2-soliton $N = -2$ as a function of the radius r for various $\nu \geq 1$. Solid line: $\nu = 2$, Dotted line: $\nu = 8$, Dashed line: $\nu = 20$.

3.4 Topological Solitons and Vortices for $0 \leq \nu \leq 1$

The range $0 \leq \nu \leq 1$ exhibits all three vacua, one of which shows the spontaneous breakdown of the $U(1)$ gauge symmetry. As demonstrated above, the breakdown of gauge symmetry means that the magnetic flux is topologically quantized. This can also easily be read off eq. (3.14), which implies $a_\infty = -1$ for f to converge. Also, the fields converge exponentially in the broken phase. These solutions are the topological vortices, see Figs. 3.7-3.10. The profile function and energy-density in the symmetric phase are displayed in Figs. 3.5-3.6. Like in so many other soliton theories, the 1-vortex is a lump while the 2-vortex is of toroidal structure.

The magnetic field has three extrema, which one can derive from (3.14): the saddle point at $r = 0$, a minimum where $\cos f_{\min} = (\nu - \sqrt{\nu^2 + 3})/3$ and a maximum where $\cos f_{\max} = (\nu + \sqrt{\nu^2 + 3})/3$. For the value of the magnetic field at the extrema this implies

$$B_\pm = -\frac{4n}{\kappa^2}\left(1 - \frac{\nu}{3}\left(\nu \pm \sqrt{\nu^2 + 3}\right)\right)\left(\nu \mp \frac{\sqrt{\nu^2 + 3}}{2}\right), \tag{3.27}$$

where the upper sign corresponds to the maximum and the lower sign to the minimum of the magnetic field with $B_- < 0$ and $B_+ \geq 0$. In the symmetric phase the field will take both extrema, see Fig. 3.9. However, for the asymmetric phase follows from the discussion above $\cos f \in [-1, \nu)$ and because $\nu^2 \leq 1$ implies that $\cos f_{\max} > \nu$, there is no maximum of the magnetic field in this phase, cf. Fig. 3.9. For $\nu = 1$ the maximum is at infinity $B_{\max} = 0$. Again, for comparison with Fig. 3.6 and Fig. 3.9 we give the numerical values of the extrema:

ϕ_∞^3	1		ν	
ν	0.5	1	0.01	0.5
$B_{\min}$	-0.030	-0.047	-0.015	-0.030
$B_{\max}$	$-.0044$	0	%	%

(3.28)

Tab. 3.3 Minima of the magnetic field for $\nu < 1$.

It is also clear from (3.14) that the magnetic field will change its sign at $\cos f = \nu$. For the symmetric phase $\phi_\infty = n$ it is therefore interesting to ask, if the magnetic flux integrates to zero. Since we are dealing with a whole family of solutions parametrized by a_∞, so in principle there is a solution with $a_\infty = 0, (\Phi = 0)$ for each N.

We fixed the CS-coupling κ to 5.0 for all simulations.

3.5   Conclusions

We obtained static sd-solutions in a CS-$O(3)$ σ-model in (2+1) dimensions. The vacuum structure of the model allows for solitons and vortices which can be either topological or non-topological. Due to the Higgs-effect, the flux is quantized in the asymmetric phase where the topological charge is non-integer. The elementary study of sdCS-solitons/vortices undertaken in this chapter provides a first step to a more general investigation of such solutions. In fact, much work on gauged sigma models has been done since this work was completed, often adapting ideas and techniques used in the Abelian Higgs model or scalar CSH-theories.

An interesting problem is, whether one could find solutions in this model with a topological charge $|N| > 1$ (in the symmetric phase, or $|M| > 1$ in the asymmetric phase) which are not on top of each other. Of course, such solutions would not be radially symmetric any longer and their energy-density could peak at up to $|N|(|M|)$ several distant points in the plane, $(x_1, \ldots, x_{|N|})$. It is natural to identify these points of maximal energy density with the positions of the solitons. These would be the canonical coordinates on the N-soliton moduli space. Due to the degeneracy of their energy, there is no potential and hence there are no forces within such a configuration. In principle, the N-soliton low-energy dynamics can be described by a moduli space approximation, which is, however, a non-trivial task due to the lack of explicit solutions. For the Abelian Higgs model it has been possible to to find a numerical scheme of computing the metric on the moduli space which is largely based on the behaviour of the Higgs field around its zeros [28]. However, for the scalar sdCS-theory any such attempts have failed so far.

Related work has been done in [63], where the static sdCS $O(3)$ σ-model was studied for $\nu = 1$ and away from the self-dual limit. For two solitons on top of each other it was found that there is an attractive and a repulsive phase depending on the coupling to the potential. In this, these results resemble very much the Abelian Higgs model.

In models like ours, which show several disconnected and degenerate vacua, there is the possibility of domain wall solutions which connect these vacua. The scalar sdCSH-theory supports domain walls as shown in [56]. In two space-dimensions the wall either separates two infinite regions and is therefore infinitely long or it surrounds a finite region in space. In the latter case the stability of the domain wall solutions against contraction or expansion is an interesting problem. Dynamically, the energy for a given flux will be minimized with respect to the radius of the enclosed domain. It was found for the sdCSH that the resulting condition on the fields is satisfied by sd-solutions, if the flux is large enough to stabilise the wall from collapse. It would be interesting to perform

similar studies in our model.

Recently, domain wall solutions in (1+1) dimensions have been studied on a dimensionally reduced scalar sdCS model [64] and very recently in the sdCS-$O(3)$ σ-model [65], a model equivalent to the one discussed above, but for $\nu = 1$. These are sd-theories where the Bogomol'nyi bound is given by a BPS-like bound with the two involved charges being the topological and the Noether charge.

Self-dual models can often be generalized to models with $N = 2$ supersymmetry (no relation to the N above), where the central charge gives the Bogomol'nyi bound. For the scalar sdCS-theory this was discussed in [66] and for the model discussed here in a recent publication [67].

Another popular idea is to generalize sd-gauged models by including an anomalous magnetic moment interaction. This is usually done by including a term proportional to the (dual) field-strength in the covariant derivative. For the scalar sdCS-model one has to introduce such an interaction to allow for simultaneous Maxwell/Yang-Mills interaction [68]. Alternatively, a neutral scalar field can be introduced [59], as mentioned in the introduction to this chapter. For the sdCS $O(3)$ σ-model such anomalous interactions have been studied by Ghosh [69], with the result that the matter equations reduce to the Liouville equation and hence they are integrable. Interestingly, this implies that these solutions are scale invariant, unlike the ones discussed here.

Finally, one can generalize the target manifold of the model to $\mathbb{CP}^N$ (again, no relation to the N above) and the gauge group to a non-Abelian one. The condition for obtaining a non-trivial bound is to have at least a global $U(1)$ symmetry left [38, 70, 71]. The gauge group is a proper subgroup of $SU(N + 1)$ and the energy bound is given again by the linear combination of Noether and topological charge. The vacuum structure if such models is rich and depends on parameters like the boundary value of the matter field and the representations of matter and gauge fields.

After much of the work of this chapter was completed, I became aware that similar results have be obtained previously [72, 73]. The essence of this work and the one presented here — the construction of a sd-potential and the numerical discussion using radially symmetric fields — is the same, although details of the exposition vary. In particular, both papers [72, 73] fail to mention the absence of solutions for $|N| = 1, \nu > 1$.
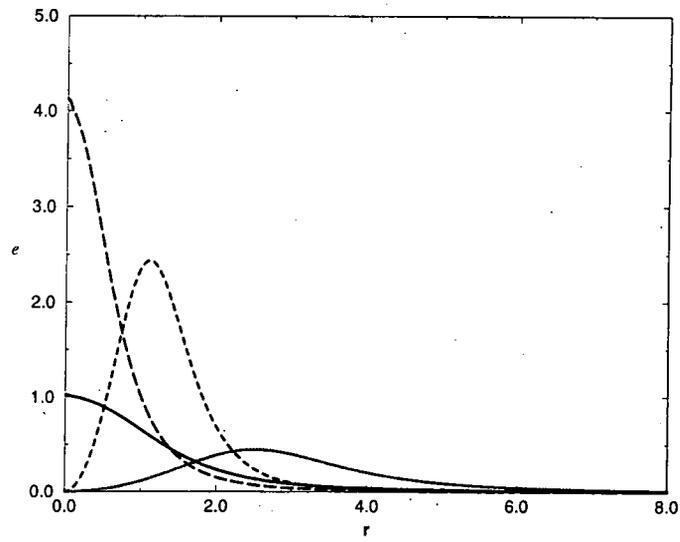
fig. 3.5: The energy density e as a function of r for the one- and two-soliton in the symmetric region, $f_\infty = 0$. Solid line $\nu = 0.5, N = -1$; dotted line $\nu = 0.5, N = -2$. Long-dashed line $\nu = 1, N = -1$; dashed line $\nu = 1, N = -2$.

fig. 3.6: The magnetic field B as a function of r for the one- and two-soliton in the symmetric region, $f_\infty = 0$. Solid line $\nu = 0.5, N = -1$; dotted line $\nu = 0.5, N = -2$. Long-dashed line $\nu = 1, N = -1$; dashed line $\nu = 1, N = -2$.
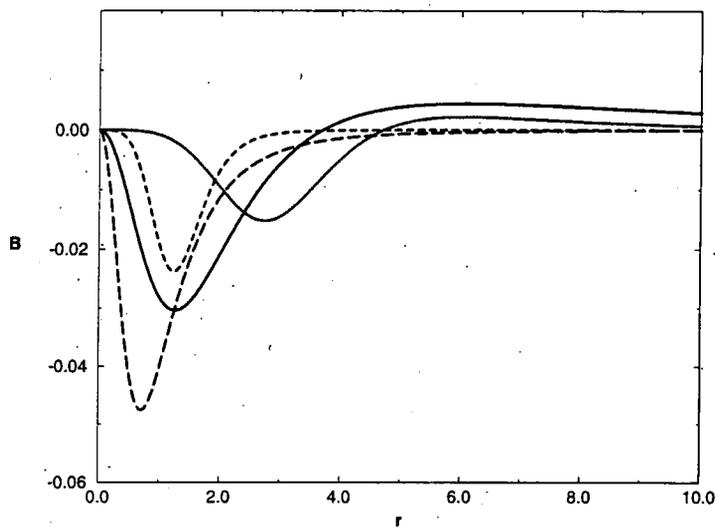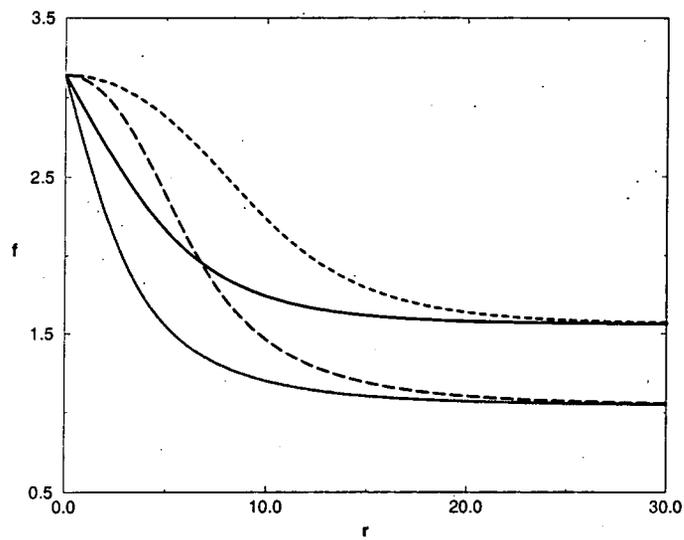
fig. 3.7: The profile function f as a function of r for the one- and two-soliton in the asymmetric region, $f_\infty = \arccos \nu$. Solid line $\nu = 0.01, N = -1$; dotted line $\nu = 0.5, N = -1$. Dashed line $\nu = 0.01, N = -2$; Long-dashed line $\nu = 0.5, N = -2$.

fig. 3.8: The gauge field a as a function of r for the one- and two-soliton in the asymmetric region, $f_\infty = \arccos \nu$. Solid line $\nu = 0.01, N = -1$; dotted line $\nu = 0.5, N = -1$. Dashed line $\nu = 0.01, N = -2$; Long-dashed line $\nu = 0.5, N = -2$.

fig. 3.9: The magnetic field B as a function of r for the one- and two-soliton in the asymmetric region, $f_\infty = \arccos \nu$. Solid line $\nu = 0.01, N = -1$; dotted line $\nu = 0.5, N = -1$. Dashed line $\nu = 0.01, N = -2$; Long-dashed line $\nu = 0.5, N = -2$.
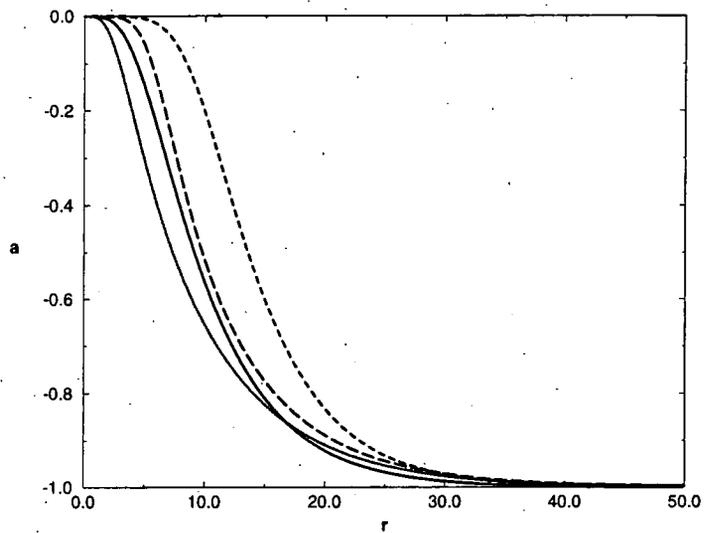

fig. 3.10: The energy density e as a function of r for the one- and two-soliton in the asymmetric region, $f_\infty = \arccos \nu$. Solid line $\nu = 0.01, N = -1$; dotted line $\nu = 0.5, N = -1$. Dashed line $\nu = 0.01, N = -2$; Long-dashed line $\nu = 0.5, N = -2$.
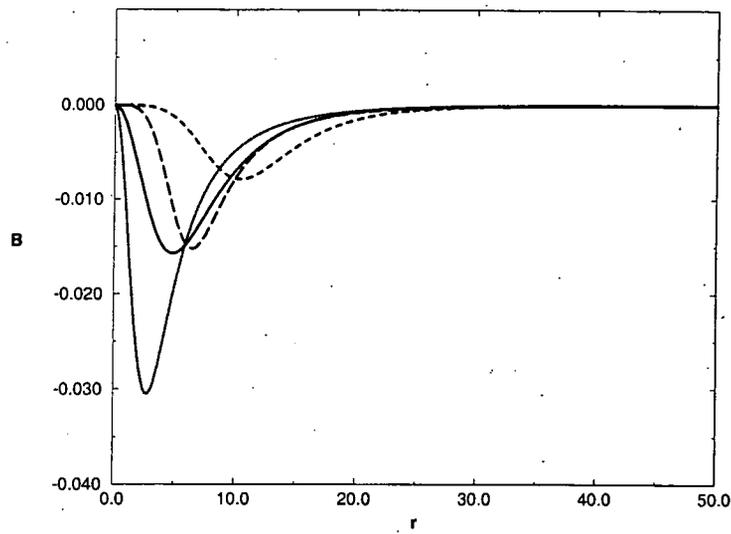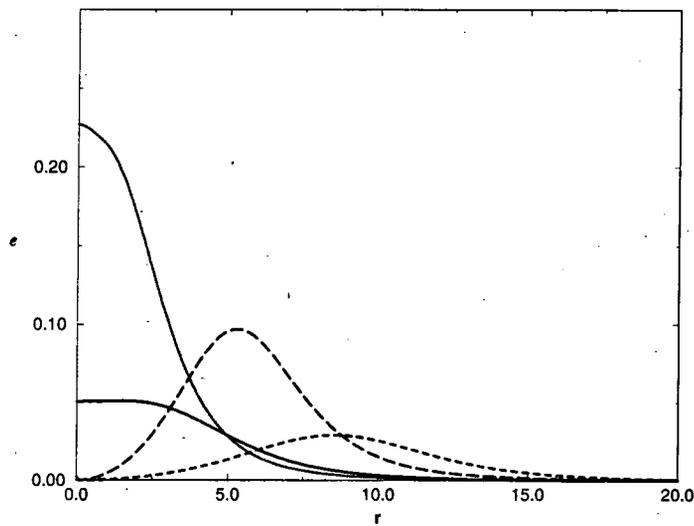
Chapter 4

Static Solitons with Non-Zero Hopf Number

The non-linear $O(3)$ σ-model in (3+1)-dimensional space-time is a scalar field-theory whose static fields are maps $\mathbb{R}^3 \cup \{\infty\} \mapsto S^2$. They can be classified by a homotopy invariant called the Hopf number. On general geometrical grounds, soliton solutions with higher Hopf number are expected to be of complicated, knotted structure. Knots are smooth embeddings of closed loops in $\mathbb{R}^3$ and are related to various problems in modern theoretical physics [32]. The systematic study of knots was originally inspired in the 19th century by Kelvin's idea of describing atoms as knots composed of ether [74], where the variety of distinct knots was supposed to take account of the different chemical elements. Kelvin's proposal resulted in an analysis of knots by Tait [75], which for many years defined the essence of mathematical knot theory. Although there are many examples of knotted structures on a macro- and mesoscopic scale, for a long time there were no further efforts to find a microscopic (that is atomistic) theory involving knots and knot theory remained of interest mainly for pure mathematicians.

From the modern nuclear physics point of view, particles modelled by knotted configurations are conceptually much in the spirit of Skyrme's original intention to describe nucleons as vortices in a mesonic fluid [4, 5], although of course the historic development was reverse and Skyrme was reportedly influenced by Kelvin's work. The recent interest in knot theory provides therefore a nice example for the cyclic evolution of science. This interest is largely fueled by work of Jones and Witten, who outlined connections of topological field theories, such as non-Abelian Chern-Simons theories, to knot theory and integrable models [32].

With respect to elementary particles one can imagine that knotted structures find an application in (cosmic and fundamental) string-theories, where the excitations of the string might be described by vibrations of a knotted configuration [76]. There are also proposals for knots in the description of gluonic flux-tubes in QCD, which could confine quarks. At present, these are just proposals and no details have been worked out, but there are other — physical and biological — systems where the occurrence of knotted structures seems more apparent. Examples for such systems are DNA-chains [77], nematic liquid crystals or vortex structures in ^{3}He superfluid [78]. There are clearly many interesting applications of knotted structures but only little can be said so far about promising field theoretical attempts to describe these configurations. The earliest proposal for a model in which stable solutions with non-vanishing Hopf number can occur, goes back some time to L.D. Faddeev [79]. It was shown later that the Hopf-number provides a lower topological bound on the potential energy of the Faddeev model [80]. However, despite several attempts which will be described below, no actual solutions to the variational equations of this model were obtained. This is undoubtedly due to the fact that very little can be done analytically and most of the results will have to be due to numerical simulations.

In this chapter we mainly study classical static solutions of Hopf-number one and two. In the next section we give an introduction to the geometry of the Hopf map. This is followed by a brief summary of previous work in the field. Our model is defined in section 4.3 where also an ansatz of azimuthal symmetry is introduced which is later used for numerical computations. In section 4.4 we present our numerical results which are minima of the potential energy functional for Hopf-number one and two. We discuss the shapes and binding energies of the solutions as well as their relation to solitons in (2+1)-dimensional theories. Our model has a self-interaction coupling parameter and we study the dependence of the energy on this coupling. In addition, the effect of a symmetry-breaking potential term is described. In section 4.5 we give a simple approximation for the excitation spectrum of a soliton slowly rotating around its axis of symmetry. We conclude with section 4.6 where we also remark on possible further investigations.

4.1   Geometry of the Hopf Map

In differential geometric terms, the Hopf map is the projection of the total space S^3 onto the base S^2 with fibre S^1 [81]. If embedded in $\mathbb{R}^3$, this fibration can be visualized as follows [82]. Consider the two-dimensional unit-disc D, centred, say, at the origin in the x/y-plane and a foliation of $\mathbb{R}^3 \cup \{\infty\}$ into concentric tori about the z-axis, see Fig. 4.1.
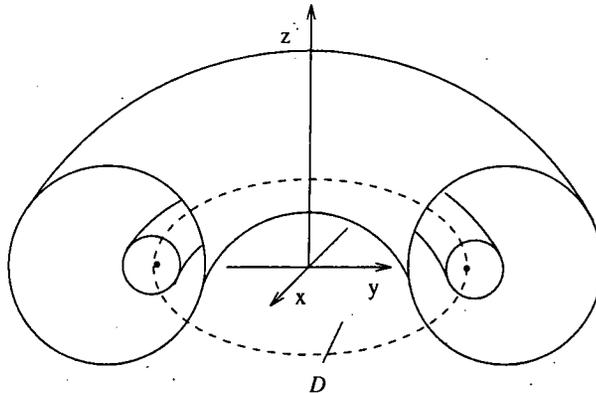

fig. 4.1: Concentric tori in $\mathbb{R}^3$

A torus has two scales, the cross-section (or "tube diameter") and the filament (mean radius). Here the tori are arranged in such a way, that the radius of their cross-section approaches zero as the mean radius tends to $\partial D = S^1$, the boundary of the disc D. On the other hand, if the mean radius tends to infinity, the cross section also tends to infinity and the meridian of the torus becomes the z-axis. The intersection of every torus with D is a loop. For a particular torus consider a closed smooth trajectory which winds around its parallel and its meridian without intersecting itself. This trajectory is classified by $\pi_1 \left(S^1 \times S^1\right)$, i.e. the number of times it winds around the meridian and the parallel, see Fig. 4.2. The fibration of S^3 is then described by the set of such trajectories with winding number (1,1) on each torus. The "field" (that is the projection onto S^2) is constant along this trajectory (the fibre). Now consider all the tori in $\mathbb{R}^3$, then the fibre approaches ∂D as the cross-section approaches zero. Therefore the field is constant along ∂D which is identified with a point on target S^2. Consequently, D can be one-point compactified to an S^2, and every point of this two-sphere has a fibre "attached" to it, because each fibre intersects D once. Each of the fibres is linked with every other fibre, because S^3 is a non-trivial bundle over S^2. An adequate picture is that any fibre intersects the surface spanned by any other one.
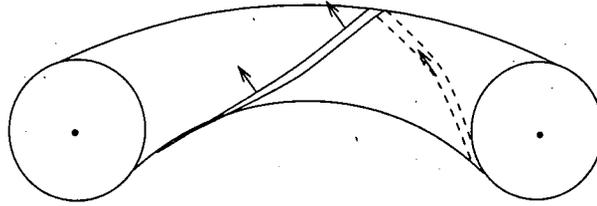
fig. 4.2: Trajectory of winding number (1,1) on the torus. The S^2 valued field, indicted by a vector of constant length, is constant along the fibre.

Hopf maps are classified topologically by $\pi_3\left(S^2\right)$, which is isomorphic to the group of integers. This integer which labels the homotopy class is called the Hopf-number H and has an elementary geometrical interpretation. As explained above, the pre-image of every point of the target space S^2 is isomorphic to a circle. It can be shown, that the Hopf-number equals the multiplicity by which two arbitrary circles are linked.

H also has a differential geometric representation [13]: be ϕ the projection onto S^2 and be ω the normalized volume element of S^2. The pullback $\phi^*\omega$ is necessarily exact since $H^2_{\mathrm{DR}}(S^3) = 0$. Hence there is a 1-form A on S^3 with $\phi^*\omega = dA$ and $H \sim \int A \wedge dA$.

In coordinate language, the dual of $\phi^*\omega$ is $B_i = \varepsilon_{ijk}\,\phi \cdot \partial_j\phi \times \partial_k\phi$ and

$$H = -\frac{1}{(8\pi)^2}\int d^3x\,\mathbf{B}\cdot\mathbf{A}\,.\tag{4.1}$$

There are several analytical expressions for the standard Hopf map. They are of course all equivalent, but here seems to be the right place to compile a little selection:

1. Let $z = (z_1 + iz_2, z_3 + iz_4) \in \mathbb{C}^2, |z|^2 = 1$ and $\phi \in S^2$. Then

$$\phi_a = z^\dagger\sigma_a z\tag{4.2}$$

is the Hopf map, where $\sigma_a\,(a = 1, 2, 3)$ are the Pauli matrices.

2. Let $W \in \mathbb{CP}^1 = S^2$ and the field z as above. Thus

$$W = \frac{z_1 + iz_2}{z_3 + iz_4}\,.\tag{4.3}$$

The connection to the fields ϕ is given by stereographic projection onto the complex plane.

$$W = \frac{\phi_1 + i\phi_2}{1 + \phi_3}. \tag{4.4}$$

By inserting (4.2) into (4.4) one obtains expression (4.3).

3. Let $R \in SO(3)$ and a function of the four-dimensional, space-dependent, unit vector $n_a = (n_0, \mathbf{n})$. In components:

$$R_{ab} = \delta_{ab} + 2(n_a n_b - \mathbf{n}^2 \delta_{ab}) - 2\varepsilon_{abc} n^c n_0. \tag{4.5}$$

If this matrix is applied to a constant vector, say, $\mathbf{c}=(0,0,1)$, the Hopf map is obtained and one can identify $\phi_a \equiv R_{ab} c^b$. A short calculation verifies that this map is equivalent to (4.2) with n_0 being replaced by z_1, n_1 by z_2 and so on.

In the course of this chapter we are not just interested in the standard Hopf map but in a map which "deforms" the standard Hopf map in such a way that its topology is preserved but the fields correspond to a minimum of a positive valued functional. To achieve this, we let the field $z \in S^3$ become space-dependent, i.e. $z(\mathbf{r})$, $\mathbf{r} \in \mathbb{R}^3$. For finite energy, we will restrict ourselves to configurations which tend to constants at spatial infinity. This allows us to compactify $\mathbb{R}^3 \cup \{\infty\}$ to S_x^3, such that

$$\mathbf{z} : S_x^3 \mapsto S_z^3. \tag{4.6}$$

This means that there are now two topological invariants to be considered: firstly the Hopf-number arising from (4.2) and secondly the degree of (4.6), being characterized by $\pi_3(S^3) = \mathbb{Z}$. Diagrammatically this is described by

$$S_x^3 \xrightarrow{z} S_z^3$$
$$\downarrow \phi$$
$$S_\phi^2$$

Denote the degree of the map z, $k = \deg[z]$. Then a theorem in Algebraic Geometry states that $\deg[\phi \circ z] = k \deg[\phi] = kH$ [8].

From the geometrical considerations given above it seems obvious that the problem is canonically described by toroidal coordinates (η, β, α, a). The map to more conventional cylindrical coordinates (r, z, α) is given by:

$$r = \frac{a \sinh \eta}{\cosh \eta - \cos \beta}, \qquad z = \frac{a \sin \beta}{\cosh \eta - \cos \beta}, \qquad \alpha = \alpha. \tag{4.7}$$

The tori are labelled by η, while their surface is parametrised by β, α, the latter being the azimuthal angle and the former the inner angle of the "tube", see Fig. 4.3. Thus the range for each angle is $[0, 2\pi]$.
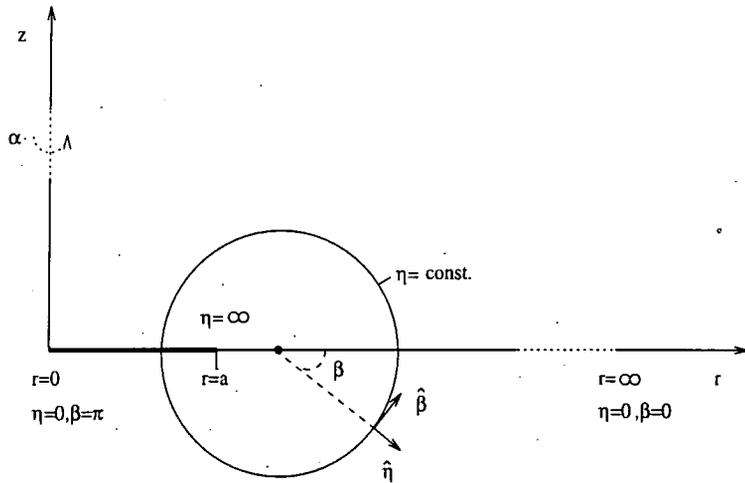

fig. 4.3: Toridal coordinates (η, β, α) and their relation to cylindrical coordinates.

The metric tensor of $\mathbb{R}^3$ is in toroidal coordinates

$$g_{ij} = \frac{a^2}{\tau^2} \begin{pmatrix} 1 & 0 & 0 \\ 0 & 1 & 0 \\ 0 & 0 & \sinh^2 \eta \end{pmatrix}, \tag{4.8}$$

where $\tau = \cosh \eta - \cos \beta$. From this the metric determinant is easily read off $\sqrt{|\det g|} = a^3 \sinh \eta / \tau^3$. Fig. 4.3 shows the coordinates for constant α, which clearly corresponds to a plane. The surfaces of constant η, on the other hand, are tori, with the two degenerate cases of $\eta = 0$ (which yields the z-axis or the sphere at infinity, depending on β) and $\eta = \infty$ (these "tori" are circles of radius a). Thus a is the mean radius of the circle of cross-section zero. The fields at this circle get mapped to the south-pole of target S^2. Using (4.7), we observe for $\beta = const.$ that:

$$r^2 + (z - a \cot \beta)^2 = \frac{a^2}{\tau^2 \sin^2 \beta} \left(\sinh^2 \eta \sin^2 \beta + (1 - \cosh \eta \cos \beta)^2 \right) = \frac{a^2}{\sin^2 \beta}. \tag{4.9}$$

Therefore the surface of constant β is a sphere of radius $a / \sin \beta$, centered at $z = a \cot \beta$.

4.2 Early Work

There are some previous attempts to find soliton solutions which are topologically stable due to their fields being of non-zero H. The direct approach of solving the complete equations of motion for any such theory in three space dimensions involves finding solutions of a set of coupled PDE's for two functions (the coordinates on the target manifold), depending on the three space coordinates each. This seems hopeless analytically and is of considerable effort numerically. Therefore the common strategy was so far to truncate the configuration space and to investigate only fields of certain symmetries, which seem inherent to the problem. It will be explained below that the results obtained in these models cannot be quantitatively correct. However, the discussion of these theories gives a good introduction to the subject and points out relevant problems that should be addressed, which is why we include a review here.

Following Faddeev's initial proposal, some of the first applications where fields of non-zero H have been investigated, are effective field-theories for three-dimensional ferromagnets [83] and superfluid ^{3}He [78]. In such theories of Ginzburg-Landau type, the fields are order-parameters and their time-evolution is governed by a first-order time-derivative of the fields. To first approximation, the static energy is expressed by second-order terms of the field-gradient. For a ferromagnet one can formulate the theory in terms of the normalized magnetization $\mathbf{n} = \mathbf{M(r)}/M_0$, $\mathbf{r} \in \mathbb{R}^3$, where M_0 is the saturation magnetization. To allow (semi-) localized configurations, the magnetization has to be homogeneous as $|\mathbf{r}| \to \infty$, thus one can one-point compactify $\mathbb{R}^3$ to S^3. Since $\mathbf{n}^2 = 1$:

$$\mathbf{n} : S^3 \mapsto S^2 . \tag{4.10}$$

For an isotropic ferromagnet the first approximation to the static energy is given by

$$V[\mathbf{n}] \propto \int d^3x \, (\partial_i \mathbf{n})^2 . \tag{4.11}$$

The minima of this functional are harmonic maps. As shown in ref. [84], all non-constant harmonic maps are orthogonal projections $\mathbb{R}^3 \mapsto \mathbb{R}^2$, followed by a harmonic map $\mathbb{R}^2 \mapsto S^2$ and therefore have infinite energy. Consistently, simple scaling arguments along the line of the Hobart-Derrick theorem show that, without further constraints, the solutions are unstable against rescaling.

Related work was performed by deVega [85], where toroidal configurations are investigated in the general context of classical field-theory. The energy functional is there equivalent to (4.11) but by contrast the fields are interpreted as free classical fields. The ring size of the torus is a parameter

of the energy which has to be minimized with respect to it. Scaling arguments show that for a functional of type (4.11) this is the case when the ring size goes to zero. In this paper it was shown that the addition of a Skyrme-term provides the energy with bounds and the configuration with non-zero radius. Both the bounds and the radius are estimated numerically. For the computation, an ansatz in toroidal coordinates (η, β, α) with unit Hopf-number is proposed:

$$\phi_1 + i\phi_2 = \sin f(\eta)\, e^{i(\beta+\alpha)}\,, \qquad \phi_3 = \cos f(\eta). \qquad (4.12)$$

The possible relevance of toroidal excitations (or "vortex excitations" as they are sometimes called) in Weinberg-Salam-Higgs theory was outlined in [86], where it was shown that the theory supports configurations for which the Higgs-field is expelled from a toroidal region. The model's constituents are two fields, the Higgs and a neutral vector boson. The latter gives rise to a non-zero flux which is trapped inside the torus. It turns out that this flux is too strong for the vortex to be stable (i.e. it overcomes the Higgs pressure which tends to collapse the vortex) and hence the vortex decays. For the actual computation ansatz (4.12) was used.

Another interesting possible application for toroidal configurations in non-linear sigma models was given in ref. [87]. There the Lagrangian was constructed as an effective chiral theory for the description of low-energy hadron dynamics – and in that attempt as being similar to the Skyrme model. The hope was there to model possible superheavy fermions in the few TeV range as bound states of solitons. Consequently, some aspects of Hopf solitons (or Hopfions, as we will call them) in the Skyrme model were investigated [88, 89, 90]. It is interesting to see how the Hopfion fits into the framework of the Skyrme model. The Skyrme model is an effective chiral model where the static fields are maps $U : \mathbb{R}^3 \mapsto SU(2)$. They can be written in a quaternionic basis $\sigma_a = (\mathbb{1}, i\sigma)$ using the four-vector $\phi_a = (\phi_0, \phi)$:

$$U = \sigma_a \phi^a\,. \qquad (4.13)$$

$U^\dagger U = 1$ implies $\phi_a \phi^a = 1$ due to the algebraic properties of the Pauli matrices. From U a conserved chiral current can be constructed $L_i = U^\dagger \partial_i U$. This current is invariant under left transition $\delta U = \epsilon U$, where ϵ is an element of the algebra $su(2)$. In terms of L_i the potential energy density $\mathcal{V}$ of the Skyrme model is

$$\mathcal{V} = \mathcal{V}_2 + \mathcal{V}_4 = -\frac{f^2}{4}\,\mathrm{Tr}\, L_i L^i + \frac{1}{32e_0^2}\,\mathrm{Tr}\, [L_i, L_j]\,[L^i, L^j]\,, \qquad (4.14)$$

where f and e_0 are free parameters. For finite energy one has to impose the boundary condition $U \to \mathbb{1}$ (or to any other constant matrix) as $r \to \infty$. Then $\mathbb{R}^3$ can be one-point compactified to

S^3 and the Skyrmion's [1] static energy or mass, the integral over $\mathcal{V}$, is bounded from below by a multiple of the homotopy index of $\pi_3(S^3) = \mathbb{Z}$. This index B is interpreted as the baryon number of the soliton and its integrand is given by

$$\mathcal{B} = \frac{1}{24\pi^2} \operatorname{Tr} \varepsilon^{ijk} \left(L_i L_j L_k \right) . \tag{4.15}$$

In the Skyrme model, Hopfions can principally be constructed by restricting the field-manifold to S^2, e.g. by setting $\phi_0 = 0$. This new model also possesses a lower topological bound on the potential energy (the integral over (4.14)) but now the bound is given in terms of the Hopf-number [80]. It holds

$$V \geq c|H|^{\frac{3}{4}} , \tag{4.16}$$

with positive non-zero c [91].

The baryon density $\mathcal{B}$ necessarily vanishes upon "Hopfization" (i.e. restriction of the target manifold to S^2). Thus the soliton configurations can be thought of as being composite of a Skyrmion with $B = H$ and an anti-Skyrmion with $B = -H$. In paper ref. [88], a hedgehog ansatz is employed in the $B = 1$ sector to map $\mathbb{R}^3 \mapsto S^3$. This is followed by a standard Hopf map (4.2). More explicitly, be $U = \exp(if(r)\boldsymbol{\sigma} \cdot \hat{r})$, where $\hat{r}$ is the radial unit vector. Then a new field $W(\mathbf{x})$ can be defined, such that

$$W = iU\sigma_3 U^\dagger . \tag{4.17}$$

The field $W \in SU(2)$ and from it a new current $\tilde{L}_i \in su(2)$ can be constructed,

$$\tilde{L}_i = W^\dagger \partial_i W = U(\sigma_3 L_i \sigma_3 - L_i)U^\dagger . \tag{4.18}$$

$\sigma_3 L_i \sigma_3$ describes a rotation of L_i by π around the $a = 3$ axes in iso-space. This means that a $U(1)$ degree of freedom has been singled out in (4.18) and since $SU(2)/U(1) = S^2$, it follows that W is a map to S^2. One can therefore think of this Hopf model as being a $U(1)$-gauged Skyrme model.

A further attempt for a computation of a solution with $H \neq 0$ in the Skyrme model was made in [92, 93] where again ansatz (4.12) was employed. There it was in addition suggested to generalize the quartic term in (4.14) by using all possible forth-order Lorentz covariant terms and giving them different couplings (although one of these couplings can be scaled away). Introducing couplings g_1 and g_2,

---

[1] The soliton solution of topological charge one is called the Skyrmion.

$$V_4 = g_1 \operatorname{Tr} \, [L_i \, , L_j] \, [L^i \, , L^j] + g_2 \operatorname{Tr} \, (L_i)^2 \, (L_j)^2 \, . \qquad (4.19)$$

It was argued that for such a model, after "Hopfization" the parameter ranges for g_1 and g_2 which support hedgehog Skyrmions also support Hopfions [88].

To find an adequate description of nuclear matter which is based on solitons, they have to be quantised in the sense that quantum fluctuations around a classical configuration are computed. The eigenvalues of the energy fluctuation tensor (the second variation of the energy with respect to the fields) determine whether the soliton is in a stable state. The energy of the fluctuations is proportional to the squared frequency of the oscillations around the classical ground state, which is given by the Hopf-soliton. For negative eigenvalues this frequency becomes imaginary and thus the fluctuations grow exponentially in time, indicating an unstable configuration. This turns out to be the case in for the (unit) Hopf-soliton in the Skyrme model as shown in [90]. This work also uses ansatz (4.12).

However, all the previous work described so far suffers from an essential problem. It relies on ansätze (4.12) and (4.17); however, it was shown in [89] that both ansätze are not consistent with the equations of motion, in the sense that these do not permit a consistent separation of the variables in the variational equations. Therefore the results obtained in these papers cannot be correct quantitatively. On the other hand, solitons with a small Hopf-number (one or two) are expected to exhibit some symmetry and both ansätze (4.12) and (4.17) might be good approximations to the actual static solutions.

4.3   Hopf Maps and Toroidal Ansatz

We are almost exclusively interested in static solutions and therefore we define our model by the following potential energy functional on $\mathbb{R}^3$, with V_4 given essentially by (4.19) (we renamed the couplings)

$$V\,[\phi] = \Lambda \int d^3x \, \frac{1}{2} \, (\partial_i \phi)^2 + \frac{g_1}{8} \, (\partial_i \phi \times \partial_j \phi)^2 + \frac{g_2}{8} \, (\partial_i \phi)^2 \, (\partial_j \phi)^2 \, . \qquad (4.20)$$

For $g_2 = 0$ this is equivalent to the static energy of the Faddeev-Skyrme model [35, 80]. The vector ϕ is the $O(3)$ σ-model field introduced in chapter 1. The cross-product is taken in field-space and the coordinate indices i, j run from 1 to 3. For the reasons laid out in section 4.2 we include the fourth-order terms in the field-gradient, more precisely the most general combination of global $O(3)$-invariant fourth-order terms. The minimum energy configurations will then not be

described by harmonic maps, but will be of a definite scale. The parameter Λ is a constant of dimension energy/length and determines the model's energy unit. The couplings g_1 and g_2 are of dimension (length)^2. The ratio g_1/g_2 is the only physically relevant coupling since an overall scaling of g_1 and g_2 can be absorbed by a rescaling of length and energy units. Using $(\partial_i\phi \times \partial_j\phi)^2 = (\partial_i\phi)^2(\partial_j\phi)^2 - (\partial_i\phi \cdot \partial_j\phi)^2$ and the inequality

$$2\sum_{ij}(\partial_i\phi \cdot \partial_j\phi)^2 \geq \sum_{ij}(\partial_i\phi)^2(\partial_j\phi)^2 \geq \sum_{ij}(\partial_i\phi \cdot \partial_j\phi)^2 \,, \qquad (4.21)$$

one sees that the allowed ranges for the coupling constants are $g_2 \geq 0$ and $g_1 > -2g_2$. We prove the first inequality in the appendix to this chapter, while the second inequality is a version of the Schwarz inequality for the vectors $\partial_i\phi$.

As before for finite energy solutions we require $\phi \to \mathbf{n}$ as $|\mathbf{x}| \to \infty$, where $\mathbf{n}$ is a constant unit vector. Thus $\mathbb{R}^3$ can be one-point compactified to S^3 and the fields ϕ are maps

$$\phi: \quad S^3 \mapsto S^2. \qquad (4.22)$$

As mentioned above, it was proved in [80] that the energy eq. (4.20) has a lower topological bound in terms of H. For $g_1 \geq 0$ it is given by (4.16)

$$V \geq \Lambda c |H|^{3/4} \,, \qquad (4.23)$$

where $c = \sqrt{2g_1}(2\pi)^2 3^{3/8}$.

At this point it is instructive to look at the symmetries of the field. It was shown in ref. [91] that the maximal subgroup of $O(3)_X \otimes O(3)_I$ under which fields with non-vanishing Hopf-number can be invariant is

$$G = \mathrm{diag}\,[O(2)_X \otimes O(2)_I]. \qquad (4.24)$$

Here $O(2)_X$ and $O(2)_I$ denote rotations about a fixed axis in space and iso-space respectively. We choose the z- and ϕ_3-axis as the axes of symmetry. According to the Coleman-Palais theorem we expect to find the minimal energy solution in the class of G-invariant configurations [7]. Therefore we use the most general G-invariant ansatz, written in terms of two functions $w(\xi_1, \xi_2)$ and $v(\xi_1, \xi_2)$. They depend on coordinates ξ_1 and ξ_2 which form an orthogonal coordinate system together with α, the angle around the z-axis:

$$\phi_1 + i\phi_2 = \sqrt{1 - w^2(\xi_1, \xi_2)}e^{i(N\alpha + v(\xi_1, \xi_2))}, \qquad \phi_3 = w(\xi_1, \xi_2). \qquad (4.25)$$

We have checked the consistency of this ansatz with the variational equations derived from (4.20). The components ϕ_1 and ϕ_2 have to vanish along the z-axis for the field to be well-defined. This is realized by setting $\phi(0,0,z) = \mathbf{n} = (0,0,1)$, which also defines the vacuum state of the theory. In order to describe a non-trivial map, ϕ has to be surjective. Hence there is at least one point $\mathbf{x}_0$ with $\phi(\mathbf{x}_0) = -\mathbf{n}$. Under the action of G, $\mathbf{x}_0$ represents a circle around the z-axis. We fix our coordinate system such that this circle lies in the xy-plane and define initially $a \equiv |\mathbf{x}_0|$. On every trajectory from the circle to the z-axis or infinity, $w(\xi_1, \xi_2)$ runs at least once from -1 to 1. Therefore the surfaces of constant w are homeomorphic to tori, in agreement with the discussion given above.

This structure prompts us to choose toroidal coordinates (r, z, α, a), see (4.7), and to identify $\xi_1 = \eta, \xi_2 = \beta$. The function $w(\eta, \beta)$ is subject to the boundary conditions $w(0, \beta) = 1, w(\infty, \beta) = -1$ and is periodic in β. $v(\eta, \beta)$ is an angle around ϕ_3 and can include windings around β. Therefore we set $v(\eta, \beta) = M\beta + v_0(\eta, \beta)$ where $v_0(\beta) : S^1 \mapsto S^1$ is homotopic to the constant map. Since v is ill-defined for $w = \pm 1$, it is not restricted by any boundary condition at $\eta = 0, \infty$.

The "potential" $\mathbf{A}$ and the "field-strength" $\mathbf{B}$ for this ansatz are given by

$$A_\alpha = 2\frac{\tau}{a \sinh \eta} N(w-1), \qquad A_\beta = 2\frac{\tau}{a}(M + \dot{v}_0)(w+1), \qquad A_\eta = 2\frac{\tau}{a}v_0'(w+1),$$

$$B_\alpha = 2\frac{\tau^2}{a^2}(w'(M + \dot{v}_0) - v_0'\dot{w}), \qquad B_\beta = -2\frac{\tau^2}{a^2 \sinh \eta}Nw', \qquad B_\eta = 2\frac{\tau^2}{a^2 \sinh \eta}N\dot{w},$$

$$(4.26)$$

where the dot and prime denote derivatives with respect to β and η respectively. Note that the field $\mathbf{A}$ is well defined on all of $\mathbb{R}^3$. The gauge has been chosen such that A_α vanishes for $\eta = 0$ (where the coordinate α is ill-defined) and analogously A_β vanishes for $\eta = \infty$.

Eq. (4.1) then gives $H = NM$ in agreement with the linking number interpretation of H given above. The potential energy (4.20) of ansatz (4.25) is given by

$$
\begin{aligned}
V[w(\eta, \beta), v(\eta, \beta), a] &= \pi\Lambda \int d\eta\, d\beta\, \frac{a^3 \sinh \eta}{\tau^3} \left\{ \frac{(\nabla w)^2}{1 - w^2} + (1 - w^2)\left((\nabla v)^2 + \frac{N^2\tau^2}{a^2 \sinh^2 \eta}\right) \right. \\
&\quad + \frac{g_1}{2}\left(\frac{N^2\tau^2}{a^2 \sinh^2 \eta}(\nabla w)^2 + (\nabla w \times \nabla v)^2\right) \\
&\quad \left. + \frac{g_2}{4}\left[\frac{(\nabla w)^2}{1 - w^2} + (1 - w^2)\left((\nabla v)^2 + \frac{N^2\tau^2}{a^2 \sinh^2 \eta}\right)\right]^2 \right\}.
\end{aligned}
$$

$$(4.27)$$

In toroidal coordinates the gradient includes a factor a^{-1}. Hence the term quadratic in the gradients is proportional to a while the quartic terms are inverse proportional to it. For soliton solutions, the energy functional has to be varied with respect to w, v and a.

4.4 Numerical Results

The variational equations for eq. (4.27) are highly non-linear coupled PDE's and numerically hard to tackle. Therefore we solved the problem by a minimization of the potential energy functional which was discretized on an (η, β) grid. The search for the minimum in a high-dimensional space is feasible using the NETLIB routine *ve08* with an algorithm described in [94]. This method is applicable if the objective function is a sum $f(\mathbf{x}) = \sum f_i(\mathbf{x})$ of simpler functions f_i, each of which is non-constant only for a few components of the (multi-dimensional) vector $\mathbf{x}$. Thus the Hessian matrix is very sparse and can be updated locally. This saves a considerable amount of memory and time compared to a more naive implementation of a conjugate gradient search.

We obtain field-configurations as displayed in Fig. 4.4 where the Hopf-number equals 1. In this plot the field ϕ is viewed from above the north pole of target S^2. Iso-vectors in the northern hemisphere terminate in a cross, those in the southern hemisphere in a dot. The toroidal structure of the fields is clearly visible. Also note that the fields in the southern hemisphere span a torus indeed.

There is an interesting interpretation of such configurations in terms of the $O(3)$ σ-model in (2+1) dimensions, the solutions of which we call (anti-) baby Skyrmions. The fields in the positive and negative x-halfplane of Figs. 4.4–4.6 are baby Skyrmions and anti-baby Skyrmions respectively. This can be understood in the following way. Wilczek and Zee [41] show that a (2+1)-dimensional configuration of Hopf-number one can be produced by creating a baby Skyrmion/anti-baby Skyrmion pair from the vacuum, rotating the (anti-) Skyrmion adiabatically by 2π and then annihilating the pair. In our model time corresponds to the third space dimension, hence Figs. 4.4–4.6 displays a "snapshot" at the time when the anti-baby Skyrmion is rotated by π. Baby Skyrmions are classified by a homotopy invariant $Q \in \mathbb{Z}$ due to $\pi_2(S^2) = \mathbb{Z}$. The analytic expression for Q is given by

$$Q = \frac{1}{4\pi} \int d^2x \, \phi \cdot \partial_1 \phi \times \partial_2 \phi, \tag{4.28}$$

where 1 and 2 denote cartesian coordinates in $\mathbb{R}^2$, see (1.10). The topological charge density is half the α-component of $\mathbf{B}$ (4.1). The integral over the whole plane vanishes because the contributions

for negative and for positive x exactly cancel. However, if integrated over the positive halfplane only (4.28) yields the baby Skyrmion number for ansatz (4.25):

$$Q = \frac{1}{8\pi} \int_0^{2\pi} d\beta \int_0^\infty d\eta \, \frac{a^2}{\tau^2} B_\alpha = M \,, \tag{4.29}$$

where we use B_α of (4.26).

Next we turn to Hopfions of topological charge two. For parametrisation (4.25) there are two ways of creating a Hopfion with $H = 2$, namely by setting either N or M to 2. Both cases correspond to two Hopfions sitting on top of each other. In order to determine which configuration represents the true ground state we computed their energies and found that the configuration with $N = 2, M = 1$ yields the lower energy for all couplings. The interpretation of the $H = 2$ solutions in terms of a (2+1)-dimensional soliton/anti-soliton pair is equivalent to the one given above for the 1-Hopfion. Because the multiplicity of the azimuthal rotation is $N = 2$ for the 2-Hopfion, the anti-baby Skyrmion in the negative x-halfplane (see Fig. 4.5) has a relative angle of π compared to the anti-baby Skyrmion of Fig. 4.4.

It is instructive to investigate how the inclusion of a potential term $U[\phi]$ alters the configuration. Its energy can be lowered by rescaling $\mathbf{x} \to \lambda\mathbf{x}$, $(\lambda \to 0)$ under which $U \to \lambda^3 U$. This means that the potential term induces a "shrinkage" of the configuration in the sense that the favoured position of the fields is closer to their vacuum value. This effect is counter-balanced by the higher-order derivatives in the energy functional (4.20), compare the discussion given in chapter 1.

Any potential explicitly breaks the model's global $O(3)$ symmetry because $O(3)$ acts transitively on the target space. We chose $U = m^2 \int d^2x \, (1 - \mathbf{n} \cdot \boldsymbol{\phi})$, where the parameter m is of dimension (length)$^{-1}$ and, in a quantum version of the theory, becomes the mass of the elementary excitations. The minimum energy solution for $m = 4$ can be seen in Fig. 4.6. The tube-like region where the field is in the southern hemisphere has clearly shrunk. Adding a linear potential term also means that the fields fall off exponentially at large distances. The reason is that the equations of motion become in the asymptotic limit those of the massive Klein-Gordon equation.

The fields of minimal energy correspond, via (4.20), to distributions of the potential energy which are displayed in Figs. 4.7–4.8. Despite the toroidal structure of the fields, we find that the potential energy for the Hopfion of $H = 1$ is lump-shaped, see Fig. 4.7. Although unexpected, this is not entirely unlikely, because the field changes far more rapidly within the disc $|\mathbf{x}| \le a$ than outside it. Hence the gradient energy, which determines the energy distribution can be concentrated in the vicinity of the origin.

If the potential term U becomes very large compared to the gradient terms one expects the energy to become more localized around the filament where the fields are far away from the vacuum. We observe this transition to a toroidal energy distribution at $m \approx 4$ for $g_1 = 1, g_2 = 0$.

The energy distribution of the 2-Hopfion is of toroidal shape (for all m), as shown in Fig. 4.8. It is a common feature in many soliton theories that solutions of topological charge two are tori, notably for Skyrmions, baby Skyrmions and magnetic monopoles. The numerical values for the potential energy V are plotted in Fig. 4.9, which also shows the topological bound eq. (4.16). For a pure Skyrme coupling we obtain energies of 197Λ and $2 * 158\Lambda$ for the 1-Hopfion and 2-Hopfion respectively. Moreover, it turns out that for all couplings the 2-Hopfion has a lower energy per topological unit than the 1-Hopfion. It is interesting to ask whether the 2-Hopfion is in a stable state or likely to decay into two Hopfions of charge one. The potential energy equals the negative force integrated from zero to infinity. The negative mass gap between the 2-Hopfion and two single Hopfions therefore means that at least in a finite region in space the forces must be attractive. If this attractive range includes the region of small $\mathbf{r}$, the relative distance of the two Hopfions, then the toroidal configuration Fig. 4.8 is stable under perturbations. Naturally, there can be a range of $\mathbf{r}$ in which the forces are repulsive, however, an investigation of such interactions would require a full (3+1)-dimensional simulation which is beyond our present means. Also note that the gap between the energies per Hopfion is largest when the fourth-order terms are purely the Skyrme term. On the other hand, for $g_1 \rightarrow -2g_2$, (i.e. $g \rightarrow 1$) the energy of the quartic terms tends to zero. Hence, by taking the limit the energy of the soliton vanishes as a consequence of the above mentioned Hobart-Derrick theorem.

4.5   Spinning Hopfions

Finally, we study the effect of a slow rotation around the axis of symmetry. For this we use a Lorentz-invariant extension of our model into (3+1)-dimensional space-time. The energy of the rotating Hopfion $E = T + V$, where V is the potential energy given by eq. (4.20) and T is the kinetic energy functional:

$$T[\phi] = \Lambda \int d^3x \, \frac{1}{2} \left(\partial_t \phi\right)^2 + \frac{g_1}{8} \left(\partial_t \phi \times \partial_i \phi\right)^2 + \frac{g_2}{8} \left(\partial_t \phi\right)^2 \left(\partial_i \phi\right)^2 + O\left(\left(\partial_t \phi\right)^4\right) . \qquad (4.30)$$

In the spirit of a moduli space approximation we assume that the configuration does not alter its shape due to the rotation ("rigid rotor"), i.e. it is given at any time by a static solution (see [7] for a review on similar treatment of the Skyrmion). T is then given by, including second-order

terms only, $T = J_{ij}\omega^i\omega^j/2$, where J_{ij} is the tensor of inertia. For simplicity, we restrict ourselves to rotations around the z-axis, i.e. $J = J_{\alpha\alpha}$, $\omega = \omega_\alpha$. We then impose time dependence on the azimuthal angle by $\alpha \to \alpha + \frac{\omega}{N}t$ with constant velocity ω. T leads to a term in the energy that is proportional to ω^2:

$$E = \frac{J}{2}\omega^2 + V, \tag{4.31}$$

where terms $O(\omega^4)$ are neglected. Using (4.25), J is given by

$$J = 2\pi\Lambda \int d\eta d\beta \left[1 + \frac{g_1}{2}\frac{(\nabla w)^2}{1-w^2} + \frac{g_2}{2}\left(\frac{(\nabla w)^2}{1-w^2} + \left((\nabla v)^2 + \frac{N^2\tau^2}{a^2\sinh^2\eta}\right)(1-w^2)\right)\right](1-w^2). \tag{4.32}$$

J can be measured explicitly on the individual solution. We plotted the values for $H = 1$ and $H = 2$ in Fig. 4.10. The moment of inertia per Hopfion is always larger for the $H = 1$ solution, with an increasing gap for decreasing g. This should be compared with the dependence of V on g.

The functional V (4.20) is invariant under α-rotations while the fields of ansatz (4.25) are clearly not. Therefore, upon quantization, the coordinate α describes a zero-mode and requires treatment as a collective coordinate. This is similar to the problem of the rotating radially symmetric Skyrmion. In analogy to the Skyrme model we therefore use, as a first approximation, the spectrum obtained by a straightforward quantization. The canonical momentum is $l = i\frac{d}{d\alpha}, (\hbar = 1)$ and the rotational energy $T = -l^2/2J$. It is then trivial to solve the eigenvalue problem $T\psi = \lambda\psi$, which gives $\lambda_n = \frac{n^2}{2J}$.

The rotations around the x_1- and x_2-axis are also zero-modes of the potential energy. However, because of the symmetry $z \to -z$ one would have to identify configurations that differ by an angle of π, which means that only even eigenvalues are allowed.

4.6 Conclusions

We have studied topological solitons in a generalized non-linear $O(3)$ σ-model in three space dimensions. Physically one may think of them as a model for hadronic matter or topological defects in a condensed matter system. By using a general ansatz for the fields we obtained explicit numerical solutions for soliton number one and two. Unexpectedly, the energy of the 1-Hopfion is distributed as a lump. We also observed that two solitons sitting on top of each other have a

lower energy than two infinitely separated solitons, thus indicating an attractive range between two lumps.

As far as the relation to knot theory is concerned, the 2-Hopfion is a torus which is the simplest form of a knot, the so-called "unknot". However, this feature also occurs for Skyrmions and BPS-monopoles. From the numerical evidence of the 1-Hopfion we conclude that, although the field-configuration of higher topological charges might be of knotted structure, the potential energy distribution may well be of much simpler shape. To decide this, a genuine three-dimensional simulation is necessary.

There are several interesting questions which remain unanswered. In particular, the stability of Hopfions of higher topological charge deserves some scrutiny. It is worthwhile asking how multi-solitons which sit on top of each other, or at least are very close, behave under induced perturbations. In analogy to planar $O(3)$ σ-models there might be several decay channels into less symmetric configurations [47].

At the opposite end of the scale, it would be instructive to look in greater detail at the interaction potential of two or more well-separated Hopfions. This is also interesting in comparison to the well-studied dynamics of Skyrmions and monopoles. Clearly, a first step in such an investigation would be to determine the asymptotic fields of the Hopf soliton. It seems obvious that inter-soliton forces will depend on the orientation of the Hopfions.

The complete description of Hopfion dynamics would require a huge numerical effort which can, however, possibly be reduced by an appropriate approximation scheme. For Bogomol'nyi solitons, the low-energy behaviour can be approximated via the truncation of the dynamics to the moduli space. Although our numerical results show that Hopfions are not of Bogomol'nyi type, given that the static forces between them are weak, there is a chance that their dynamics can be described by some kind of moduli space approximation, in analogy to Skyrmions (which are also not of Bogomol'nyi type).

Finally, it seems worth to study spinning Hopfions in a more sophisticated way. This should include an assessment of the back-reaction of the rotation on the matter fields. From this one expects a non-trivial shift of the energy levels in the rotation spectrum and possibly radiation of excessive energy.

Appendix

We prove that for $\phi \in S^2$ holds:

$$2 \sum_{i,j=1}^{3} (\partial_i \phi \cdot \partial_j \phi)^2 \geq \sum_{i,j=1}^{3} (\partial_i \phi)^2 (\partial_j \phi)^2 . \qquad (4.33)$$

To shorten the notation, we rename $\partial_1 \phi = a, \partial_2 \phi = b, \partial_3 \phi = c$. Then we can write:

$2 \sum_{i,j=1}^{3} (\partial_i \phi \cdot \partial_j \phi)^2 - \sum_{i,j=1}^{3} (\partial_i \phi)^2 (\partial_j \phi)^2$ $\qquad = $

$a^4 + b^4 + c^4 + 4 \left((ab)^2 + (ac)^2 + (bc)^2 \right) - 2(a^2 b^2 + a^2 c^2 + b^2 c^2)$ $\qquad = $

$\frac{1}{2}(a^2 - b^2)^2 + \frac{1}{2}(a^2 - c^2)^2 + \frac{1}{2}(c^2 - b^2)^2 + 4 \left((ab)^2 + (ac)^2 + (bc)^2 \right) - (a^2 b^2 + a^2 c^2 + b^2 c^2)$ $\quad \geq$

$4 \left((ab)^2 + (ac)^2 + (bc)^2 \right) - (a^2 b^2 + a^2 c^2 + b^2 c^2) .$

$$\qquad (4.34)$$

Now we use that a, b and c are vectors in a plane perpendicular to ϕ. This means we can express $(ab)^2$ as $a^2 b^2 \cos^2 \gamma_1$, where γ_1 is the angle between a and b. Defining γ_2 as the angle between b and c we can write the rhs of (4.34) as:

$$a^2 b^2 (4 \cos^2 \gamma_1 - 1) + a^2 c^2 (4 \cos^2 \gamma_2 - 1) + b^2 c^2 (4 \cos^2(\gamma_1 + \gamma_2) - 1) . \qquad (4.35)$$

The remainder of the proof is to show that this expression is positive definite. To accomplish this, we assume without loss of generality, that $a \geq b \geq c$, from which follows that (4.35) is larger or equal than

$$c^4 (4(\cos^2 \gamma_1 + \cos^2 \gamma_2 + \cos^2(\gamma_1 + \gamma_2)) - 3) \equiv \Gamma(\gamma_1, \gamma_2) . \qquad (4.36)$$

Γ defines a surface in $\mathbb{R}^3$ which is parametrized by γ_1 and γ_2. It can be discussed using standard calculus tools. This yields that for $\gamma_1, \gamma_2 \in [0, 2\pi)$, $\Gamma = 0$ is the minimum at $\gamma_1 = \gamma_2 = \pi/3$ and $\gamma_1 = \gamma_2 = 2\pi/3$. These cases differ by the transformation $b \to -b$ and correspond to a symmetric arrangement of a, b, c.
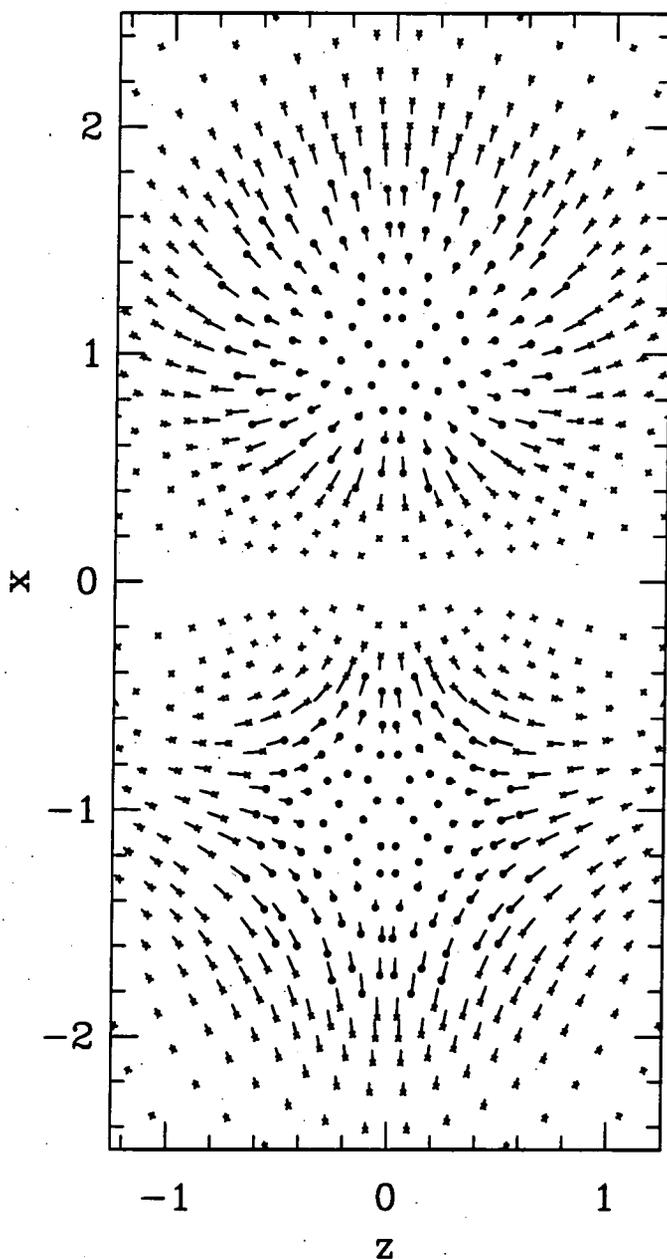
fig. 4.4: Field configuration in the xz-plane for $H = 1, g_1 = 0.4, g_2 = 0.4$. The field is projected into the $\phi_1\phi_2$-plane. A cross indicates $\phi_3 > 0$, a dot $\phi_3 < 0$. Therefore the vacuum state is denoted by a cross only.
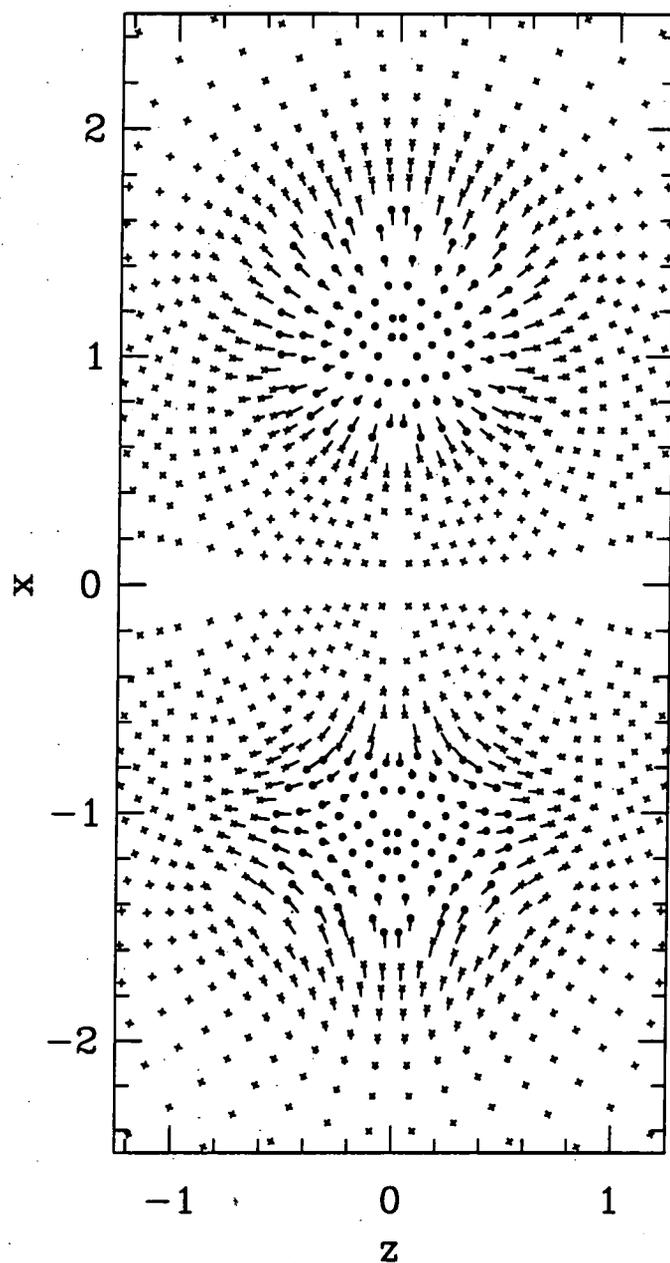
fig. 4.5:   Field-configuration of $H = 2, g_1 = 0.4, g_2 = 0.4$.
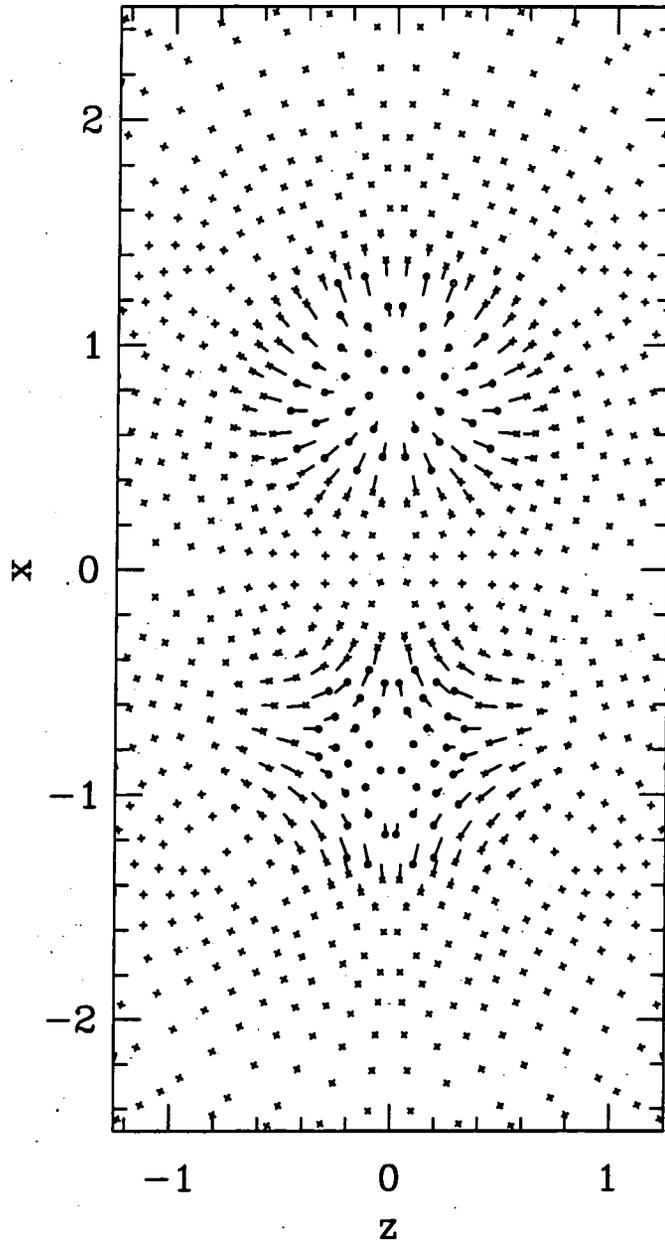
fig. 4.6: Field-configuration with potential term, $H = 1, g_1 = 1, g_2 = 0, m = 4$.
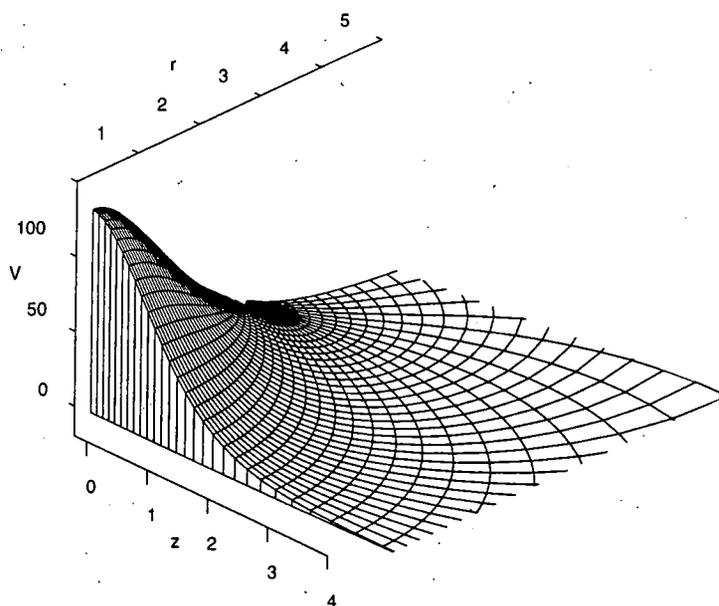
fig. 4.7: Potential energy density $\mathcal{V}$ (arbitrary units) for $H = 1, g_1 = 0.4, g_2 = 0$ in cylindrical coordinates r, z. The Hopfion is pancake-shaped.
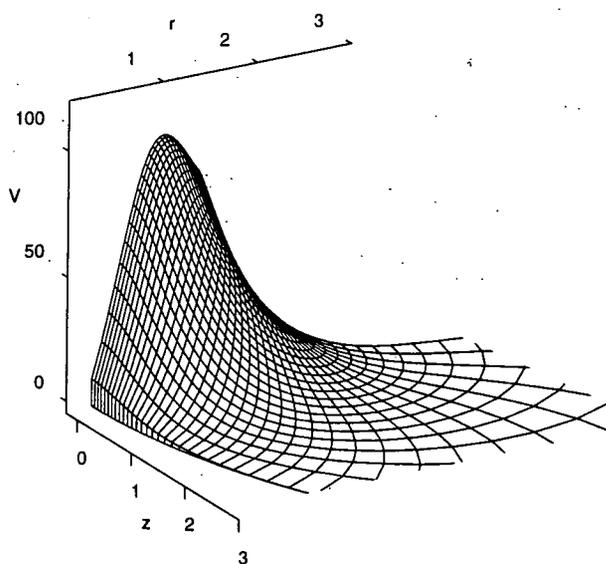

fig. 4.8: Potential energy density $\mathcal{V}$ for $H = 2, g_1 = 0.4, g_2 = 0.8$ over r, z. The configuration is torus-shaped.
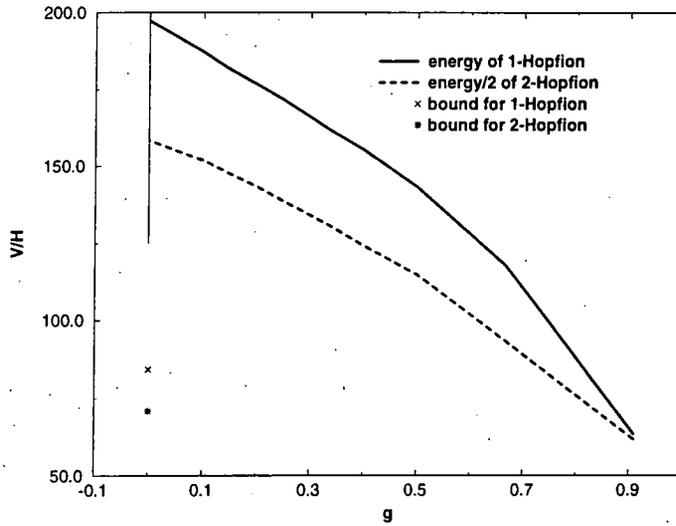
fig. 4.9:   Dependence of the potential energy V per Hopfion on the quartic couplings. They are parametrized as $g_1 = 1 - 3g, g_2 = g$. Hence $g = 0$ corresponds to pure $(\partial_i \phi \times \partial_j \phi)^2$ coupling, $g = 1/3$ to pure $(\partial_i \phi)^2 (\partial_j \phi)^2$ coupling and $g = 1$ to the case $(\partial_i \phi)^2 (\partial_j \phi)^2 - 2(\partial_i \phi \times \partial_j \phi)^2$. The energy is given in units of Λ. The topological bounds for pure Skyrme coupling are also displayed.

fig. 4.10: Dependence of the moment of inertia J in α-direction per Hopfion on the coupling g, defined as above.

Chapter 5

Solitons in the CP^2 Baby Skyrme Model

The investigations in the previous chapters are based on the $O(3)$ σ-model and its modifications by the introduction of gauge fields or higher-derivative terms. On a classical level and without gauge field dynamics, the $O(3)$ $\sigm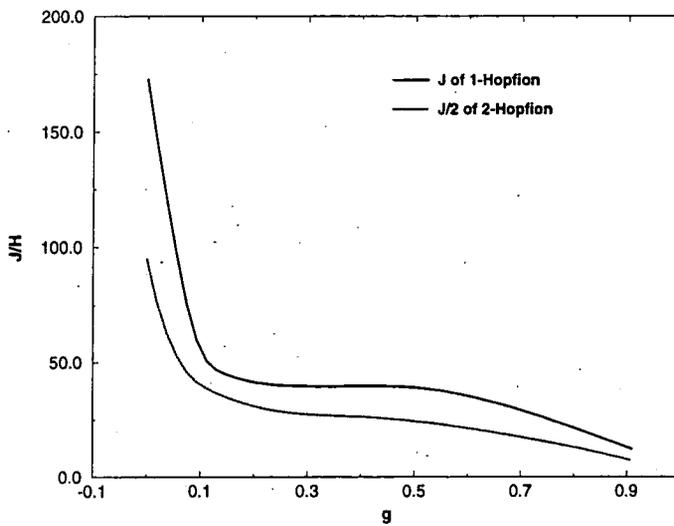a$-model is equivalent to the $\mathbb{CP}^1$-model. The natural generalizations of these models to higher target-manifolds are the $O(N+1)$ σ-models and the $\mathbb{CP}^{N-1}$-models respectively, which, however, differ in their topology and in their soliton solutions for $N > 2$. The non-linear $O(N+1)$ σ-models are straightforward generalizations of the $O(3)$ σ-model. The fields ϕ are $(N+1)$-component vectors, subject to $\phi_a\phi^a = 1$ and thus taking values on S^N. The action is equivalent to (1.6) and is invariant under global rotations $\phi_a \rightarrow R_{ab}\phi^b$, $R \in O(N+1)$. Among these models of particular interest is the $O(4)$ σ-model with a Skyrme term in (3+1) dimensions : it is equivalent to the $SU(2)$-Skyrme model, cf. (4.13), chapter 4.

One reason to work in enlarged target-spaces is that in general there will be a greater number of parameters and thus possibly a richer variety of static solutions and diverse time-evolutions. An example which illustrates this are time-dependent lumps in the $\mathbb{CP}^2$-model. During a collision of two solitons their energy densities overlap and they can form a ring *or* a lump, depending on some internal parameters. In the $\mathbb{CP}^1$-model, all scattering goes through a toroidal state [95].

It is also interesting to see how lower-dimensional models and their solutions fit into an extended theory, in particular, one can ask about the nature of embeddings and their symmetry transformations. Often solutions of a lower-dimensional model correspond to subspaces of the parameter-space of solutions to the higher-dimensional theory. Another interesting aspect is that

the number of possible terms in the action for a given set of conditions, such as Lorentz-invariance, global symmetries or positiveness, can increase with the dimension of the target-manifold, thus adding to the choice of models. These are some of the questions that we address in this chapter. It is often difficult though, to examine all these problems for a general N and therefore a good tactics is to start looking at small N first, which can indicate more general features in an inductive way. Consequently, we concentrate here on the $\mathbb{CP}^2$-model, but first we review some known general properties of the $\mathbb{CP}^{N-1}$-models.

The $\mathbb{CP}^{N-1}$-models in (2+1) dimensions are an obvious object of interest for various reasons. Their static solutions are known analytically, which allows to model their low-energy dynamics by a moduli space approximation. This was investigated some time ago by Ward [52] for the $\mathbb{CP}^1$-model, by Stokoe and Zakrzewski for $\mathbb{CP}^{N-1}$-model [96] and later more detailed for the $\mathbb{CP}^1$-model by Leese [97]. For the $\mathbb{CP}^1$ baby Skyrme model a moduli space approximation was performed by Sutcliffe [98]. It was generally found that in a head-on collision two solitons can scatter at right angles or back to back depending on the initial conditions, although the complete discussion in [97] shows that the details are more subtle and other scattering angles are possible. Right angle scattering of two solitons was also observed in studies on the dynamics of solitons in a $\mathbb{CP}^2$-model by Piette et al. in [95]. There the dynamics were altered by adding a term that involves three derivatives which are contracted by an antisymmetric tensor ε_{ijk}, thus making this term metric-independent. Such a term resembles the Hopf-term of the $\mathbb{CP}^1$-model, but by contrast for $\mathbb{CP}^2$ it is not a total derivative and thus contributes to the equations of motion. Consequently, it alters the dynamics of the solitons and this happens by giving them a non-zero angular momentum.

Another interesting observation was made by Hindmarsh in [99]. There it was shown that the $\mathbb{CP}^{N-1}$-model can be obtained from an extended Abelian Higgs model in (2+1) dimensions, where the domain of the fields is $\mathbb{C}^N$. For a specific choice of the gauge potential and in the limit of small momenta, the model can be mapped to the $\mathbb{CP}^{N-1}$-model with a Skyrme term. The Maxwell term in the action of the Abelian Higgs model under this transformation corresponds to the Skyrme term.

In this chapter we mainly study a related model, namely the $\mathbb{CP}^2$-model in (2+1) dimensions with a Skyrme term. Here the solitons are stabilized by a potential and fourth-order terms in the action, which are however, not unique for $\mathbb{CP}^2$. We find a family of analytic static one-soliton solutions and study the two-soliton configuration numerically in a gradient-flow equation on the moduli space.

5.1 CP^{N-1}-models Revisited

CP^{N-1}-models are examples of theories where the field-space is given by a Grassmanian manifold. This is a complex manifold which describes an M-dimensional subspace of the N-dimensional complex Euclidean space $\mathbb{C}^N$. It can be written as a coset $G(M, N)$:

$$G(M,N) = \frac{U(N)}{U(M) \times U(N - M)} . \tag{5.1}$$

The complex projective spaces are the sets of lines through the origin in $\mathbb{C}^N$ and correspond to $M = 1$. The canonical coordinates on $\mathbb{C}^N$ are the homogeneous or cartesian coordinates $z = (z_1, \ldots, z_N)$. According to the definition given above, CP^{N-1} can be described as the complex space in which all the z that differ by a complex number are identified, $z \sim \lambda z, z \neq 0, \lambda \in \mathbb{C}$. Therefore

$$CP^{N-1} = \left(\mathbb{C}^N - \{0\}\right)/\mathbb{C}^* , \tag{5.2}$$

where $\mathbb{C}^*$ is the group of non-zero complex numbers. In order to write the CP^{N-1}-model in terms of homogeneous coordinates, one has to impose the equivalence relation $z \sim \lambda z$. The first step is to fix the magnitude of z by setting $z^\dagger z = 1$ which restricts the field to values on $S^{2N-1} = U(N)/U(N - 1)$. Geometrically, this sphere is a $U(1)$-bundle over base-space CP^{N-1}, which illustrates formula (5.1) for $M = 1$. The second step is thus to impose local $U(1)$-gauge invariance on the action which removes any dependence of the model on the corresponding phase. Consequently, the usual quadratic expression $\partial_\alpha z^\dagger \partial^\alpha z/2$ in the Lagrangian is replaced by

$$\mathcal{L}_2 = \frac{1}{2} (D_\alpha z)^\dagger (D^\alpha z) , \tag{5.3}$$

where the dagger indicates hermitian conjugation and the covariant derivative is

$$D_\alpha z = \partial_\alpha z + i A_\alpha z . \tag{5.4}$$

($\alpha = 0, 1, 2$). The equations of motion for A_α yield:

$$A_\alpha = i z^\dagger \partial_\alpha z , \tag{5.5}$$

which also shows that the CP^{N-1}-models are a non-linear theory. Although A_α is not an independent field and in particular not related to any electromagnetic interactions, because of the formal

analogy, we will refer to it as a gauge field and generally adopt the notation of gauge theory. The model (5.3) has a global $SU(N)$-symmetry, resulting in $N^2 - 1$ conserved global charges and the local $U(1)$-symmetry.

The projective space $\mathbb{CP}^{N-1}$ can also be described in terms of the inhomogeneous coordinates W. In a region where $z_a \neq 0$, they are defined as follows

$$W = (w_1, \ldots, w_{N-1}) \equiv \frac{z_1}{z_a}, \ldots \frac{z_{a-1}}{z_a}, \ldots \frac{z_{a+1}}{z_a}, \ldots \frac{z_N}{z_a}, \tag{5.6}$$

which is by construction independent on the choice of the representative z of the equivalence class; let z, $\tilde{z}$ be elements of such class: $\tilde{z}_b/\tilde{z}_a = \lambda z_b/\lambda z_a = z_b/z_a$. On a patch which includes $z_a = 0$, but $z_c \neq 0$ one defines:

$$\tilde{W} = (\tilde{w}_1, \ldots, \tilde{w}_{N-1}) \equiv \frac{z_1}{z_c}, \ldots \frac{z_{c-1}}{z_c}, \ldots \frac{z_{c+1}}{z_c}, \ldots \frac{z_N}{z_c}. \tag{5.7}$$

In the regions, where both patches overlap, the transformation between the inhomogeneous coordinates W and $\tilde{W}$ is obtained by

$$W = \frac{z_c}{z_a} \tilde{W}. \tag{5.8}$$

The complex projective space $\mathbb{CP}^{N-1}$ is a Kähler manifold. This implies that there is a hermitian metric $\tau_{a\bar{b}}$ and associated with this metric is a closed, antisymmetric and real two-form $\Omega = \tau_{a\bar{b}} dz^a \wedge d\bar{z}^b$, $d\Omega = 0$. In terms of the cartesian coordinates on $\mathbb{C}^N$, $\tau_{a\bar{b}}$ is given by:

$$\tau_{a\bar{b}} = \frac{\delta_{ab} |z|^2 - z_a \bar{z}_b}{|z|^4}. \tag{5.9}$$

This expression is called the Fubini-Study metric and is the natural metric on $\mathbb{CP}^{N-1}$, if embedded in $\mathbb{C}^N$.

The Kähler potential, which corresponds to (5.9), is patchwise defined. In a region U_a, where $z_a \neq 0$ it is

$$K_a = \ln \left(\left| \frac{z_1}{z_a} \right|^2 + \ldots + \left| \frac{z_N}{z_a} \right|^2 \right), \tag{5.10}$$

such that

$$\tau_{a\bar{b}} = \frac{\partial^2 K_a}{\partial \bar{z}_a \partial z_b}. \tag{5.11}$$

The imposition of the phase invariance for homogeneous coordinates is equivalent to changing the metric on $\mathbb{C}^N$ from the flat-space metric to the Fubini-Study metric, i.e.

$$\partial_\alpha \bar{z}_a \partial^\alpha z_b \delta^{ab} \to \partial_\alpha \bar{z}_a \partial^\alpha z_b \tau^{a\bar{b}} , \tag{5.12}$$

which can be verified by using (5.5). From the topological point of view the existence of solitons in the $\mathbb{CP}^{N-1}$-model on $\mathbb{R}^2$ is based on

$$\pi_2 \left(\mathbb{CP}^{N-1} \right) = \mathbb{Z} , \qquad N > 1 . \tag{5.13}$$

The non-triviality of this homotopy stems from the topology of maps from the (compactified) plane to $\mathbb{CP}^1$ subspaces of $\mathbb{CP}^{N-1}$. Explicitly, the degree is given by

$$Q = \frac{1}{4\pi} \int d^2 x \, \varepsilon_{ij} \, (D_i z)^\dagger (D_j z) . \tag{5.14}$$

Here, to avoid confusion with the target-space dimension N, we changed our notation and we have called the topological charge Q rather than N as before. Interestingly, there are two ways to look at the topological charge in the $\mathbb{CP}^{N-1}$-models. For finite energy, the covariant derivative has to vanish at spatial infinity

$$\lim_{|\mathbf{x}| \to \infty} D_i z = 0 . \tag{5.15}$$

For the gauge field this implies

$$A_i = \frac{i \partial_i z_a}{z_a} , \qquad \forall a . \tag{5.16}$$

A_i is real and independent on a, which leads to

$$\lim_{|\mathbf{x}| \to \infty} z = z_\infty e^{i2\pi h(\theta)} , \tag{5.17}$$

where z_∞ is a fixed unit-vector and θ is the polar angle on $\mathbb{R}^2$. In analogy to the Abelian Higgs model, single-valuedness of z implies $h(2\pi) = h(0) + n$, $n \in \mathbb{Z}$. Thus there is an associated topological charge which stems from $\pi_1(S^1) \neq 0$ and counts the winding number of the gauge field at infinity:

$$Q = \frac{1}{2\pi} \oint_{S^1} d\theta A_\theta = \frac{1}{2\pi} \left(h(2\pi) - h(0) \right) = n . \tag{5.18}$$

The relation to formula (5.14) can be established using Stokes' theorem, the integrand of (5.14) corresponds to the "magnetic field" $F_{12} = \partial_1 A_2 - \partial_2 A_1$.

All the pure $\mathbb{CP}^{N-1}$-models are of Bogomol'nyi-type and the corresponding argument generalizes almost trivially from $\mathbb{CP}^1$. The potential energy can be written as:

$$V[z] = \frac{1}{2} \int d^2x \, |D_1 z \pm iD_2 z|^2 \mp 4\pi Q \,. \tag{5.19}$$

Minima are obtained for

$$(D_1 \pm iD_2)z \equiv D_\pm z = 0 \,, \tag{5.20}$$

where $D_\pm z$ indicates the derivative with respect to $x_\pm = x_1 \pm ix_2$. The n-soliton solutions to this equation can be written in terms of (anti-) holomorphic functions P_n:

$$z = \frac{P_n}{|P_n|} \,, \tag{5.21}$$

where, in full generality, for a holomorphic P_n

$$P_n = \begin{pmatrix} \lambda_1(x_+ - a_1^1) & \dots & (x_+ - a_n^1) \\ \vdots & & \vdots \\ \lambda_N(x_+ - a_1^N) & \dots & (x_+ - a_n^N) \end{pmatrix} \,. \tag{5.22}$$

It is interesting to ask, how many of the parameters (λ_r, a_i^s), $(r, s = 1 \dots N; i = 1 \dots n)$ correspond to physically distinct fields, in other words, we ask for the dimension of the n-soliton moduli space. The way it is written above, P_n has $2N(n+1)$ real parameters. Two of these are redundant because the model lives on the projective space, i.e. $z \sim \lambda z$; the $U(1)$-gauge degree of freedom and further two real parameters, corresponding to a choice of the origin in $\mathbb{R}^2$ should also not be counted. The multiplicative factors in front of each component can be transformed to unity by using the global $SU(N)$-symmetry. This removes a further $(2N - 2)$ degrees of freedom, leaving $2Nn - 1$.

Skyrme terms

It has been mentioned before in this thesis that in space-dimensions greater than one there has to be a higher-order derivative term in the Lagrangian in order to allow non-singular solutions. If one imposes the constraint that such a term respects the symmetries of the theory (global $SU(N)$ and local $U(1)$) and includes only second-order terms of derivatives with respect to any variable (especially the time-derivative), one is left for $\mathbb{CP}^{N-1}$-models with two generically different Skyrme terms which can be written in terms of the tensor $A_{\alpha\beta}$ [100]:

$$A_{\alpha\beta} \equiv (D_\alpha z)^\dagger (D_\beta z) \,. \tag{5.23}$$

Note that $\bar{A}_{\alpha\beta} = A_{\beta\alpha}$ and hence A is hermitian. Now we decompose $A_{\alpha\beta}$ into its real symmetric and its imaginary antisymmetric part:

$$F_{\alpha\beta} = -i(A_{\alpha\beta} - A_{\beta\alpha}) \quad = -2\mathrm{Im}\,(A_{\alpha\beta}) \quad = i\left(z_\alpha^\dagger z_\beta - z_\beta^\dagger z_\alpha\right) = \partial_\alpha A_\beta - \partial_\beta A_\alpha \quad = \left[D_\alpha^\dagger, D_\beta\right]_- ,$$

$$G_{\alpha\beta} = A_{\alpha\beta} + A_{\beta\alpha} \qquad = 2\mathrm{Re}\,(A_{\alpha\beta}) \quad = z_\alpha^\dagger z_\beta + z_\beta^\dagger z_\alpha + 2A_\alpha A_\beta \qquad = \left[D_\alpha^\dagger, D_\beta\right]_+ , \tag{5.24}$$

such that $A_{\alpha\beta} = (G_{\alpha\beta} + iF_{\alpha\beta})/2$. To shorten the notation we have introduced here $z_\alpha = \partial z/\partial x^\alpha$. F and G are manifestly gauge invariant and can be included in the Lagrangian as

$$\mathcal{L}_4^{\mathrm{G}} = \frac{1}{8}\,(\,\mathrm{Tr}\,G)^2 - \frac{1}{8}\,\mathrm{Tr}\,G^2 , \qquad \mathcal{L}_4^{\mathrm{F}} = \frac{1}{4}\,\mathrm{Tr}\,F^2 . \tag{5.25}$$

Giving the fourth-order terms different couplings μ_{F} and μ_{G} respectively, the $\mathbb{C}P^{N-1}$ Skyrme model is defined by:

$$\mathcal{L} = \mathcal{L}_2 + \mu_{\mathrm{G}}\mathcal{L}_4^{\mathrm{G}} + \mu_{\mathrm{F}}\mathcal{L}_4^{\mathrm{F}} + \mu_{\mathrm{U}}U . \tag{5.26}$$

$\mathcal{L}_4^{\mathrm{F}}$ is what is usually called the Skyrme term. For $N = 2$ it turns out that $\mathcal{L}_4^{\mathrm{F}}$ and $\mathcal{L}_4^{\mathrm{G}}$ are equivalent [100]. This can be indicated by using the equivalence of the $\mathbb{C}P^1$ and the $O(3)\,\sigma$-model. In the latter model the fields are three-component real vectors $\phi \in S^2$. The relation to the z-fields is given by the Hopf map $\phi_a = z^\dagger\sigma_a z$, $(a = 1, 2, 3)$ where σ_a are the Pauli matrices, cf. (4.2). Then the following equalities hold:

$$(\,\mathrm{Tr}\,G)^2 = 8\sum_\alpha \left(\partial_\alpha\phi \cdot \partial^\alpha\phi\right)^2 ,$$

$$\mathrm{Tr}\,G^2 = 8\sum_{\alpha\beta} \left(\partial_\alpha\phi \cdot \partial_\beta\phi\right)^2 , \tag{5.27}$$

$$\mathrm{Tr}\,F^2 = 4\sum_{\alpha\beta} \left(\partial_\alpha\phi \times \partial_\beta\phi\right)^2 .$$

To derive this we can use

$$\sigma_a^{ij}\sigma_a^{kl} = 2\delta^{ij}\delta^{kl} - \delta^{ij}\delta^{kl} , \qquad \sigma_a^{ij}\sigma_b^{kl}\sigma_c^{mn}\varepsilon^{abc} = 4(\delta^{il}\delta^{jm}\delta^{kn} - \delta^{in}\delta^{jk}\delta^{lm}) , \tag{5.28}$$

$(a, b, c = 1, 2, 3)$. The equation $\mathcal{L}_4^{\mathrm{G}} = \mathcal{L}_4^{\mathrm{F}}$ is then equivalent to the Lagrange identity:

$$(\partial_\alpha\phi \cdot \partial^\alpha\phi)^2 - (\partial_\alpha\phi \cdot \partial_\beta\phi)^2 = (\partial_\alpha\phi \times \partial_\beta\phi)^2 . \tag{5.29}$$

It is interesting to ask for the geometrical interpretations of the fourth-order terms $\mathcal{L}_4^{\mathrm{G}}$ and $\mathcal{L}_4^{\mathrm{F}}$. We showed above that the integral over the "field-strength" F_{12} is integer valued and counts the

windings of the gauge field at infinity. *A priori* there is no topological invariant related to G. As a possible way of thinking about the geometry of the model (5.26) we remind ourselves of the geometrical way in which Manton described the potential energy in the Skyrme model [101]. The argument is very general and does not even require the target-manifold to be a Lie-group; it applies to any Riemannian manifold. Given a map f between two such manifolds $\mathcal{M}$ and $\mathcal{N}$ endowed with orthonormal frames e^i and κ^a respectively, the Jacobi matrix of the map f is

$$J_{k\dot{r}} = e_k^i \partial_i f^a \kappa_r^a. \tag{5.30}$$

Using this, one defines a strain tensor $D = JJ^\dagger$, which is a measure of the local deformation induced by the map. It is constructed in a way such that it carries only indices of the base-space. Hence the number of its invariants (eigenvalues) equals the dimension m of $\mathcal{M}$, the physical space. Manton showed, that the potential energy functional of the Skyrme model (where $\mathcal{M} = \mathbb{R}^3$ and $\mathcal{N} = S^3$) can be expressed in terms of eigenvalues of D. Geometrically, the quadratic term in the energy is a measure for the distortion due to changes in the length of the local frame vectors while the Skyrme term indicates how the area spanned by two respective vectors gets deformed due to the map. This is to say, the Skyrme term energetically favours isometries.

For the case of interest to us $\mathcal{M} = \mathbb{R}^2$, $\mathcal{N} = \mathbb{C}^N$ and $f = z$. Given, that $\kappa_i^a \bar{\kappa}_i^b = \tau^{a\bar{b}}$ is the Fubini-Study metric on $\mathbb{C}^N$, one finds that the potential energy can be expressed in a similar fashion to the Skyrme model, where A_{ij} plays the role of D_{ij}. In two space-dimensions $(\text{Tr } A)^2 - \text{Tr } A^2 = 2 \det A$ and the potential energy that corresponds to $\mathcal{L}_2 + \mathcal{L}_4^G + \mathcal{L}_4^F$ can be expressed as

$$V = \int d^2x \, \frac{1}{2} \text{Tr } A + \frac{1}{2} \det A. \tag{5.31}$$

5.2   The CP^2 baby Skyrme Model

Equipped with the general framework described above, we will now investigate a concrete example, namely the $\mathbb{C}P^2$ Skyrme model. According to (5.1), the $\mathbb{C}P^2$-manifold is described by

$$\mathbb{C}P^2 = \frac{U(3)}{U(2) \times U(1)}. \tag{5.32}$$

We define the inhomogeneous coordinates on the patch, where $z_1 \neq 0$, $W = (z_2, z_3)/z_1 \equiv (w, v)$, related to the cartesian coordinates $z = (z_1, z_2, z_3)$ as follows:

$$z = \frac{(1, w, v)}{\sqrt{1 + |w|^2 + |v|^2}} .$$ (5.33)

In terms of W, the tensor $A_{\alpha\beta}$ becomes:

$$A_{\alpha\beta} = \frac{1}{M^4} \left\{ \left(1 + |w|^2\right) \bar{v}_\alpha v_\beta + \left(1 + |v|^2\right) \bar{w}_\alpha w_\beta - \bar{v} w \bar{w}_\alpha v_\beta - \bar{w} v \bar{v}_\alpha w_\beta \right\} ,$$ (5.34)

where $M = 1 + |w|^2 + |v|^2$ and $W_\alpha = \partial W / \partial x^\alpha$ for each component of W. The Lagrangian $\mathcal{L}_2$ is, in terms of W:

$$\mathcal{L}_2 = \frac{1}{2M^2} \left\{ |w_\alpha|^2 + |v_\alpha|^2 + |w_\alpha v - v_\alpha w|^2 \right\} ,$$ (5.35)

where the summation over α is assumed. The difference of the fourth-order terms is proportional to

$$\Delta \mathcal{L}_4 = \mathcal{L}_4^{\mathrm{G}} - \mathcal{L}_4^{\mathrm{F}} = 4(A_\alpha^\alpha A_\beta^\beta - A_{\alpha\beta} A^{\beta\alpha}) .$$ (5.36)

For time-independent fields, this difference can be expressed in terms of W as follows :

$$\Delta \mathcal{L}_4 = \frac{4}{M^3} \left| w_{x_1} v_{x_2} - w_{x_2} v_{x_1} \right|^2 .$$ (5.37)

Let $W^a = W_{\mathrm{Re}}^a + i W_{\mathrm{Im}}^a$ where the index a indicates the component ($a = 1, 2; W^1 = w, W^2 = v$) then $\Delta \mathcal{L}_4 = 0$ if

$$\frac{\partial W_{\mathrm{Re}}^a}{\partial x_1} = \frac{\partial W_{\mathrm{Im}}^a}{\partial x_2} , \qquad \frac{\partial W_{\mathrm{Re}}^a}{\partial x_2} = -\frac{\partial W_{\mathrm{Im}}^a}{\partial x_1} ,$$ (5.38)

which are the Cauchy-Riemann equations. Therefore the two fourth-order terms are identical for static holomorphic functions and especially for solutions to the pure $\mathbb{CP}^2$-model.

5.3   Solutions to the CP^2 Skyrme Model

We know that the static solutions of the pure $\mathbb{CP}^2$-model are given in terms of rational functions (5.22). The question naturally arises, whether one can find static analytic solutions to a model which includes a Skyrme term and a potential term. A systematic method is to use the freedom in the choice of the potential and reconstruct it from the equations of motion for a given ansatz of the fields. For $\mathbb{CP}^1$ Skyrme models there is a slightly more elegant method; one can adapt the Bogomol'nyi argument where the potential energy density is given by

$$\mathcal{V} = \frac{1}{2} (D_i z)^\dagger (D^i z) + \frac{\mu_{\mathrm{F}}}{4} F_{12}^2 + \mu_{\mathrm{U}} \mathcal{U} .$$ (5.39)

We rewrite the potential energy as

$$V_{\text{cp1}} = \int d^2x \, \frac{1}{2} \left(D_1 z \pm iD_2 z \right)^\dagger \left(D_1 z \pm iD_2 z \right) + \frac{\mu_\text{F}}{4} \left(F_{12} \pm 2\sqrt{\frac{\mu_\text{U}}{\mu_\text{F}}} \sqrt{\mathcal{U}} \right)^2$$
$$\mp 4\pi Q \mp \sqrt{\mu_\text{U} \mu_\text{F}} \int d^2x \, F_{12} \sqrt{\mathcal{U}} \, . \tag{5.40}$$

It can be shown that the last term also describes the topology $\pi_2(S^2)$ and is, in this sense, equivalent to the topological charge Q [102]. We know that the term F_{12} is proportional to the topological charge density (5.14), the pullback of the volume form on S^2. Geometrically, multiplication with the scalar function $\sqrt{\mathcal{U}}$ changes the "shape" of the target S^2 but not its topology and corresponds to a renormalization of the volume element on target S^2. Therefore one finds two self-dual equations, the solutions of which saturate the modified Bogomol'nyi bound

$$F_{12} = \mp 2\sqrt{\frac{\mu_\text{U}}{\mu_\text{F}}} \sqrt{\mathcal{U}} \, , \qquad D_1 z = \mp iD_2 z \, . \tag{5.41}$$

From the first equation, a potential can be constructed for a given holomorphic field which will automatically satisfy the second. In the $\mathbb{CP}^1$-model the field W consists of one complex component w and for $w = \lambda x_+$ the potential $\mathcal{U} = 8/(1 + |w|^2)^4$ was found to satisfy (5.41), [102].

For higher $\mathbb{CP}^{N-1}$, $N > 2$, this trick does not work any longer, the term $F_{12}\sqrt{\mathcal{U}}$ is in general not a total derivative (or, in differential geometric terms, not a closed two-form). However, one can, for a given holomorphic field, construct a potential which satisfies the variational equations

$$\partial_i \frac{\partial F_{12}^2}{\partial (\partial_i W_a)} = \frac{4\mu_\text{U}}{\mu_\text{F}} \frac{\partial \mathcal{U}}{\partial W_a} \, . \tag{5.42}$$

Solutions to these equations will not saturate the Bogomol'nyi bound and their stability or instability will have to be shown be different methods. Returning to the $\mathbb{CP}^2$-model, for the field

$$w = \lambda(x_+ - a) \, , \qquad v = b \, , \tag{5.43}$$

one finds the potential

$$\mathcal{U} = 8 \frac{\left(1 + |v|^2\right)^4}{\left(1 + |v|^2 + |w|^2\right)^4} \tag{5.44}$$

together with the constraint

$$2\sqrt{\frac{\mu_\text{U}}{\mu_\text{F}}} = \frac{|\lambda|^2}{1 + |b|^2} \, . \tag{5.45}$$

This potential preserves the $SU(2) \times U(1)$ symmetry of the model. The potential energy of this solution is given by $V = 2\pi(1 + 8/3\sqrt{\mu_U \mu_F})$. The parameter λ is a measure of the size of the soliton while a gives its position. The interpretation for b is less clear but, in a way, it describes how the CP^1-manifold spanned by w is embedded into CP^2. For constant b one observes that the solution above is a CP^1 embedding because all that v does in this case is to renormalize the couplings and the fields by a factor $(1 + |v|^2)$. The discussion of section 5.1 tells us that, after fixing the origin in the plane (by, say, setting $a = 0$), the one-soliton moduli space is three-dimensional. Due to the residual symmetry of the potential one can take λ to be real. The time-evolution of such a single lump is rather simple: unless it is pushed, it will sit there and possibly change its shape. One can study the time-evolution of a single or multiple soliton configuration in a moduli space approximation. This means that the dynamics of the full theory is truncated to the subspace of minimal energy solutions. The motion of the soliton is then described by the geodesic motion of a point-particle on the background of a Riemannian metric induced by the kinetic energy functional. Let ξ be the vector of the n-soliton solution parameter, $\mathcal{M}_n$ the n-soliton moduli space and $L = T - V$ the Lagrange function. The ξ are the coordinates on $\mathcal{M}_n$, while the metric $g_{ab}(\xi)$ on $\mathcal{M}_n$ is defined by

$$T = \frac{1}{2} g_{ab}(\xi) \dot{\xi}^a \dot{\xi}^b. \tag{5.46}$$

If one can neglect energy modes orthogonal to the direction of zero-modes, the motion in the moduli space is a good approximation to the solution of the full variational equations. Picturely speaking, the dynamics is described by a trajectory in the configuration space along the bottom of the valley defined by the potential energy. As long as the energies of the solitons are small, the solitons cannot climb up the potential well too much and their true trajectories will stay close to the moduli space. Due to the Skyrme terms and the potential $\mathcal{U}$, the original moduli space possesses a potential and the true energetic minima are subspaces of it (the quadratic term contributes only an irrelevant constant to this potential). However, given that the forces between the individual solitons are relatively weak, i.e. the moduli space is sufficiently flat, one can approximate the low-energy dynamics in the spirit of a perturbation theory.

For a single lump, however, the metric $g_{ab}(\xi)$ has divergent components, unless one chooses a compact domain for the theory. This means it requires infinite energy to change the solution in the corresponding direction. For the fields (5.43) given above, $\xi = (\lambda, b, a)$ and the divergent direction corresponds to $g_{\lambda\lambda}$. One can, however, study the soliton dynamics on $\mathcal{M}_2$, the 2-soliton moduli space, where the metric is finite. An ansatz for the 2-soliton field which has the correct

asymptotic behaviour for a large a is given by

$$w = \frac{\lambda}{2a}(x_+ + a)(x_+ - a), \qquad v = b.$$
(5.47)

It is, however, not clear how this ansatz relates to a true minimum of the potential energy. A way to study this problem numerically is the gradient-flow. In this procedure one starts with a point in the moduli space which is not a global minimum of V such that the two solitons exert a mutual force given by the gradient of the potential in the moduli space. They undergo a dissipative time-evolution which reduces the potential energy until a fixpoint is reached for $t \to \infty$. In practice one will, of course, truncate after a finite time. This time-evolution corresponds to a flow down the valley of potential energy with respect to the induced metric. The gradient-flow equations are:

$$g_{ab}\dot\xi^b = -\frac{\partial V[\xi]}{\partial \xi^a}.$$
(5.48)

For the 2-soliton configuration, there are three possibilities for the global minimum: the solitons are infinitely separated, coalesce or assume a stable state at a finite distance. For the actual computation, we modify the expression (5.47) and decompose ξ into magnitudes ψ and phases χ such that in polar coordinates $x_+ = r \exp(i\theta)$:

$$w = \psi_1 r^2 e^{i(2\theta + \chi_1)} + \psi_2 e^{i\chi_2}, \qquad v = \psi_3 e^{i\chi_3}.$$
(5.49)

The metric $g_{ab}(\psi, \chi)$, $(a, b = 1, 2, 3)$ is hermitian which implies for its components

$$|\psi_a| |\psi_b| g_{\psi_a \psi_b} = g_{\chi_a \chi_b}.$$
(5.50)

The metric gets contributions from $(D_0 z)^2$, $G_{00}G_{ii} - G_{i0}^2$ and F_{i0}^2. It can be computed in terms of hypergeometric functions and its explicit form is given in the appendix to this chapter. The potential on the moduli space that corresponds to (5.26), is, for a given topological sector Q of the configuration space, in polar coordinates (r, θ):

$$
\begin{aligned}
V_Q[\psi, \chi] =\ & 4\pi|Q| + \int dr d\theta\, r \left\{ \frac{(\mu_G + \mu_F)}{4r^2} F_{r\theta} + \mu_U \mathcal{U} \right\} \\
=\ & 4\pi|Q| + \int dr d\theta\, r \left\{ \frac{8(1 + \psi_3^2)^2((\mu_G + \mu_F)\psi_1^2 r^2 + \mu_U(1 + \psi_3^2)^2)}{(1 + \psi_1^2 r^4 + \psi_2^2 + \psi_3^2 + 2\psi_1\psi_2 r^2 \cos(2\theta - \chi_1 - \chi_2))^4} \right\}.
\end{aligned}
$$
(5.51)

Remember that for holomorphic static fields the two fourth-order terms are identical. The integration ranges over $\mathbb{R}^2$ and can be carried out explicitly. The result is presented in the appendix. Note that the phases χ_1, χ_2 only provide a shift in the angle of a π-periodic function whose range of integration is $[0, 2\pi]$. Therefore the result will not depend on χ. This implies for the gradient-flow that $\dot{\chi} = 0$ is a solution of (5.48) and thus we can restrict the discussion to the three-dimensional problem:

$$g_{ab}(\psi)\dot{\psi}^b = -\frac{\partial V[\psi]}{\partial \psi^a} \,. \tag{5.52}$$

Figures 5.1-5.3 show the potential $V[\psi]$. Note, that the ansatz of the fields can be written as

$$w = \psi_1 \left(x_+ + \sqrt{\frac{\psi_2}{\psi_1}} \right) \left(x_+ - \sqrt{\frac{\psi_2}{\psi_1}} \right) \,, \qquad v = \psi_3 \,, \tag{5.53}$$

such that $\sqrt{\psi_2/\psi_1}$ is a measure for the separation of the lumps and a change of sign in ψ_2 means that the lumps move from the real to the imaginary axis and vice versa. The coordinate ψ_1 cannot become zero during a time-evolution, because this would imply a change of topological charge. Correspondingly, one sees a divergent potential for $\psi_1 \to 0$ in Figs. 5.1 and 5.2. The difference of the two fourth-order terms is for ansatz (5.43):

$$\Delta \mathcal{L}_4 = \frac{4}{M^3} \left| \partial_i w \dot{\psi}_3 \right|^2 \,, \tag{5.54}$$

which implies that the metric is only different in their component $g_{\psi_3 \psi_3}$.
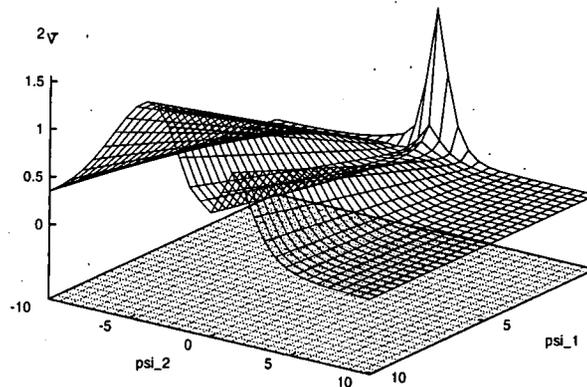

fig. 5.1: Potential V as a function of ψ_1 and ψ_2. The third component $\psi_3 = 0$, so this is the potential of the $\mathbb{C}P^1$ subspace. The couplings are $\mu_F = 0.01$, $\mu_U = 0.1$.
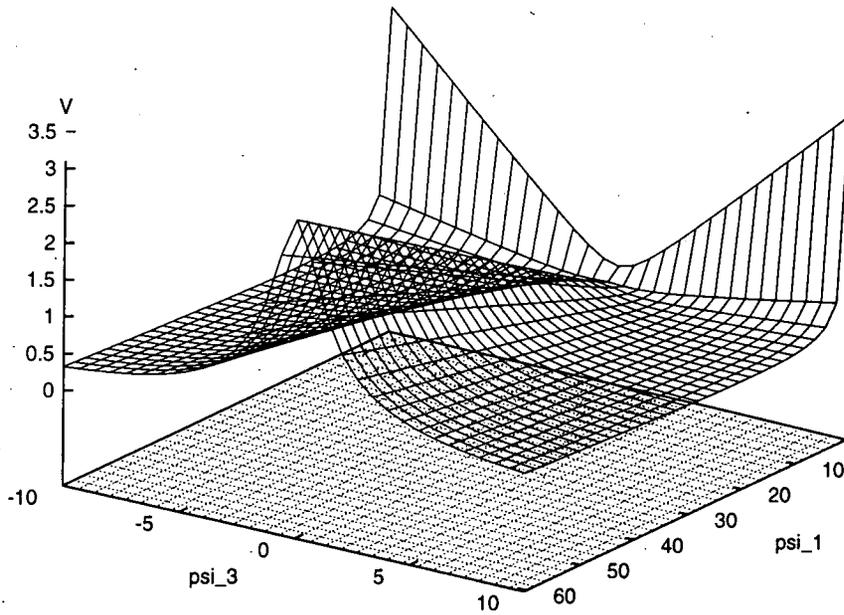
fig. 5.2: Potential V as a function of ψ_1 and ψ_3. In this plot $\psi_2 = 0.1$. The couplings are $\mu_F = 0.01$, $\mu_U = 0.1$.
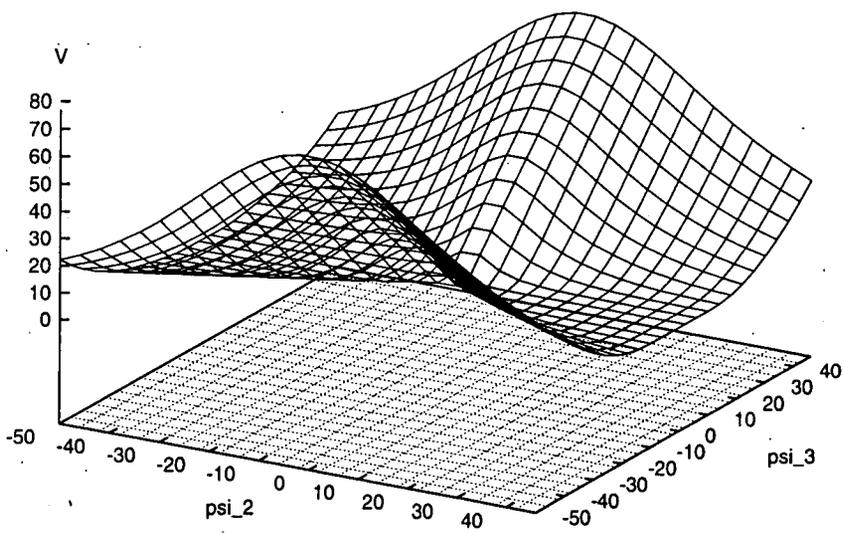

fig. 5.3: Potential V as a function of ψ_2 and ψ_3. In this plot $\psi_1 = 0.1$. The couplings are $\mu_F = 0.01$, $\mu_U = 0.1$.

5.4 Numerical Results and Outlook

We studied the gradient-flow equations (5.52) numerically, where the potential energy $V = V_2 + V_4 + U$ with $V_4 = \mu_{\mathrm{F}} F_{12}^2$. We used a fourth-order Runge-Kutta method for the time-evolution, where the metric g_{ab} was diagonalized at each timestep. We found that the two solitons always repel. If initially placed at a certain distance (by chosing $\psi_2 > 0$), they started to move apart and gradually slowed down. The potential energy $V[\psi]$ decreased and converged against twice the energy of one soliton, as expected; see Fig. 5.5. If we placed the two lumps initially on top of each other the potential energy had a maximum and a small perturbation was sufficient to induce the decay into two separate lumps which repelled. The numerical errors due to the truncation of floating point variables are sufficient to provide this perturbation. This is what we show in Figs. 5.6-5.7. Because the distance between the lumps is proportional to $\sqrt{\psi_2}$, we expect it to converge only asymptotically. This behaviour is different from ψ_1 and ψ_3 who are related to the size of the solitons and approach constant values at a finite time, see Fig. 5.4.

The behaviour of ψ_3 is interesting because it is a measure of how the $\mathbb{CP}^1$-submanifold, which is described by w, is embedded into $\mathbb{CP}^2$. If initially put to zero, ψ_3 remains at this value and the fields do not leave the $\mathbb{CP}^1$ subspace on which they started. If ψ_3 was initially non-zero, the force that pushes the lumps apart increased and thus the time-evolution of ψ_2 was accelerated. This is also indicated in Fig. 5.3, where V is plotted as a function of ψ_3. The gradient of the potential grows with increasing ψ_3 for constant ψ_2. In addition, Figs. 5.2-5.3 also show the symmetry of V under $\psi_3 \to -\psi_3$ and consequently no features can depend on the sign of ψ_3. We have verified this numerically.

An important question is the stability of the one-soliton solution (5.43) for the potential $\mathcal{U}$. Although the holomorphic fields (5.43) minimize the quadratic term of the potential energy V_2, there may be fields which have a lower potential energy. They would have be non-analytic fields, because the only possible analytic alteration is to replace ψ_3 by $\psi_3 x_+ + \psi_4$, which leads, via (5.51), to a divergent V. The stability of the one-soliton against radially symmetric deformations has been studied numerically [103] with the result that the configuration obtained by minimizing V is equivalent to (5.43).

The results of this chapter should be seen as first results of an ongoing investigation. Several interesting questions remain to be answered and various routes are open to do this. One can study the motion of two (or more) solitons in a non-dissipative moduli space approximation which involves the time-evolution of the metric g_{ab}. From the results obtained so far we predict a repulsion or a

back-to-back scattering for certain small impact paramenters. There will probably be a transition to a 90° scattering if the impact parameter becomes large enough. One can also drop the restriction of a real ξ and allow for non-constant χ which will allow the solitons to move anywhere in the plane of motion. It will be interesting to compare this to full simulations. Such simulations are another project that is presently under way and the first results confirm the repulsion of lumps that we have observed here.

The problems that lie ahead for the $\mathbb{CP}^2$-Skyrmions are manifold. First of all, their statics and dynamics are interesting in comparison to the $\mathbb{CP}^1$-solitons. Secondly, an unanswered question for $\mathbb{CP}^2$ is the difference in the dynamics due to the choice of the Skyrme term. For the two-soliton field (5.47) we have observed that the metric g_{ab} only differs in one component ($g_{\psi_3\psi_3}$), so the time-evolution described by $\mathcal{L}_4^G$ and $\mathcal{L}_4^F$ will probably not be too distinct. Another problem lies at hand. As mentioned above, one can think of the solitons on $\mathbb{CP}^2$ as being embedded $\mathbb{CP}^1$ lumps, in the sense that their topology is described by maps into $\mathbb{CP}^1$ submanifolds. It would be instructive to gain a better understanding of the geometry of these embeddings and their relation to the potential energy. Manton's interpretation of the potential energy of the Skyrmion in terms of local deformations induced by the field also applies to the $\mathbb{CP}^1$-model [49]. It might be possible to exploit this idea for the $\mathbb{CP}^2$ Skyrme model further, with the addition that here deformation *and* embedding should play a role.

Finally, the choice of the potential $\mathcal{U}$ is free which has allowed us to construct a specific $\mathcal{U}$ for a given field, this being done directly from the equations of motion. It would be interesting to investigate if one can conclude from given fields directly which potential satisfies these equations. In summary, there are many questions left to be answered, some that have been looked at in the $\mathbb{CP}^1$-model and different ones that stem from the geometry of a larger target-space.
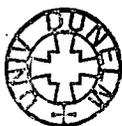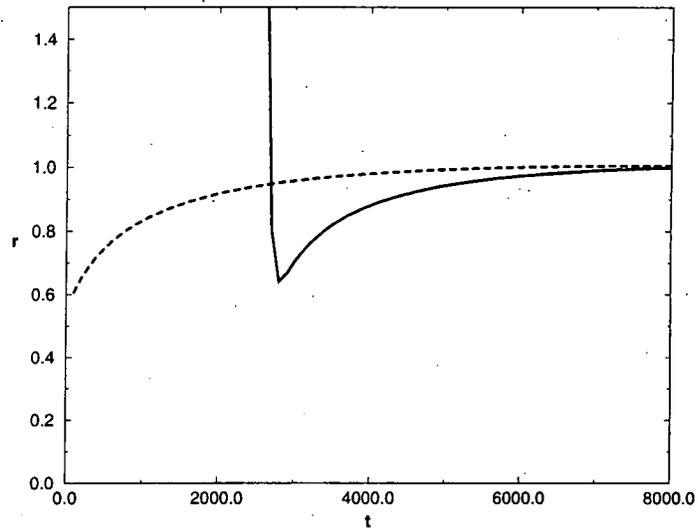
fig. 5.4: Time-evolution of ratio $r = \sqrt{\mu_U/\mu_F}(1 + \psi_3^2)/(4\psi_1\psi_2)$. The initial values were $\psi_1 = 1.0, \psi_2 = 0.0, \psi_3 = 0.0$ (solid line) and $\psi_1 = 1.5, \psi_2 = 0.2, \psi_3 = 1.0$ (dashed line). The couplings are $\mu_U = 0.01$ and $\mu_F = 0.1$.

fig. 5.5: Time-evolution of potential energy V in units of the theoretical value $V_t = 4\pi(1 + \sqrt{2\mu_U\mu_F})/3$. The initial values were here $\psi_1 = 1.0, \psi_2 = 0.0, \psi_3 = 0.0$ (solid line) and $\psi_1 = 1.5, \psi_2 = 0.2, \psi_3 = 1.0$ (dashed line). The couplings are $\mu_U = 0.01$ and $\mu_F = 0.1$.
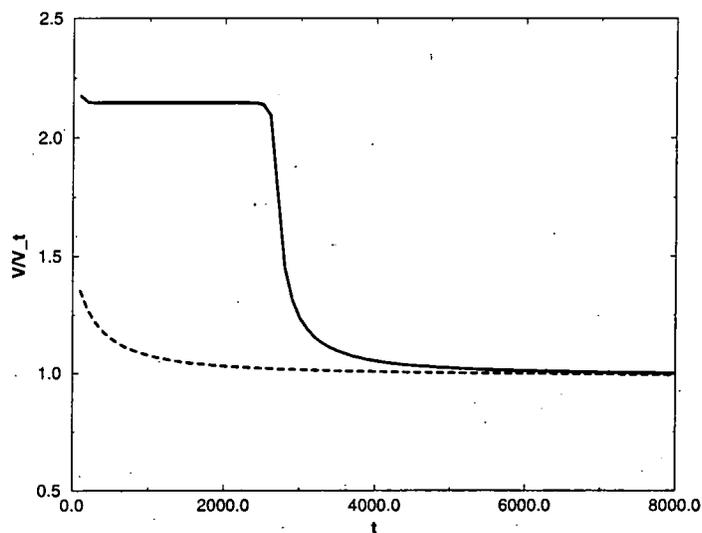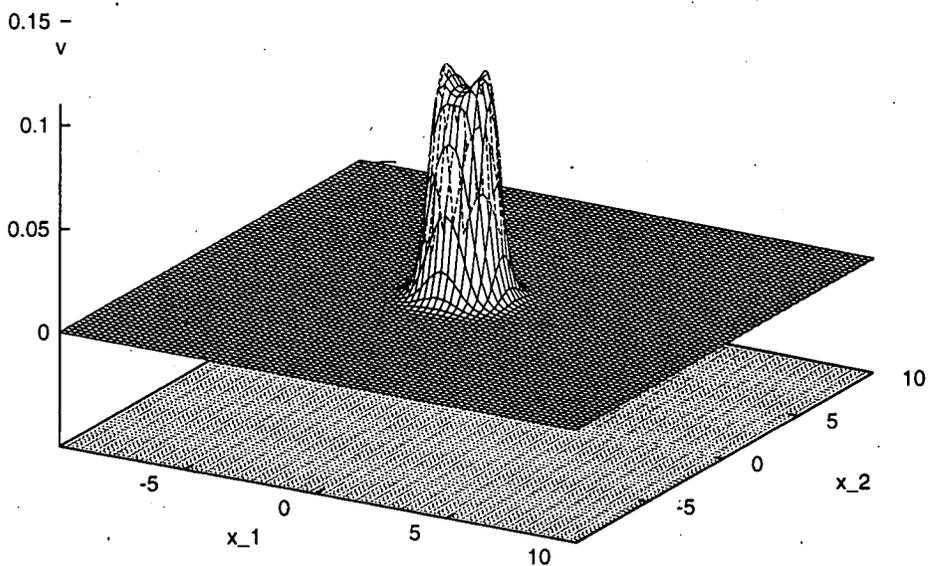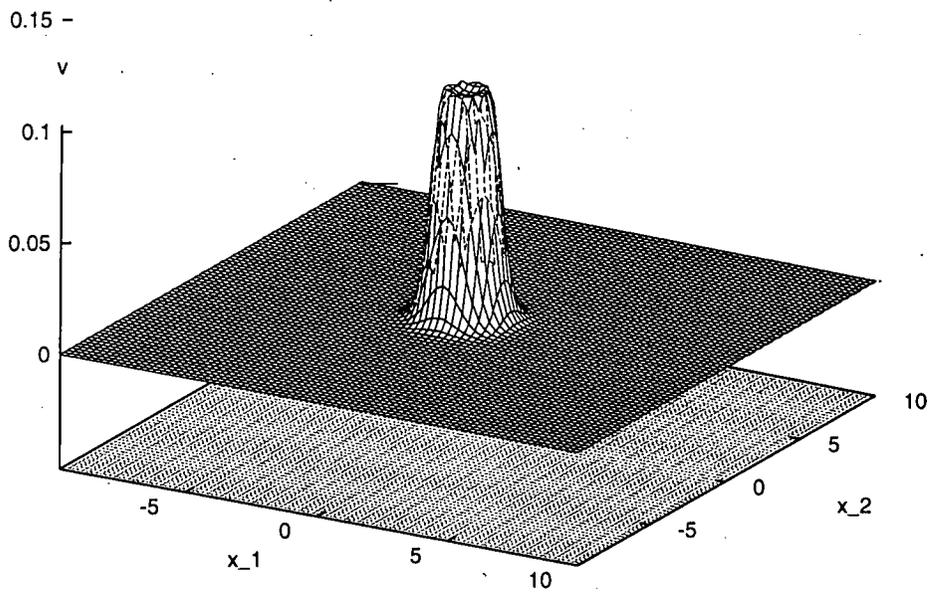
fig. 5.6: Gradient-flow for two-soliton configuration after 2000 timesteps (top) and 12000 timesteps (bottom). The initial values are $\psi_1 = 0.05$, $\psi_2 = 0$, $\psi_3 = 0.1$. The couplings are $\mu_F = 0.1$ and $\mu_U = 0.01$.
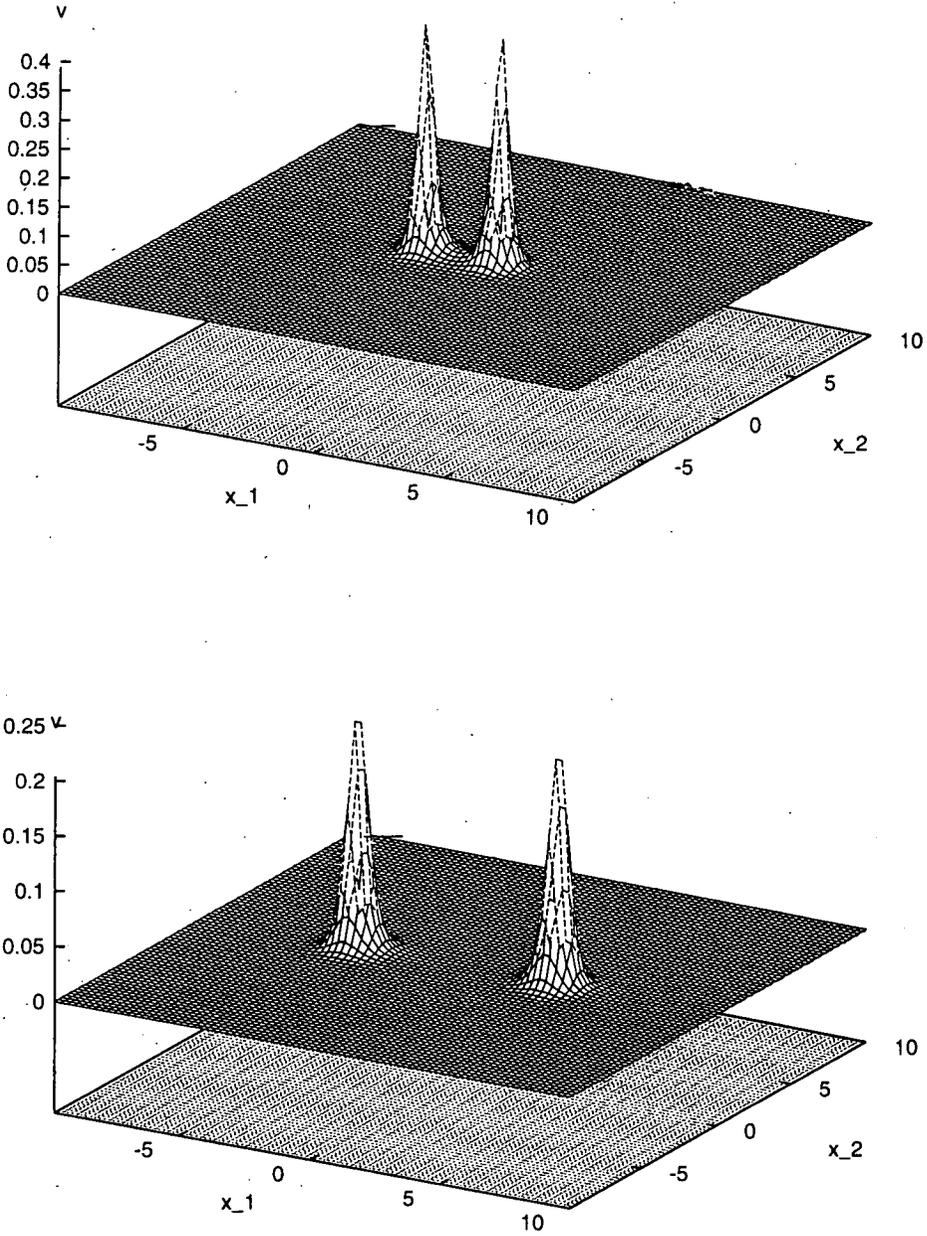
fig. 5.7:   Gradient-flow for two-soliton configuration of Fig.5.6 after 14000 timesteps (top) and 40000 timesteps (bottom).

Appendix

Potential

The potential on the moduli space can be written in terms of an auxiliary function $\mathsf{L}_m^n(\psi_2, \psi_3)$, defined as

$$\mathsf{L}_m^n(\psi_2, \psi_3) = B\left(\frac{n+1}{4}, 2m - \frac{n+1}{4}\right) {}_2F_1\left(\frac{n+1}{8}, m - \frac{n+1}{4}; m + \frac{1}{2}; 1 - E^2\right), \qquad (5.55)$$

where $E = (1 + \psi_3^2 - \psi_2^2)/(1 + \psi_3^2 + \psi_2^2)$, such that $|E| \leq 1$. B is here the Beta-function and ${}_2F_1$ the hypergeometric function. The potential on the moduli space $V[\psi]$ can be expressed as a series in L_m^n. In the following expression $m = 7/2$ for all L and will be omitted.

$$
\begin{aligned}
V[\psi] = \ & 4\pi \left(1 + \psi_3^2\right)^2 \Big\{ \\
& \mu \left(8\,\psi_1^{10}\mathsf{L}^{17} + 24\psi_1^8 \left(1 + \psi_3{}^2 + 3\psi_2{}^2\right) \mathsf{L}^{13} + \right. \\
& 24\psi_1^6 \left(1 + \psi_3^2 + 3\psi_2^2\right)\left(1 + \psi_3^2 + \psi_2^2\right)\mathsf{L}^9 + 8\left(1 + \psi_3{}^2 + \psi_2{}^2\right)^3 \psi_1{}^4 \mathsf{L}^5 \Big) + \\
& \mu_{\mathsf{U}} \left(\psi_1{}^6 \left(1 + \psi_3{}^2\right)^2 \mathsf{L}^{13} + 3\,\psi_1{}^4 \left(1 + \psi_3{}^2 + 3\psi_2{}^2\right)\left(1 + \psi_3{}^2\right)^2 \mathsf{L}^9 + \right. \\
& 3\,\psi_1{}^2 \left(1 + \psi_3{}^2 + 3\psi_2{}^2\right)\left(1 + \psi_3{}^2 + \psi_2{}^2\right)\left(1 + \psi_3{}^2\right)^2 \mathsf{L}^5 + \\
& \left(1 + \psi_3{}^2 + \psi_2{}^2\right)^3 \left(1 + \psi_3{}^2\right)^2 \mathsf{L}^1\Big)\Big\}
\end{aligned}
\qquad (5.56)
$$

where $\mu = \mu_{\mathsf{F}} + \mu_{\mathsf{G}}$.

Metric

We denote the six components of the metric as $g_{ab} = g_{\psi_a \psi_b}$, $(a, b = 1, 2, 3)$ and express them generally as

$$g_{ab} = K_{ab} \sum_{mn} R_{mn}^{ab} \mathsf{L}_m^n, \qquad (5.57)$$

where $R_{mn}(\psi)$ is a coefficient matrix that is given below.

$$a = 1, \qquad b = 1, \qquad K_{11} = \pi(1 + \psi_3^2)\psi_1^2$$

$$\mathbf{R}^{11}$$

m	$3/2$	$7/2$
n		
5	$(1 + \psi_2^2 + \psi_3^2)$	0
7	0	$\mu 8(1 + \psi_3^2)(1 + \psi_2^2 + \psi_3^2)^3$
9	ψ_1^2	0
11	0	$24\mu\psi_1^2(1 + \psi_3^2)(1 + \psi_2^2 + \psi_3^2)(1 + 3\psi_2^2 + \psi_3^2)$
15	0	$24\mu\psi_1^4(1 + \psi_3^2)(1 + 3\psi_2^2 + \psi_3^2)$
19	0	$8\mu\psi_1^6(1 + \psi_3^2)$

$$a = 1, \qquad b = 3, \qquad K_{13} = -16\pi(1 + \psi_3^2)\psi_1^3\psi_3$$

$$\mathbf{R}^{13}$$

m	$3/2$	$7/2$
n		
5	$(1 + \psi_2^3 - \psi_3^2)/(8\psi_1^2(1 + \psi_3^2))$	0
7	0	$\mu(1 + \psi_2^2 + \psi_3^2)^2(1 + \psi_3^2 - 3\psi_2^2)^2$
9	$(8(1 + \psi_3^2))^{-1}$	0
11	0	$\mu\psi_1^2((1 + \psi_3^2)(1 + 4\psi_2^2 + \psi_3^2) - 3\psi_2^4)$
15	0	$\mu\psi_1^4(3 + 5\psi_2^2 + 3\psi_3^2)$
19	0	$\mu\psi_1^6$

$$a = 2, \qquad b = 2, \qquad K_{22} = 4\pi(1 + \psi_3^2)^2\psi_1^2$$

$$\mathbf{R}^{22}$$

m	$3/2$	$7/2$
n		
1	$(1 + \psi_2^3 + \psi_3^2)/(4\psi_1^2(1 + \psi_3^2))$	0
3	0	$\mu(1 + \psi_2^3 + \psi_3^2)^3$
5	$1/(4(1 + \psi_3^2))$	0
7	0	$\mu\psi_1^2(1 + \psi_2^2 + \psi_3^2)^2(3 + 3\psi_3^2 + 19\psi_2^2)^2$
11	0	$\mu\psi_1^4(3 + 3\psi_3^2 + 19\psi_2^2)$
15	0	$\mu\psi_1^6$

$$a = 1, \qquad b = 2, \qquad K_{12} = -64\pi(1 + \psi_3^2)^2 \psi_1^3 \psi_2$$

$$\mathbf{R}^{12}$$

m n	3/2	7/2
5	$(16(1 + \psi_3^2)\psi_1^2)^{-1}$	0
7	0	$\mu\psi_1^4$
11	0	$\mu\psi_1^2(2 + 2\psi_3^2 + 3\psi_2^2)$
15	0	$\mu(1 + \psi_2^2 + \psi_3^2)$

$$a = 2, \qquad b = 3, \qquad K_{23} = 8\pi(1 + \psi_3^2)^2 \psi_1^2 \psi_2 \psi_3$$

$$\mathbf{R}^{23}$$

m n	3/2	7/2
1	$-(1 + \psi_2^3 + \psi_3^2)/(4\psi_1^2(1 + \psi_3^2))$	0
3	0	$-\mu(1 + \psi_2^3 + \psi_3^2)^3$
5	$1/(4(1 + \psi_3^2))$	0
7	0	$\mu\psi_1^2(1 + \psi_2^2 + \psi_3^2)^2(5 + 5\psi_3^2 - 11\psi_2^2)^2$
11	0	$\mu\psi_1^4(13 + 13\psi_3^2 + 5\psi_2^2)$
15	0	$\mu 7\psi_1^6$

$$a = 3, \qquad b = 3, \qquad K_{33} = 2\pi\psi_1^3 \psi_3^2$$

$$\mathbf{R}^{33}$$

m n	3/2	7/2
1	$\dfrac{(1 + \psi_3^2)(1 + \psi_2^2) + \psi_2^2(1 + \psi_2^2)}{(2\psi_1^2\psi_3^2)}$	0
3	0	$2\mu(1 + \psi_2^2 + \psi_3^2)^3$
5	$(1 + \psi_3^3 - \psi_2^2)/(2\psi_3^2)$	0
7	0	$\mu(1 + \psi_2^2 + \psi_3^2)(2(1 + \psi_3^2)^2 + \psi_2^2(5\psi_2^2 - 9(1 + \psi_3^2)))$
9	$1/(2\psi_3^2)$	0
11	0	$\mu 2\psi_1^4(1 + \psi_2^2 + \psi_3^2)(6 - 11\psi_2^2 + 6\psi_3^2)$
15	0	$\mu 6\psi_1^6(2 + \psi_2^2 + 2\psi_3^2)$
19	0	$\mu 4\psi_1^8$

General Conclusions

The theories studied in this thesis describe various aspects of statics and dynamics of extended objects in relativistic σ-models, therefore it makes sense to look back and summarize what features they have in common and what future research might be of relevance to all of them.

Almost all the objects discussed here are "textures" which owe their topological stability to the behaviour of the fields at the interior of the physical space. The topological charge provides a bound on the potential energy and prevents the lumps of non-zero degree from decaying into radiation during their time-evolution. Thus all the models studied here can have solutions that are in principle suitable to model dynamical interactions.

Two areas of further study are of common interest to all of the theories, albeit for different physical reasons. The first one of these is the investigation of solutions of higher topological degree, especially non-radially symmetric solutions and their time-dependence. For the self-dual solutions of chapter 3 this would be interesting in comparison to the well-studied vortices of the Abelian Higgs model. Perturbation theory around the self-dual point will lead to forces between the separated lumps who will begin to move under the influence of this force. For the Hopfion described in chapter 4 there is, for higher topological charges, the possibility that knot-like structures occur: the dynamics of "multi-knots" would be interesting in various contexts such as the behaviour of cosmic strings and their scattering. Open questions include the existence of bound states, the dynamics of rotating Hopfions and generally the structure of the moduli space of the theory. These are also questions of interest to the $\mathbb{C}P^2$ baby Skyrme model of chapter 5. Furthermore, for the Hopf-model one can think of an extended theory which includes Skyrmions and Hopfions. Their interactions could be diverse and promise a rich playground for investigations. Some topological properties of such a theory have been looked at in [104].

The second area of interest that is shared between the models is a quantum mechanical description of the solutions. We have not discussed such work at all here (apart from a brief aside in

chapter 4), but clearly this is a question of great interest. To construct a quantum field theory for solitons is a hard task and the general approach used so far has involved the truncation of the theory to a finite-dimensional system and quantization of the degrees of freedom in the moduli space. Semiclassical computations of fluctuations around the classical ground state have been performed in the Skyrme model, where one method involved the analysis of the vibrational normal modes and the study of the Fourier spectrum of the fields after a perturbation. Similar techniques should be applicable to the models described in this thesis, especially the Hopfions.

Each of the theories that we discussed is interesting in its own right but they might also provide ideas for investigations of the other models that we have studied. For instance, it would be interesting to look at a $U(1)$-gauged Hopfion and to compare it to a gauged Skyrmion. It would also be instructive to see if one can construct a better bound on the potential energy for such a model. On the other hand, it is an interesting problem to impose an angular time-dependence on the fields in the models of chapter 2 and 3, similar to the Hopfion or to Coleman's Q-balls.

To summarize, despite the obvious differences between the various models described in this thesis, they represent many interesting areas of research and provide inspiration for further investigations.

Bibliography

[1] J. Gladikowski. "Topological Chern-Simons Vortices in the $O(3)\,\sigma$-model". *Z. Phys.*, **C73**:181, 1996.

[2] J. Gladikowski and M. Hellmund. "Static Solitons with Non-Zero Hopf Number" . to appear in Phys. Rev. D.

[3] P.G. Drazin and R.S. Johnson. *Solitons: an Introduction*. Cambridge University Press, Trumpington Street, Cambridge, 1989.

[4] T.H.R. Skyrme. "A Nonlinear Field Theory". *Proc. Roy. Soc. Lond.*, **A260**:127, 1961.

[5] T.H.R. Skyrme. "A Unified Field Theory of Mesons and Baryons". *Nucl. Phys.*, **31**:556, 1962.

[6] E. Witten. "Current Algebra, Baryons and Quark Confinement". *Nucl. Phys.*, **B223**:433, 1983.

[7] V. G. Makhanov, Y.P. Rybakov and V.I. Sanyuk. *The Skyrme Model*. Springer-Verlag, Berlin Heidelberg, 1993.

[8] P.J. Hilton. *Introduction to Homotopy theory*. Cambridge University Press, Trumpington Street, Cambridge, 1964.

[9] M. Gell-Mann and M. Lèvy. "The Axial Vector Current in Beta Decay". *Nouvo Cimento*, **16**:705, 1960.

[10] A.M. Polyakov. *Gauge Fields and Strings*. Cambridge University Press, Trumpington Street, Cambridge, 1989.

[11] W.J. Zakrzewski. *Low Dimensional Sigma Models*. Adam Hilger, Bristol and Philadelphia, 1989.

[12] M. Nakahara. *Geometry, Topology and Physics.* Institute of Physics Publishing, Techno House, Bristol, 1990.

[13] R. Bott and L.W. Tu. *Differential Forms in Algebraic Topology.* Springer-Verlag, Berlin Heidelberg, 1982.

[14] E. M. Bogomol'nyi. "The Stability of Classical Solutions". *Sov. J. Nucl. Phys.*, **24**:449, 1976.

[15] A.Belavin and A.M. Polyakov. "Metastable States of Two-Dimensional Isotropic Ferromagnets". *JETP. Lett.*, **22**:245, 1975. *Pisma ZETF* **22**:503.

[16] N.S. Manton. "A Remark on the Scattering of BPS-Monopoles". *Phys. Lett.*, **110B**:54, 1982.

[17] R. Hobart. "On the Instablility of a Class of Unitary Field Models". *Proc. Phys. Soc. Lond.*, **82**:201, 1963.

[18] G.H. Derrick. "Comments on Non-Linear Wave-Equations as Models for Elementary Particles". *J. Math. Phys.*, **5**:1252, 1964.

[19] B. Piette and W.J. Zakrzewski. "Shrinking of Solitons in the (2+1)-dimensional S^2 Sigma Model". *Nonlinearity,* **9**:897, 1996.

[20] R.S. Ward. "Stable Topological Skyrmions on the 2D Lattice". *Lett. Math. Phys.*, **35**:385, 1995.

[21] R.S. Ward. "Bogomol'nyi Bounds for Two-Dimensional Lattice Systems". *Comm. Math. Phys.*, **184**:397, 1996.

[22] Clifford and Taubes. *Vortices and Monopoles.* Birkhäuser, Bristol, New York, 1980.

[23] M.J. Speight. *On the Dynamics of Topological Solitons.* PhD thesis, Durham University, 1995.

[24] L. Jacobs and C. Rebbi. "Interactions of Superconducting Vortices". *Phys. Rev.*, **B 19**:4486, 1979.

[25] N.S. Manton. "The Force between 't Hooft-Polyakov Monopoles". *Nucl. Phys.*, **B 126**:525, 1977.

[26] N.S. Manton. "Vortices and Anyons". *Phys. Rev. Lett.*, **67**:1462, 1991.

[27] I.A.B. Strachan. "Low-Velocity Scattering of Vortices in a Modified Abelian Higgs Model". *J. Math. Phys.*, **33**:102, 1992.

[28] T.M. Samols. "Vortex Scattering". *Comm. Math. Phys.*, **145**:149, 1992.

[29] P.A. Shah. "Vortex Scattering at Near-critical Coupling". *Nucl. Phys.*, **B429**:259, 1994.

[30] E. Corrigan. "Knot Physics". *Physics World*, June 1993.

[31] S. Deser, R. Jackiw and S. Templeton. "Topologically Massive Gauge Theories". *Ann. Phys. NY*, **140**:372, 1982.

[32] M. Atiyah. *The Geometry and Physics of Knots.* Cambridge University Press, Trumpington Street, Cambridge, 1990.

[33] S. Deser and R. Jackiw. "Self-Duality of Topological Massive Gauge Theories". *Phys. Lett.*, **B139**:371, 1984.

[34] F. Wilczek. *Fractional Statistics and Anyon Superconductivity.* World Scientific, PO Box 128, Farrer Road, Singapore 9128, 1990.

[35] L.D. Faddeev. "Some Comments on the Many Dimensional Solitons". *Lett. Math. Phys.*, **1**:289, 1976.

[36] G.S. Adkins, C.R. Nappi and E. Witten. "Static Properties of Nucleons in the Skyrme Model". *Nucl. Phys.*, **B228**:552, 1983.

[37] I.E. Dzyaloshinskii, A.M. Polyakov and P.B. Wiegmann. "Neutral Fermions in Paramagnetic Insulators". *Phys. Lett.*, **A127**:112, 1988.

[38] G. Nardelli. "Magnetic Vortices From a Non-Linear Sigma Model with Local Symmetry". *Phys. Rev. Lett.*, **73**:2524, 1994.

[39] M.A. Mehta, J.A. Davis and I.J.R. Aitchinson. " Stable Soliton Solutions of the $\mathbb{CP}^1$ Model with a Chern-Simons Term". *Phys. Lett.*, **B281**:86, 1992.

[40] B.M.A.G. Piette, D.H. Tchrakian and W.J. Zakrzewski. " Chern-Simons Solitons in a $\mathbb{CP}^1$ Model". *Phys. Lett.*, **B339**:95, 1994.

[41] F. Wilczek and A.Zee. "Linking Number, Spin and Statistics of Solitons". *Phys. Rev. Lett.*, **51**:2250, 1983.

[42] B.J. Schroers. "Bogomol'nyi Solitons in a Gauged $O(3)$ σ-Model". *Phys. Lett.*, **B356**:291, 1995.

[43] S. Coleman. *Aspects of Symmetry*. Cambridge University Press, Trumpington Street, Cambridge, 1985.

[44] J.J.M. Verbaarschot et.al. "Symmetry And Quantization Of The Two Skyrmion System: The Case Of The Deuteron". *Nucl. Phys.*, **A468**:520, 1986.

[45] V.B. Kopeliovich and B.E. Stern. " Exotic Skyrmions". *Pis'ma v ZhETF*, **45**:165, 1987.

[46] H. Weigel, B. Schwesinger and G. Holzwarth. "Exotic Baryon Number B = 2 States In The SU(2)-Skyrme Model ". *Phys. Lett.*, **B168**:321, 1986.

[47] B.M.A.G. Piette, B.J. Schroers and W.J. Zakrzewski. "Multisolitons in a Two-Dimensional Skyrme Model". *Z. Phys.*, **C 65**:165, 1995.

[48] J. Gladikowski, B. Piette and B.J. Schroers. "Skyrme-Maxwell Solitons in (2+1) dimensions". *Phys. Rev.*, **D53**:844, 1996.

[49] B.M.A.G. Piette, B.J. Schroers and W.J. Zakrzewski. "Dynamics of Baby Skyrmions". *Nucl. Phys.*, **B439**:205, 1995.

[50] R. Rajaraman. *Solitons and Instantons*. North Holland, Elsevier Science Publishers B.V. P.O. Box 211, 1000 AE Amsterdam, The Netherlands, 1982.

[51] V.E. Zakharov and A.V. Mikailov. "Example of Nontrivial Soliton Interaction in Classical Field Theory". *JETP*, **47**:1017, 1978.

[52] R.S. Ward. "Slowly Moving Lumps in the $\mathbb{C}P^1$ Model in (2+1) Dimensions". *Phys. Lett.*, **B158**:424, 1985.

[53] G. Dunne. "Self-Dual Chern-Simons Theories". In *Lecture Notes in Physics, m36*. Springer-Verlag, July 1995. hep-th/9410065.

[54] R. Jackiw and S.Y. Pi. "Classical and Quantal Nonrelativistic Chern-Simons Theory". *Phys. Rev.*, **D 42**:3500, 1990. erratum ibid. **D 48**, 3929 (1990).

[55] G.V. Dunne, R. Jackiw, S.Y. Pi and C.A. Trugenberger. "Self-dual Chern-Simons Solitons and Two-Dimensional Nonlinear Equations". *Phys. Rev.*, **D 43**:1332, 1996.

[56] R. Jackiw, K. Lee and E.J. Weinberg. "Self-Dual Chern-Simons Solitons". *Phys. Rev.*, **D 42**:3488, 1990.

[57] J. Hong, Y. Kim and P.Y. Pac. "Multivortex solutions of the Abelian Chern-Simons-Higgs theory". *Phys. Rev. Lett.*, **64**:2230, 1990.

[58] R. Jackiw and E.J. Weinberg. "Self-dual Chern-Simons Vortices". *Phys. Rev. Lett.*, **64**:2234, 1990.

[59] C. Lee, K. Lee and H. Min. "Self-dual Maxwell-Chern-Simons Solutions". *Phys. Lett.*, **B252**:79, 1990.

[60] Y. Kim, P. Oh and C. Rim. "Self-dual Chern-Simons Solitons in the Planar Ferromagnet". Technical Report SNUTP 97-020, Seoul Nat. Univ., Korea, 1997. hep-th/9703193.

[61] R. Jackiw and S.Y. Pi. "Soliton Solutions to the Gauged Nonlinear Schrödinger Equation on the Plane". *Phys. Rev. Lett.*, **64**:2969, 1990.

[62] P.K. Ghosh and S.K. Ghosh. "Topological and Nontopological Solitons in a Gauged $O(3)\,\sigma$-model with Chern-Simons Term". *Phys. Lett.*, **B366**:199, 1996.

[63] K. Arthur. "Interaction Energy of Chern-Simons Vortices in the Gauged $O(3)\,\sigma$-model". *Phys. Lett.*, **B385**:181, 1996.

[64] H. Kao, K. Lee and T. Lee. "The BPS Domain-Wall Solution in Self-Dual Chern-Simons-Higgs systems". *Phys. Rev.*, **D 55**:6447, 1997.

[65] P.K. Ghosh. "Solitons in (1+1)-dimensional Gauged Sigma Models". Technical Report MRI-PHY/97-01, Mehta Research Inst., 1997. hep-th/9701132.

[66] C. Lee, K. Lee and E.J. Weinberg. "Supersymmetry and Self-Dual Chern-Simons Systems". *Phys. Lett.*, **B243**:105, 1990.

[67] K. Kimm and B. Sul. "N=2 Supersymmetric gauged $O(3)\,\sigma$-model". Technical Report SNUTP 97-038, Seoul National Univ., 1997. hep-th/9703185.

[68] M. Torres. "Bogomol'nyi Limit for Nontopological Solitons in a Chern-Simons Model with Anomalous Magnetic Moment". *Phys. Rev.*, **D 46**:2295, 1992.

[69] P.K. Ghosh. "Exact Self-Dual Solutions in a Gauged $O(3)\,\sigma$-model with Anomalous Magnetic Moment Interaction". *Phys. Lett.*, **B381**:237, 1996.

[70] K. Kimm, K. Lee and T. Lee. "The Self-Dual Chern-Simons $\mathbb{CP}^N$ Models". *Phys. Lett.*, **B380**:303, 1996.

[71] P.K. Ghosh. "Self-Dual Gauged $\mathbb{CP}^N$ Models". *Phys. Lett.*, **B384**:185, 1996.

[72] K. Kimm, K. Lee and T.Lee. "Anyonic Bogomol'nyi Solitons in a Gauged $O(3)\,\sigma$-model". *Phys. Rev.*, **D 53**:4436, 1996.

[73] K. Arthur, D.H. Tchrakian and Y. Yang. "Topological and Non-Topological Self-Dual Chern-Simons Solitons in a Gauged $O(3)\,\sigma$-model". *Phys. Rev.*, **D 54**:5245, 1996.

[74] W.H. Thomson. *Trans. R. Soc. Edinb.*, **25**:217, 1869.

[75] P.G. Tait. *On Knots I, II, III*, in *Scientific Papers*. Cambridge University Press, Trumpington Street, Cambridge, 1898.

[76] M. Hindmarsh and T.W.B. Kibble. "Cosmic Strings". *Rep. Prog. Phys.*, **58**, 1995.

[77] D.W.L. Summers. "Knot Theory and DNA". *Proc. Symp. Appl. Math.*, **45**, 1991.

[78] G.E. Volovik and V.P. Mineev. "Particle-Like Solutions in Superfluid ^{3}He Phases". *JETP*, **46**, 1977.

[79] L.D. Faddeev. "Quantisation of Solitons". Technical Report IAS-print 75-QS70, IAS Princeton, 1975.

[80] А.Ф. Вакуленко и Л.В. Капитанский . "Усточивост солитонов в S^2 нелинейной σ-модели". Доклады Академии наук СССР, 246:840, 1979.

[81] H. Hopf. "Über die Abbildungen der dreidimensionalen Sphäre auf die Kugelfläche". *Math. Ann.*, **104**:637, 1931.

[82] A.T. Fomenko. *Differential Geometry and Topology*. Consultants Bureau, New York, London, 1987.

[83] I.E. Dzyloshinskii and B.A. Ivanov. "Localized Topological Solitons in a Ferromagnet". *JETP Lett.*, **29**:540, 1979.

[84] P. Baird and J.C. Wood. "Bernstein Theorem for Harmonic Morphisms from $\mathbb{R}^3$ and S^3". *Math. Ann.*, **280**:579, 1988.

[85] H.J. de Vega. "Closed Vortices and the Hopf Index in Classical Field Theory". *Phys. Rev.*, **D 18**:2945, 1977.

[86] K. Huang and R. Tipton. "Vortex Excitations in the Weinberg-Salam Theory". *Phys. Rev.*, **D 23**:3050, 1981.

[87] J.M. Gipson and H.C. Tze. "Possible Heavy Solitons in the Strongly Coupled Higgs Sector". *Nucl. Phys.*, **B183**:524, 1980.

[88] K.F. Fujii, S. Otsuki and F. Toyoda. "Solitons with the Hopf Index versus Skyrmions in SU(2)-Nonlinear Sigma Model". *Lett. Progr. Theor. Phys.*, **73**:1287, 1985.

[89] A. Kundu. "Hedgehog and Toroidal Solitons of the Skyrme Model". *Phys. Lett.*, **B171**:67, 1986.

[90] Z. Hlousek and J. Shertzer. "On the Stability of the Skyrme Model Soliton with Unit Hopf Charge". *Phys. Rev.*, **D 37**:1279, 1987.

[91] A. Kundu and Y.P. Rubakov. "Closed Vortex-Type Solitons with Hopf Index". *J. Phys.*, **A 15**:269, 1982.

[92] U.G. Meissner. "Toroidal Solitons with Unit Hopf Charge". *Phys. Lett.*, **B154**:190, 1985.

[93] Y.S. Wu and A.Zee. "A Closed String (or Ring) Soliton Configuration with Non-Zero Hopf Number". *Nucl. Phys.*, **B324**:623, 1989.

[94] A. Griewank and P.L. Toint. "Partitioned Variable Metric Updates for Large Structured Optimization Problems". *Numer. Math.*, **39**:119, 1982.

[95] B. Piette, M.S.S. Rashid and W.J. Zakrzewski. "Soliton Scattering in the $\mathbb{CP}^2$ Model". *Nonlinearity*, **6**:1077, 1993.

[96] I. Stokoe and W.J. Zakrzewski. "Dynamics of Solutions of the $\mathbb{CP}^{N-1}$ Models in (2+1) Dimensions". *Z. Phys.*, **C 34**:491, 1987.

[97] R.A. Leese. "Low Energy Scattering of Solitons in the $\mathbb{CP}^1$ Model". *Nucl. Phys.*, **B344**:33, 1990.

[98] P.M. Sutcliffe. "The Interaction of Skyrme-Like Lumps in (2+1) Dimensions". *Nonlinearity*, **4**:1109, 1991.

[99] M. Hindmarsh. "Semilocal Topological Defects". *Nucl. Phys.*, **B392**:461, 1993.

[100] J.A. De Azcarraga, M.S. Rashid and W.J. Zakrzewski. "Skyrme-like and Topological Terms in Sigma Models". *J. Math. Phys.*, **32**:1921, 1991.

[101] N.S. Manton. "Geometry of Skyrmions". *Comm. Math. Phys.*, **111**:469, 1987.

[102] B. Piette and W.J. Zakrzewski. "Skyrmion Dynamics in (2+1) Dimensions". Technical Report DTP-93/41, CPT Durham, UK, 1993.

[103] M. Hellmund J. Gladikowski. in preparation.

[104] L. Brekke, S. J. Hughes and T.D. Imbo. "Rings and Balls". *Int. J. Mod. Phys.*, **A9**:3523, 1994.